nature portfolio

Peer Review File

Serum metabolic profiling enables diagnosis, prognosis, and monitoring for brainstem gliomas

Corresponding Author: Professor Jingjing Wan

This file contains all reviewer reports in order by version, followed by all author rebuttals in order by version.

Version 0:

Reviewer comments:

Reviewer #1

(Remarks to the Author)
In the current manuscript, Dr. Li and colleagues presents a comprehensive study on the use of metabolic profiling through nanoparticle enhanced laser desorption/ionization mass spectrometry (NPELDI-MS), for the therapeutic and prognostic monitoring of brainstem gliomas (BSG). The observations from this study have a potentially clinical impact for the treatment of BSG patients for which there are no biomarkers and surgical diagnosis. However, there are some concerns as described below.

Major revisions
1. In the "Results" section in Fig. 4, when discussing the diagnostic panel, can you clarify the respective roles of the metabolic markers in distinguishing BSG from healthy donors?
2. When discussing the prognostic panel, provide more information about the biological significance of the nine metabolic features selected, and how they collectively predict prognosis.
3. There are 33 cases with “unknown” WHO grade, that cause biased data evaluation. Please discuss for this concern.
4. The authors demonstrated that the static metabolic snapshots effectively differentiate brainstem glioma from normal brain. Brainstem gliomas exhibit relatively characteristic imaging findings on MRI, so it is relatively easy to distinguish from normal brains. One of major challenges in clinical practice is the comparison with multiple sclerosis. I wonder if the static metabolic snapshots could detect any differences between brainstem glioma vs. other neural diseases. Please discuss about this possibility.
5. The authors indicated that brainstem gliomas can be diagnosed using comprehensive serum metabolic snapshots. To a guidance for reader, author would provide a flowchart for the diagnostic course with metabolic profiling in brainstem glioma patients.
6. The standard treatment for brainstem gliomas is radiotherapy, but for other brain tumors including GBMs, chemotherapy is often used in combination. Metabolism is expected to change depending on the chemoradiation regimens. Please discuss about a possibility that this framework can be expanded to the combination of chemotherapy and radiation.
7. In the "Methods" section, the rationale for choosing NPELDI-MS is briefly mentioned. Could you provide more details on why this method was selected and how it compares to other metabolic profiling techniques, with more explanation on the use of nanoparticle matrices as an alternative of chromatograph in laser desorption/ionization (LDI)-MS.
8. Fig.3d showed there are significant difference between low-risk and High -risk group. In this study, author collected the samples from both H3K27-altered high grade gliomas and other IDH or BRAF mutant low-grade gliomas. Molecular classification could be a major factor for the difference OS between high- and low risk. To understand the specific risk from static metabolic snapshots, please add OS survival plots with molecular groups and discuss about advantage of the risk soccer from static metabolic snapshots that exceed molecular status.
9. Is there any paired samples data such as patient tumor biopsy samples and patient serum? To verify the findings, authors would perform preclinical animal study using either patient-derived xenograft or genetically engineered mouse models to acquire paired samples (i.e., mice brain tumor and mice serum before and after radiation) with same analysis from discovery set. It is important to know these metabolite change including lactate in high-grade gliomas treatment course in brainstem tumor itself. These animal models experiment will increase scientific rigorously and generalizability for this method.
10. In Figure 4c, the ability of BRT metabolic profiles to predict tumor volume changes is intriguing. Elaborating on the biological mechanisms underlying this predictive capability and discussing its clinical significance might add more value.
11. In the “Discussion,” consider addressing the potential clinical challenges and practicality of implementing NPELDI-MS for routine BSG diagnosis and monitoring. Are there any technical or logistical hurdles to consider?

Minor revisions
1. The manuscript is generally well written with some minor grammatical errors in phrasing some sentences (some examples of corrected sentences in yellow). There are others throughout the paper – please proofread the manuscript again and check using Grammarly or another software.
1.1. “Nevertheless, imaging modalities afford an accuracy of only 65-73% in BSG detection due to the unsatisfactory image resolution (approximately 1 mm), which could lead to the misdiagnosis of minimal lesions."
1.2. “In particular, tailored inorganic nanoparticles have been introduced as chromatography alternatives prior to MS to selectively enrich metabolites, which makes it better suited for bioanalysis toward biofluid detection.”
Rephrase the “bioanalysis toward biofluid detection” to improve clarity.
1.3. We monitored the dynamic disturbances of key metabolites during the course of therapy.
2. Rephrase this sentence to improve clarity.
2.1. “In the context of BSG, metabolism alteration disrupts homeostatic processes from tumor stress in blood, causing bioenergetic perturbation, endocrine disruption, and oxidative stress.
3. Do not present ‘Results’ in the Introduction section.
3.1. “Based on the static metabolic snapshots, we distinguished BSG patients against healthy donors (HDs) with an area under the curve of 0.923.”
3.2. “We further predicted patient survival and stratified them into high-risk and low-risk groups with significant differences in prognostic outcomes ($p < 0.05$).”

Reviewer #2

(Remarks to the Author)
The study by Li and colleagues shows the potential diagnostic and prognostic value of circulating metabolites in distinguishing BSG patients from healthy donors, as well as predicting patient survival and radiotherapy response. The manuscript is generally well-written and well-structured, making it easy to follow the research methodology and results. Overall, the manuscript is well-structured and presents a valuable contribution to the field; however, the study would benefit from additional experiments to help strengthen the main conclusions.

Major Comments:

1. The authors' analysis suggests that a unique metabolic signature exists in BSG and correlates these data with pathway-based topology analysis. However, it is not clear if the signature arises from systemic metabolic changes or if it is part of the metabolic rewiring of the tumors. To clarify this point, the authors should correlate the metabolic signature in BSG with RNAseq or expression data from patients.

2. A key missing point in the paper is the lack of experimental validation. The metabolic signature or expression signature should be validated in cell lines (e.g., CHLA-07-BSGBM).

3. Along the same lines, in Fig 3, the authors identify a nine-feature panel correlated with clinical outcomes. However, there is no indication of what the biological role of these metabolites could be. Are they generated because of the rewired metabolism of tumors? Do they correlate with genetic mutations or gene expression signatures?

Minor comments:

1. Elaborate on the clinical implications of the findings, discussing how this research could impact patient care, treatment strategies, and potential future studies

Reviewer #3

(Remarks to the Author)
Li et al., apply a MALDI-based metabolomics platform to identify serum metabolites in pediatric brainstem gliomas that could be used for diagnosis and determination of patient responses to therapy. They find metabolites that could distinguish brainstem glioma from healthy controls and predict outcomes. Additionally, using longitudinally-collected samples they identify metabolites, including lactic acid, associated with response to radiotherapy.

Brainstem gliomas represent a significant portion of CNS tumors that arise in pediatric populations and we have limited knowledge of the molecular underpinnings of this tumor type. This limits therapeutic development for these cancers. As such, studies that identify metabolic alterations associated with this tumor type are important for expanding our understanding of how these tumors develop. In this referee’s opinion, a strength of the study is the development of a patient cohort that is followed longitudinally with serial sampling of serum. Additionally, the use of their nanoparticle-based MS platform (NPELDI MS) had the potential to scale to larger patient populations. However, there are several there are key experiments missing as well as broader details on their MS platform that make it difficult to substantiate their claims.

1. There are major details/data lacking for their NPELDI-MS platform. In total they detected 402 metabolic features with 287 metabolic features changed from BSG and healthy controls. This language is confusing. Typically features refers to MS peaks that haven't been identified. Did they identify 402 metabolites from their method? It appears that metabolite identification was determined by mass. How were these IDs verified? Were authentic standards used? If so they should

show their data (MS/MS, match to standards). Additionally, the level of metabolite IDs should be stated according to the Metabolomics Standards Initiative (PMID: 24039616). The number of predictor metabolites is low, for example only seven metabolites were used to determine BSG diagnosis. This makes it essential that IDs are correct.

2. While this referee appreciates that this study is performed on pediatric patients, making recruitment challenging. The low number of patients that were used for this study is problematic, especially for validation of biomarkers. A clear strength of their NPELDI-MS platform would be sample throughput, yet the authors don't take advantage of that. Instead evaluating 73 patients (40 patients for longitudinal sampling). These low numbers are likely to make translation of the biomarkers to larger patient populations difficult. Are there historical samples that the authors could use for validation?

3. The small number of serum metabolites that are used as predictors is problematic. Performing pathway analysis on such a small set is not meaningful especially since metabolites often participate in multiple pathways. For example, ornithine participates in proline metabolism, urea cycle, and polyamine metabolism. With the single ID of ornithine, pathway assignment is not possible. Looking at the metabolite predictors, the majority of significant metabolites are amino acids. This might be due to diet (or illness impacting eating) rather than glioma. Information should be given for medication and diet if possible. I also recommend authors search for other public datasets that might correlate biological responses to their small number of metabolite changes (other cancers perhaps).

4. In the panel of nine metabolites associated with clinical outcome, dialuric acid, N,N"sulfonylbisurea, caffeic acid 3-O-glucuronide, dihydroperillic acid are not endogenous metabolites and probably come from drugs the patients are receiving. Their biological significance is not clear.

5. The rationale for use of serum metabolite biomarkers for diagnosis isn't strong. The samples were collected from brainstem glioma patients when disease was already present and confirmed by imaging. It doesn't make sense to compare glioma patients to healthy controls since the presence of a tumor would be confirmed by imaging anyway. A better (or more clinically useful) comparison in my opinion would be to try and look for metabolic changes associated with glioma that could distinguish pediatric tumors (or neurological conditions) with similar presentation.

6. The most clinically useful and interesting part of this study is the longitudinal collection of samples to determine response to therapy. However, the small number of patients limits the robustness of their biomarkers. Could the authors expand to a larger patient population?

Minor comment
In the introduction the authors mention that small molecule metabolites can pass through the blood brain barrier; however, this is not true. Polar small molecules require transport though solute carriers for entry into the brain. In the context of blood brain barrier dysfunction there may be transport-independent mechanisms for metabolites to end up in the blood, but the authors should clarify this.

Version 1:

Reviewer comments:

Reviewer #1

(Remarks to the Author)
The authors have addressed most of my concerns. However, there is a critical concern about glioblastoma (GBM) cell lines used in the new experiments in response to the comment 1, 2, and 9. Author used human GBM cell lines, U251MG and U87MG, that are gold standard GBM cell lines for research and are genetically and biologically quite different from brainstem glioma (BSG). The results from using these GBM cell lines will not reflect BSG biology and incompatible with the clinical data from BSG patient. The readers in neuro-oncology field will not accept the results using the well-established GBM cells for the study of BSG. Because few BSG cell lines are commercially available, author should use those BSG cell lines in response to the comments 1, 2, and 9. In addition, author used subcutaneous model of U87MG that is also will not reflect BSG biology. Author should use orthotopic intracranial (i.e., brainstem) xenografts with patient-derived BSG cell lines.

Reviewer #2

(Remarks to the Author)
In the revised manuscript, Li and colleagues have extensively addressed all my concerns. The data presented in the current version supports the authors' conclusions. I recommend publication in Nature Communications.

Reviewer #3

(Remarks to the Author)
This revised manuscript has improved on the study and answered many of the questions posed in the original review, including a more in-depth description on how they identified the metabolite biomarkers and adding additional patients. However, I have two concerns remaining that should be addressed prior to publication.

1. The authors have clarified that the 402 metabolic features are unidentified peaks detected in their NPELDI-MS platform

and 287 features were different between healthy and glioma patients. It is fine to report these numbers; however, comparing groups by using unidentified features as is done in Figure 1 and Figure 2a is problematic. Mass spectrometers detect noise signals in the low mass range and without positive metabolite identifications it likely that many of the peaks don't actual represent biological metabolites but are artifacts of the detection method. I don't think the authors have to identify all 402 features, but they should either eliminate these comparisons or perform the same comparisons using only metabolites that have been identified.

2.It is appreciated that the authors tried to add biological context with cell culture experiments, but the rationale and approach for these studies is confusing. It is well-known that metabolites such as lactate can impact malignant cell phenotype, but presumably a better argument is that the serum biomarkers found in the study (and associated with BSG and response to therapy) would be secreted into circulation by the tumor. It is puzzling why the authors didn't just measure excretion of their metabolite biomarkers into media? In my opinion the RNA-seq data (matched tumor/serum from mice) support a biological role for the metabolite biomarkers better than the cell culture experiments. Perhaps the authors can modify the text to spend less time on the cell culture experiments and describe the RNA-seq experiments more fully.

Minor comments:
Western blot in supplementary 10a doesn't look different between treatments in my opinion.

Language still needs to some editing. For example, Line 88 has resolution twice. Line 376-Our sampling focus on the HDs and BSG.

Version 3:

Reviewer comments:

Reviewer #1

(Remarks to the Author)
The revised manuscript has addressed my concerns about models system and metabolic makers between BSG and HDs. I recommended publication in Nature Communications.

Reviewer #3

(Remarks to the Author)
The authors have performed additional work that sufficiently addresses my previous concerns. I only have two minor comments to add.

1.The authors should indicate in the text and figure legend how many identified metabolites were used as input in their model and provide a list of metabolites in supplementary.

2.I appreciate that the authors have now focused on the RNA-seq, I am still unsure how the in vitro viability assays validate the biological activity of metabolites in the paper. The magnitude in change in viability looks marginal at best and there is no confirmation of nutrient uptake in the cells or signaling through a receptor. One path perhaps to move forward would be to acknowledge the limitations of only looking at proliferation and emphasize that more biological validation studies need to be done.

Reviewer #1 (Remarks to the Author): clinical expertise in glioma

Comment: *In the current manuscript, Dr. Li and colleagues presents a comprehensive study on the use of metabolic profiling through nanoparticle enhanced laser desorption/ionization mass spectrometry (NPELDI-MS), for the therapeutic and prognostic monitoring of brainstem gliomas (BSG). The observations from this study have a potentially clinical impact for the treatment of BSG patients for which there are no biomarkers and surgical diagnosis. However, there are some concerns as described below.*

Response: We thank the reviewer for his/her time and careful consideration. We have revised the manuscript and strengthened this work addressing the reviewer's concerns. Detailed point-by-point responses and revisions can be found below.

Major revisions

Comment 1: *In the "Results" section in Fig. 4, when discussing the diagnostic panel, can you clarify the respective roles of the metabolic markers in distinguishing BSG from healthy donors?*

Response: We thank the reviewer for the useful comment. We have performed additional experiments on cell lines to clarify the respective roles of the metabolic markers in distinguishing BSG from healthy donors.

We conducted functional studies of these biomarkers to validate the biological function of metabolite biomarkers in human glioblastoma multiforme cell line (U251MG). Reprogrammed metabolic activities such as glycolysis and amino acid metabolism play important roles in cell growth and proliferation in culture or locally aggressive tumors (Ref. 38: Faubert B, et al., Metabolic reprogramming and cancer progression. Science. 2020. 368. 152). We validated the proliferative effect of lactic acid and ornithine on glioma cells at specific concentrations via cell counting kit-8 assay ($p < 0.05$, Fig. R1a, b, corresponding to Supplementary Fig. 4a, b in

Supplementary Information). Moreover, we observed a lactic acid-induced increase in mRNA expression of hypoxia-inducible transcription factor-1-α (HIF1α) and nuclear factor kappa-B (NF-κB) in tumor cells after 12 h and 24 h treatments as determined by quantitative PCR (Fig. R1c, d). This finding confirms that lactic acid is a common byproduct of the glycolytic pathway in the tumor microenvironment (Ref. 42: Baltazar F, et al., Lactate beyond a waste metabolite: metabolic affairs and signaling in malignancy. Frontiers in Oncology. 2020. 10. 231).

To investigate the impact of leucine, valine, and threonine on tumor cells, U251MG cells were deprived of amino acids for 1.5 h and restimulated with leucine, valine, and threonine (1 mM) for another 1 h. Cell lysates were analyzed via immunoblotting for the indicated proteins and phosphorylation states. As a result, the three amino acids positively regulated the activity of mTOR complex 1 (mTORC1), a key growth regulator in tumor cells (Ref. 43: Sivanand et al., Emerging roles for branched-chain amino acid metabolism in cancer. Cancer Cell. 2020. 37. 147), as evidenced by the phosphorylation levels of ribosomal protein S6 kinase 1 (pPS6K) (Fig. R1e). This finding highlights the role of these amino acids in modulating critical signaling pathways involved in cancer cell metabolism and growth.

Overall, our results underscore the significant roles of lactic acid, ornithine, valine, leucine, and threonine in cancer cell proliferation and signaling modulation, emphasizing their potential as distinguishing factors between BSG and healthy individuals.

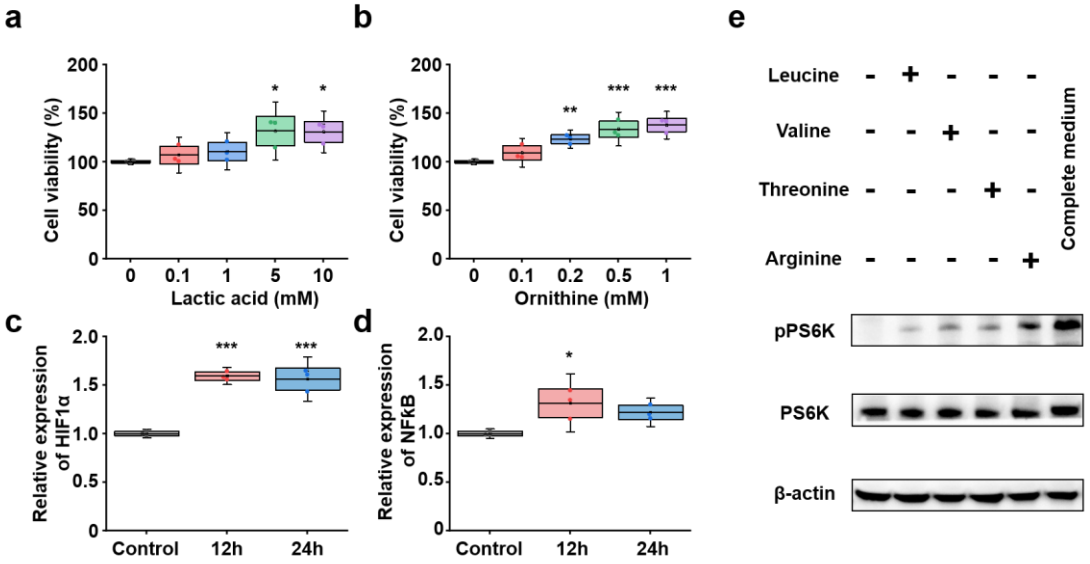

Fig. R1. Biological effects of diagnostic biomarkers on human glioblastoma multiforme (U251MG) cells. Both (a) lactic acid and (b) ornithine promoted the proliferation of tumor cells after 24 h treatment. Lactic acid induced an increase in mRNA expression of (c) HIF1α and (d) NFκB in tumor cells after 12 h and 24 h treatment, determined by quantitative polymerase chain reaction (qPCR). (e) Amino acids including leucine, valine, threonine, and arginine promoted mTOR complex 1 (mTORC1) activity, as determined by the phosphorylation of p70 ribosomal protein S6 kinase (PS6K) through western blot analysis. Cells cultured with complete medium were used as positive control sample. One-way ANOVA was used to perform statistical analyses. * $p < 0.05$, ** $p < 0.01$, *** $p < 0.001$. Experiments were repeated independently 3 times with similar results (a-d).

We have added the cell experimental results (Supplementary Fig. 4), references (Ref. 38, 42, 43), and related discussion in the manuscript and Supplementary Information as follows.

Revision:

"The metabolic signature should be validated in human-derived cell line[41]. We conducted functional studies of these biomarkers to validate the biological function of metabolite biomarkers in human glioblastoma multiforme cell line (U251MG). Reprogrammed metabolic activities such as glycolysis and amino acid metabolism play important roles in cell growth and proliferation in culture or locally aggressive tumors[38]. We validated the proliferative effect of lactic acid and ornithine on U251MG at specific concentrations via cell counting kit-8 assay ($p < 0.05$, Supplementary Fig. 4a, b).

Moreover, we observed a lactic acid-induced increase in mRNA expression of hypoxia-inducible transcription factor-1-α (HIF1α) and nuclear factor kappa-B (NFκB) in tumor cells after 12 h and 24 h treatments as determined by quantitative PCR (Supplementary Fig. 4c, d). This finding confirms that lactic acid is a common byproduct of the glycolytic pathway in the tumor microenvironment[42].

To investigate the impact of leucine, valine, and threonine on tumor cells, U251MG cells were deprived of amino acids for 1.5 h and restimulated with leucine, valine, and threonine (1 mM) for another 1 h. Cell lysates were analyzed via immunoblotting for the indicated proteins and phosphorylation states. As a result, the three amino acids positively regulated the activity of mTOR complex 1 (mTORC1), a key growth regulator in tumor cells[43], as evidenced by the phosphorylation levels of ribosomal protein S6 kinase 1 (Supplementary Fig. 4e). This finding highlights the role of these amino acids in modulating critical signaling pathways involved in cancer cell metabolism and growth." (Manuscript, Page 8)

"**1.7 Cell culture**

U87MG-Luc (a human glioblastoma cell line with luciferase fluorescent labeling) and U251MG (a human glioblastoma cell line) cells were cultured in Dulbecco's Modified Eagle Medium (DMEM, Gibco) supplemented with 10% fetal bovine serum (Corning) and 1% penicillin-streptomycin (Gibco) at 37°C in a 5% CO_2 humidified incubator. Cells in the logarithmic growth phase were selected for subsequent experiments.

1.8 *In vitro* cell experiments

Cell proliferation assay: U251MG cells were seeded in 96-well plate at the density of 1×10^4 cells per well and incubated at 37°C for 24 h. Then the cells were treated with lactic acid (0, 0.1, 1, 5, and 10 mM) or ornithine (0, 0.1, 0.2, 0.5, and 1mM) at various concentrations in triplicate for 24 h. The cell viability was determined using an enhanced cell counting kit-8 (CCK8, Beyotime). Specifically, 10 μL of CCK8 solution was added to each well. After 1 h of cell culture, optical density (OD) value at 450 nm was detected via plate reader (BioTek Synergy H1).

Quantitative polymerase chain reaction (qPCR) assay: U251MG cells were

seeded in a 12-well plate at the density of 1.5×10^5 cells per well and incubated at 37°C for 24 h. Then the cells were treated with lactic acid (10 mM) in triplicate for 12 h or 24 h. The cells were collected and subjected to RNA extraction by using SimplyP Total RNA Extraction Kit (Bioer Techology). qPCR assay was performed using HiScript III RT SuperMix Kit for qPCR (Vazyme) and ChamQ Universal SYBR qPCR Master Mix Kit (Vazyme) according to manufacturer's instructions.

Western blotting analysis: U251MG cells were seeded in culture dish (6 cm) at the density of 8×10^5 cells per dish and incubated at 37°C for 24 h. To determine the role of amino acids, the cells were starved by amino acid-depleted DMEM for 1.5 h, followed by the addition of individual amino acid (1 mM) for 1 h. Here, cells cultured with full medium for 1 h after amino acid starvation were used as positive control sample. To study the impact of glucose, the cells were treated with glucose-depleted DMEM for 24 h. Then, glucose with different concentrations (25 mM and 50 mM) were supplied for another 24 h. To assess β-nicotinamide mononucleotide (NMN), the cells were treated with NMN (0, 0.5, and 1mM) for 24 h according to literature[17]. Afterwards, the cells were collected for western blot analysis. Typically, cells were lysed in RIPA buffer (Epizyme Biotech) containing protease inhibitor (MCE) and phosphatase inhibitor cocktail (Epizyme Biotech). The concentration of protein was determined by a bicinchoninic acid (BCA) assay (Vazyme). 20 μg of cell lysate protein per sample was subjected to gel electrophoresis (Tanon). The primary antibodies include anti-phospho-p70 S6 Kinase (Thr389) antibody (CST), anti- p70 S6 Kinase (49D7) Rabbit antibody (CST), anti-PD-L1 antibody (CST), and anti-β-Actin (8H10D10) antibody (CST), while anti-rabbit IgG HRP-linked antibody and anti-mouse IgG HRP-linked Antibody (CST) were used as the secondary antibodies. The blots were imaged by CLINX ChemiScope 6000 system." (Supplementary Information, Page 6)

***Comment* 2:** *When discussing the prognostic panel, provide more information about the biological significance of the nine metabolic features selected, and how they collectively predict prognosis.*

Response: We thank the reviewer for the valuable feedback. We have conducted additional experiments on cell models to elucidate the biological significance of the prognostic panel. The panel collectively predicts prognosis by jointly affecting the immune escape, signal activation, and metastasis of glioma cells.

We confirmed the biological significance of the prognostic panel using human glioblastoma multiforme cell line (U251MG). In particular, we have already validated lactic acid in the diagnostic panel. Hence, its presence in the prognostic panel does not warrant further investigation.

Programmed death-ligand 1 (PD-L1) is significantly overexpressed in various tumor types and regulates immune evasion by binding to the inhibitory receptor PD-1 on activated T cells, leading to T cell exhaustion (Ref. 48: Kornepati A, et al., Programmed death ligand 1 signals in cancer cells. Nature Reviews Cancer. 2022. 22. 174). It has been reported that glucose and niacinamide contributed to tumor immune escape via elevating expression of PD-L1 (Ref. 49&50: He H, et al., Aerobic glycolysis promotes tumor immune evasion and tumor cell stemness through the noncanonical function of hexokinase 2. Cancer Communications. 2023. 43. 387; Lv H, et al., NAD(+) metabolism maintains inducible PD-L1 expression to drive tumor immune evasion. Cell Metabolism. 2021. 33. 110). To assess this impact on human glioblastoma multiforme cell line, U251MG cells were cultured in glucose-depleted dulbecco's modified eagle medium (DMEM) supplemented with varying glucose concentrations (0, 25, and 50 mM) for 24 h. In case of niacinamide, cells were cultured in complete medium with the addition of β-nicotinamide mononucleotide (an analog of niacinamide and a precursor to NAD^+) at selected concentrations (0, 0.5, and 1 mM) for 24 h. As a result, the increase of both glucose and niacinamide analog resulted in the up-regulation of PD-L1 expression in tumor cells (Fig. R2a, corresponding to Supplementary Fig. 10a in Supplementary Information).

We also demonstrated that arginine promoted mTORC1 activation in tumor cells through western blotting analysis, following the same protocol in exploring the biofunctions of amino acids in the diagnostic panel (Fig. R1e).

Succinic acid was secreted by tumor to promote metastasis via phosphoinositide

3-kinase (PI3K)-HIF1αaxis (Ref. 51: Wu J Y, et al., Cancer-derived succinate promotes macrophage polarization and cancer metastasis via succinate receptor. Molecular Cell. 2020. 77. 213). To verify the effect of succinic acid in human glioblastoma multiforme cell line, we conducted a cell migration experiment and observed a rise in cell migration as the concentration of succinic acid increased from 0-0.1 mM (Fig. R2b, c). The result supported succinic acid-promoted metastasis of U251MG cells.

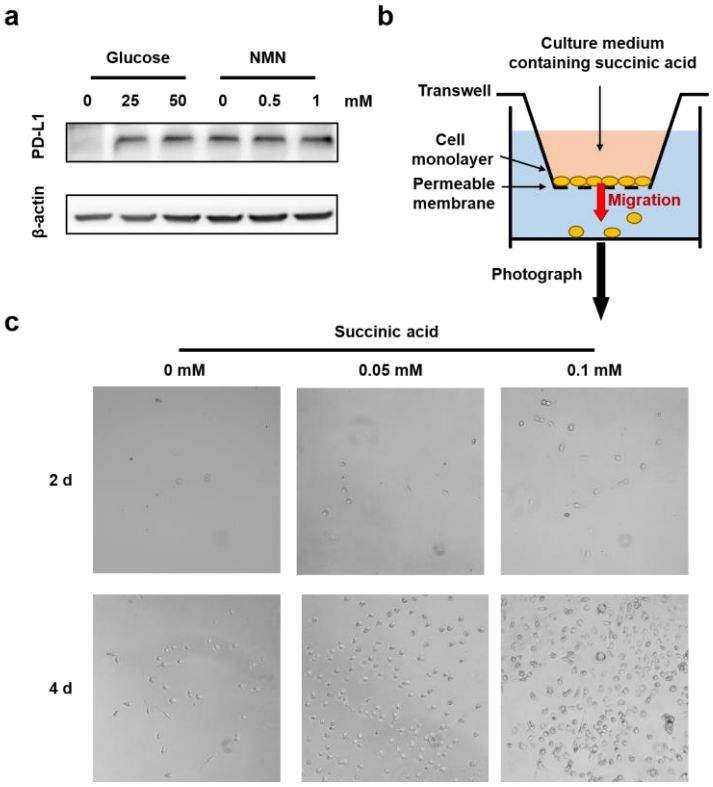

Fig. R2. Biological effects of prognostic biomarkers on human glioblastoma multiforme cells. (a) Both glucose and nicotinamide mononucleotide (NMN) improved the PD-L1 expression in U251MG cells, verified by western blot analysis. (b) U251MG cells in the upper chamber of transwell were treated with succinic acid (0.05 mM and 0.1 mM). (c) At selected time point (2 d and 4 d), migrated U251MG cells in the lower chamber were photographed under an inverted microscope using a 10× objective lens.

We have added the cell experimental results (Supplementary Fig. 4, 10), references (Ref. 48-51), and related discussion in the manuscript and Supplementary Information as follows.

Revision:

"We confirmed the biological significance of the prognostic panel using U251MG cell line. In particular, we have already validated lactic acid in the diagnostic panel. Hence, its presence in the prognostic panel does not warrant further investigation.

Programmed death-ligand 1 (PD-L1) is significantly overexpressed in various tumor types and regulates immune evasion by binding to the inhibitory receptor PD-1 on activated T cells, leading to T cell exhaustion[48]. It has been reported that glucose and niacinamide contributed to tumor immune escape via elevating expression of PD-L1[49,50]. To assess this impact on human glioblastoma multiforme cell line, U251MG cells were cultured in glucose-depleted dulbecco's modified eagle medium (DMEM) supplemented with varying glucose concentrations (0, 25, and 50 mM) for 24 h. In case of niacinamide, cells were cultured in complete medium with the addition of β-nicotinamide mononucleotide (an analog of niacinamide and a precursor to NAD^+) at selected concentrations (0, 0.5, and 1 mM) for 24 h. As a result, the increase of both glucose and niacinamide analog resulted in the up-regulation of PD-L1 expression in tumor cells (Supplementary Fig. 10a).

We also demonstrated that arginine promoted mTORC1 activation in tumor cells through western blotting analysis, following the same protocol in exploring the biofunctions of amino acids in the diagnostic panel (Supplementary Fig. 4e).

Succinic acid was secreted by tumor to promote metastasis via phosphoinositide 3-kinase-HIF1α axis[51]. To verify the effect of succinic acid in human glioblastoma multiforme cell line, we conducted a cell migration experiment and observed a rise in cell migration as the concentration of succinic acid increased from 0-0.1 mM (Supplementary Fig. 10b, c). The result supported succinic acid-promoted metastasis of U251MG cells." (Manuscript, Page 11)

"**1.7 Cell culture**

U87MG-Luc (a human glioblastoma cell line with luciferase fluorescent labeling) and U251MG (a human glioblastoma cell line) cells were cultured in Dulbecco's Modified Eagle Medium (DMEM, Gibco) supplemented with 10% fetal bovine serum (Corning) and 1% penicillin-streptomycin (Gibco) at 37°C in a 5% CO_2 humidified incubator. Cells in the logarithmic growth phase were selected for subsequent

experiments.

1.8 *In vitro* cell experiments

Cell proliferation assay: U251MG cells were seeded in 96-well plate at the density of 1×10^4 cells per well and incubated at 37°C for 24 h. Then the cells were treated with lactic acid (0, 0.1, 1, 5, and 10 mM) or ornithine (0, 0.1, 0.2, 0.5, and 1mM) at various concentrations in triplicate for 24 h. The cell viability was determined using an enhanced cell counting kit-8 (CCK8, Beyotime). Specifically, 10 μL of CCK8 solution was added to each well. After 1 h of cell culture, optical density (OD) value at 450 nm was detected via plate reader (BioTek Synergy H1).

Quantitative polymerase chain reaction (qPCR) assay: U251MG cells were seeded in a 12-well plate at the density of 1.5×10^5 cells per well and incubated at 37°C for 24 h. Then the cells were treated with lactic acid (10 mM) in triplicate for 12 h or 24 h. The cells were collected and subjected to RNA extraction by using SimplyP Total RNA Extraction Kit (Bioer Techology). qPCR assay was performed using HiScript III RT SuperMix Kit for qPCR (Vazyme) and ChamQ Universal SYBR qPCR Master Mix Kit (Vazyme) according to manufacturer's instructions.

Western blotting analysis: U251MG cells were seeded in culture dish (6 cm) at the density of 8×10^5 cells per dish and incubated at 37°C for 24 h. To determine the role of amino acids, the cells were starved by amino acid-depleted DMEM for 1.5 h, followed by the addition of individual amino acid (1 mM) for 1 h. Here, cells cultured with full medium for 1 h after amino acid starvation were used as positive control sample. To study the impact of glucose, the cells were treated with glucose-depleted DMEM for 24 h. Then, glucose with different concentrations (25 mM and 50 mM) were supplied for another 24 h. To assess β-nicotinamide mononucleotide (NMN), the cells were treated with NMN (0, 0.5, and 1mM) for 24 h according to literature[17]. Afterwards, the cells were collected for western blot analysis. Typically, cells were lysed in RIPA buffer (Epizyme Biotech) containing protease inhibitor (MCE) and phosphatase inhibitor cocktail (Epizyme Biotech). The concentration of protein was determined by a bicinchoninic acid (BCA) assay (Vazyme). 20 μg of cell lysate protein per sample was subjected to gel electrophoresis (Tanon). The primary antibodies include anti-phospho-

p70 S6 Kinase (Thr389) antibody (CST), anti- p70 S6 Kinase (49D7) Rabbit antibody (CST), anti-PD-L1 antibody (CST), and anti-β-Actin (8H10D10) antibody (CST), while anti-rabbit IgG HRP-linked antibody and anti-mouse IgG HRP-linked Antibody (CST) were used as the secondary antibodies. The blots were imaged by CLINX ChemiScope 6000 system.

Cell migration: U251MG cells were seeded on the upper chamber of a 24-well transwell plate at the density of 2×10^4 cells per well and treated with succinic acid of different concentrations (0.05 mM and 1 mM) according to literature[18]. After 2 d or 4 d simulation, cells migrated to the lower chamber and were photographed under an inverted microscope using a 10× objective lens." (Supplementary Information, Page 6)

Comment 3: *There are 33 cases with unknown WHO grade, that cause biased data evaluation. Please discuss for this concern.*

Response: We thank the reviewer for the valuable suggestions. While the WHO grade was unknown for 33 cases, their disease status was carefully confirmed based on clinical symptoms and imaging findings according to the established clinical guidelines (Ref.: Louis D N, et al., The 2021 WHO classification of tumors of the central nervous system: a summary. Neuro-Oncology. 2021. 23. 1231). Strict diagnostic procedures were followed to avoid the potential biased data evaluation.

The BSG cohort was recruited over a period of 6 years (from November 2017 to May 2023). Given the complexities and inherent risks associated with performing biopsies in brainstem tumors, particularly in cases of diffuse intrinsic pontine glioma, obtaining WHO grades for all patients presents challenges especially before 2020 (Ref. 34: Grimm S A, et al. Brainstem glioma: a review. Current Neurology and Neuroscience Reports. 2013. 13. 346). In cases where pathological biopsies were not feasible, diagnostic decisions were based on the integration of clinical symptoms and imaging characteristics (Ref.: Hargrave D, et al. Diffuse brainstem glioma in children: critical review of clinical trials. Lancet Oncology. 2006. 7. 241). To ensure the accuracy of patient enrollment and diagnosis as BSG cases, the diagnosis of each patient was

collaboratively reviewed by 2 oncologists and imaging specialists. If conflicting opinions arose, senior physicians were consulted to avoid any potential biases in data evaluation.

We have added the related discussion and references (Ref. 34) in the manuscript and Supplementary Information as follows.

Revision:

"Given the complexities and inherent risks associated with performing biopsies in brainstem tumors, particularly in cases of diffuse intrinsic pontine glioma, obtaining WHO grades for all patients presents challenges especially before 2020[34]. To ensure the accuracy of patient enrollment and diagnosis as BSG cases, the diagnosis of each patient was collaboratively reviewed by 2 oncologists and imaging specialists. If conflicting opinions arose, senior physicians were consulted to avoid any potential biases in data evaluation." (Manuscript, Page 5)

"BSG patients were diagnosed based on abnormalities observed in magnetic resonance imaging (MRI) images of the brainstem and confirmed by two independent oncologists and imaging specialists. All individuals with BSG were confirmed through the use of radiological imaging and clinical symptoms." (Supplementary Information, Page 2)

Comment 4: *The authors demonstrated that the static metabolic snapshots effectively differentiate brainstem glioma from normal brain. Brainstem gliomas exhibit relatively characteristic imaging findings on MRI, so it is relatively easy to distinguish from normal brains. One of major challenges in clinical practice is the comparison with multiple sclerosis. I wonder if the static metabolic snapshots could detect any differences between brainstem glioma vs. other neural diseases. Please discuss about this possibility.*

Response: We thank the reviewer for the useful advice. We newly collected clinical samples from patients with other neural diseases and added the comparison between

BSG and other neural diseases through the static metabolic snapshots. We confirmed that the static metabolic snapshots could detect differences between BSG vs. other neural diseases.

The typical age of onset for multiple sclerosis is 20-40 years old, which differs from the age range of 6-10 years old observed in the BSG cohort enrolled in this study (Ref.: Graves J S, et al., Ageing and multiple sclerosis. Lancet Neurology. 2023. 22. 66-77). Therefore, we mainly focus on differentiating other neurological diseases (encephalitis and idiopathic epilepsy) commonly occurring in children. We newly collected 68 serum samples from 28 encephalitis cases and 40 idiopathic epilepsy cases.

We adopted the same protocol to detect the differences between BSG vs. other neurological diseases based on static metabolic snapshots (Fig. R3a, corresponding to Supplementary Fig. 7a in Supplementary Information). As a result, the models also achieved outstanding performance in differentiating BSG from encephalitis and idiopathic epilepsy, with area under receiver operating characteristic of 0.929 and 0.923, respectively (Fig. R3b).

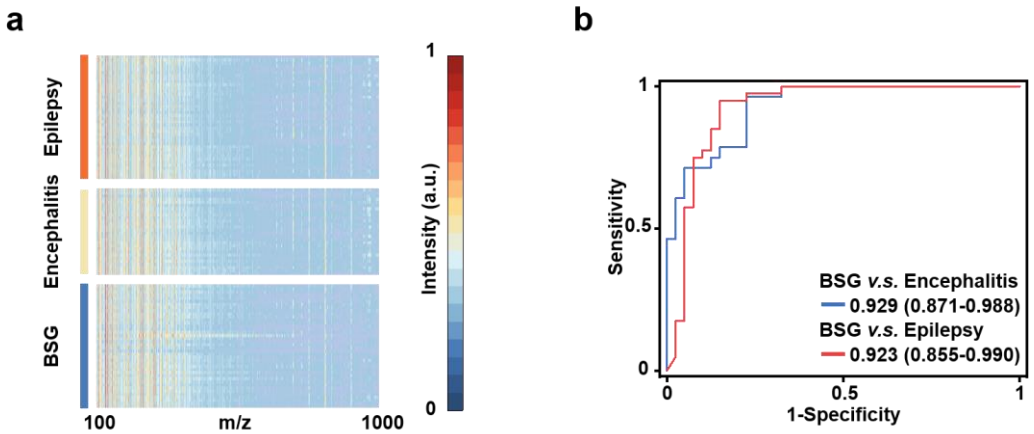

Fig. R3. Static metabolic snapshots of other neural diseases. (a) Heatmap of serum metabolic profiles from 40 BSG patients, 28 encephalitis patients, and 40 epilepsy patients. (b) ROC curves for differentiating BSG patients from encephalitis and epilepsy patients via the static metabolic snapshots, respectively.

We have added the related results (Supplementary Fig. 7) and discussion in the manuscript as follows.

Revision:

"Another major challenge in clinical practice is the differentiation of BSG from other neural diseases by MRI imaging[44]. We added the comparison between BSG and other neural diseases (28 encephalitis cases and 40 idiopathic epilepsy cases) through the static metabolic snapshots. We adopted the same protocol to detect the differences (Supplementary Fig. 7a). As a result, the models also achieved outstanding performance in differentiating BSG from encephalitis and idiopathic epilepsy, with AUC of 0.929 and 0.923, respectively (Supplementary Fig. 7b)." (Manuscript, Page 9)

Comment 5: *The authors indicated that brainstem gliomas can be diagnosed using comprehensive serum metabolic snapshots. To a guidance for reader, author would provide a flowchart for the diagnostic course with metabolic profiling in brainstem glioma patients.*

Response: We thank the reviewer for the valuable suggestion. We have provided a flowchart (Fig. R4, corresponding to Supplementary Fig. 15 in Supplementary Information) for the diagnostic course with metabolic profiling in BSG patients.

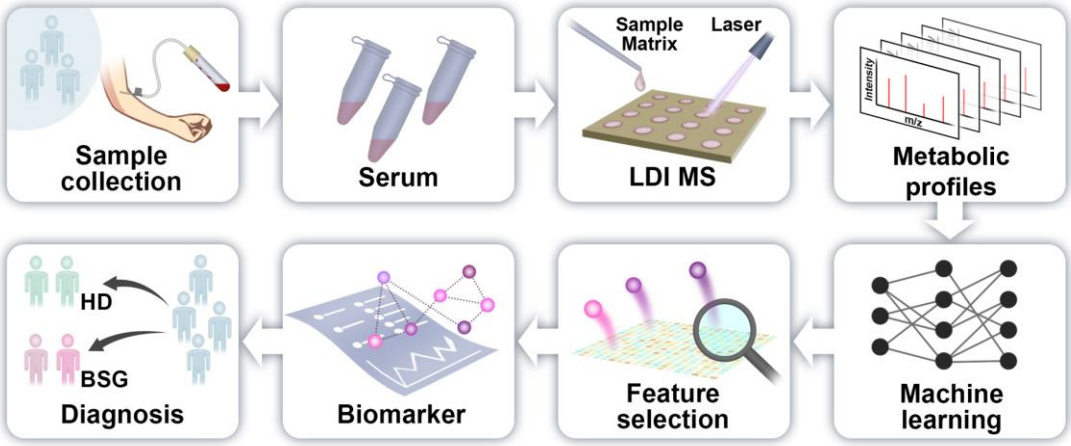

Fig. R4. Flowchart for the diagnostic course with metabolic profiling in BSG patients.

Revision:

"Notably, both diagnostic and prognostic assays were built on a novel NPELDI-

MS platform (see workflow in Supplementary Fig. 15), featuring little sample pretreatment (~min) and fast analytical speed (2 s per sample) for metabolic profiling of tracing serum sample (down to 100 nL)." (Manuscript, Page 17)

Comment 6: *The standard treatment for brainstem gliomas is radiotherapy, but for other brain tumors including GBMs, chemotherapy is often used in combination. Metabolism is expected to change depending on the chemoradiation regimens. Please discuss about a possibility that this framework can be expanded to the combination of chemotherapy and radiation.*

Response: We thank the reviewer for the insightful comment. This framework indeed has the potential for expansion to encompass the combination of chemotherapy and radiation in the treatment of BSG.

While radiotherapy is the standard treatment for BSG, chemotherapy is often utilized in combination with radiotherapy for other brain tumors like glioblastomas (GBMs). The metabolism of tumors is expected to undergo changes based on the chemoradiation regimens employed (Ref. 67: Xiao Y, et al., Emerging therapies in cancer metabolism. Cell Metabolism. 2023. 35. 1283). Importantly, we have previously observed significant alterations in carbohydrates and amino acids during the chemotherapy process for various cancer types such as gastric cancer, pancreatic cancer, and breast cancer (Ref. 29&68: Xu Z, et al., Efficient plasma metabolic fingerprinting as a novel tool for diagnosis and prognosis of gastric cancer: a large-scale, multicentre study. Gut. 2023. 72. 2051; Vernieri C, et al., Targeting cancer metabolism: dietary and pharmacologic interventions. cancer discovery. 2016. 6. 1315-1333). Thus, it is feasible to extend this framework to incorporate the combined use of chemotherapy and radiation in brain tumor treatment. Our goal is to offer a more in-depth understanding of how metabolic profiles are affected by diverse treatment strategies, ultimately enhancing the precision and efficacy of therapeutic interventions for brain tumors.

We have added the related references (Ref. 29, 67, 68) and discussion in the manuscript as follows.

Revision:

"While radiotherapy is the standard treatment for BSG, chemotherapy is often utilized in combination with radiotherapy for other brain tumors like GBMs. The metabolism of tumors is expected to undergo changes based on the chemoradiation regimens employed[67]. Importantly, we have previously observed significant alterations in carbohydrates and amino acids during the chemotherapy process for various cancer types such as gastric cancer, pancreatic cancer, and breast cancer[68]. Thus, it is feasible to extend this framework to incorporate the combined use of chemotherapy and radiation in brain tumor treatment." (Manuscript, Page 17)

Comment 7: *In the "Methods" section, the rationale for choosing NPELDI-MS is briefly mentioned. Could you provide more details on why this method was selected and how it compares to other metabolic profiling techniques, with more explanation on the use of nanoparticle matrices as an alternative of chromatograph in laser desorption/ionization (LDI)-MS.*

Response: We thank the reviewer for his/her helpful advice. NPELDI-MS was selected for its fast detection capability compared to other metabolic profiling techniques. We have also provided more explanation on the use of nanoparticle matrices as an alternative of chromatograph in laser desorption/ionization (LDI)-MS in the "Methods" section.

Current metabolic profiling techniques mainly include nuclear magnetic resonance (NMR) and mass spectrometry (MS). LDI-MS stands out for its ability to rapidly detect metabolites in high-throughput manner. Throughout the analysis process, the abundance of metabolites and the complexity of samples significantly affect MS analysis, necessitating rigorous pretreatment procedures to separate and enrich metabolites from complex biological mixtures. Utilizing nanomaterials as substrates and fine-tuning the interaction interfaces between molecules and substrate materials by controlling the physicochemical properties of the material interface can significantly

enhance the detection efficiency of LDI-MS.

Ferric nanoparticle as an alternative of chromatograph in LDI-MS possesses three advantages: (1) nano-scale surface roughness and large-scale uniformity that enables the swift and selective laser desorption/ionization of metabolites; (2) optimized surface charge that promotes ion formation and facilitates electron transfer; and (3) ease of mass-production with cost-effectiveness that are suitable for extensive clinical applications (Supplementary Ref. 11: Huang L, et al. Machine learning of serum metabolic patterns encodes early-stage lung adenocarcinoma. Nature Communications. 2020. 11. 3556). Based on these advantages, our NPELDI-MS platform avoids the necessity for sample pretreatment, leading to faster analysis speed (~seconds) and a significant reduction in sample consumption (100 nL) by approximately 2-3 orders of magnitude.

We have added the related discussion in the Supplementary Information as follows.

Revision:

"Current metabolic profiling techniques mainly include nuclear magnetic resonance (NMR) and mass spectrometry (MS). LDI-MS stands out for its ability to rapidly detect metabolites in high-throughput manner. Throughout the analysis process, the abundance of metabolites and the complexity of samples significantly affect MS analysis, necessitating rigorous pretreatment procedures to separate and enrich metabolites from complex biological mixtures. Utilizing nanomaterials as substrates and fine-tuning the interaction interfaces between molecules and substrate materials by controlling the physicochemical properties of the material interface can significantly enhance the detection efficiency of LDI-MS.

Ferric nanoparticle as an alternative of chromatograph in LDI-MS possesses three advantages: (1) nano-scale surface roughness and large-scale uniformity that enable the rapid and selective laser desorption/ionization of metabolites; (2) optimized surface charge that promotes ion formation and facilitates electron transfer; and (3) ease of mass-production with cost-effectiveness that are suitable for extensive clinical applications[11]. Based on these advantages, NPELDI-MS platform avoids the necessity

for sample pretreatment, leading to faster analysis speed (~seconds) and a significant reduction in sample consumption (100 nL) by approximately 2-3 orders of magnitude." (Supplementary Information, Page 4)

Comment 8: *Fig.3d showed there are significant difference between low-risk and High -risk group. In this study, author collected the samples from both H3K27-altered high grade gliomas and other IDH or BRAF mutant low-grade gliomas. Molecular classification could be a major factor for the difference OS between high- and low risk. To understand the specific risk from static metabolic snapshots, please add OS survival plots with molecular groups and discuss about advantage of the risk soccer from static metabolic snapshots that exceed molecular status.*

Response: We thank the reviewer for the thoughtful analysis and constructive suggestions. The original Fig. S4 already includes overall survival (OS) plots with molecular groups, as indicated. With the expansion of the total sample size from 244 to 405, we have updated the OS plots for molecular subtypes in a larger cohort from 40 to 67 patients with molecular features and prognostic information, revealing the consistent ability for differentiation based on the H3K27M mutation. The advantage of the risk score from static metabolic snapshots that exceed molecular status lies in the higher patient compliance and rapid detection capabilities.

While Fig. 3d revealed significant differences between the low-risk and high-risk groups based on static metabolic snapshots, it is acknowledged that molecular classification plays a crucial role in distinguishing the OS outcomes between high- and low-risk patients (Ref.: Chen L H, et al., The integrated genomic and epigenomic landscape of brainstem glioma. Nature Communications. 2020. 11. 3077). The study involved the collection of samples from various molecular genotypes, including H3K27M- and TP53-altered gliomas. In further exploration of the specific risks identified from static metabolic snapshots, we assessed the prognostic impact of H3K27M mutation ($p = 0.004$, log-rank test, Fig. R5a, corresponding to Supplementary Fig. 12a in Supplementary Information) and TP53 mutation ($p = 0.554$, log-rank test,

Fig. R5b).

Significantly, the H3K27M mutation demonstrated superior distinguishing ability between high- and low-risk groups compared to the risk scores via static metabolic snapshots ($p = 0.031$, log-rank test, Fig. 3d). Unlike molecular testing on tissue biopsies, risk scores from static metabolic snapshots were derived from serum samples, facilitating treatment monitoring through serial liquid biopsy. Furthermore, metabolic profiling using NPELDI MS technology offers rapid and cost-effective analysis compared to sequencing methodologies. Overall, regular monitoring of metabolic snapshots allows for prompt assessment of the patients' treatment effectiveness and provide valuable support in clinical decision-making processes.

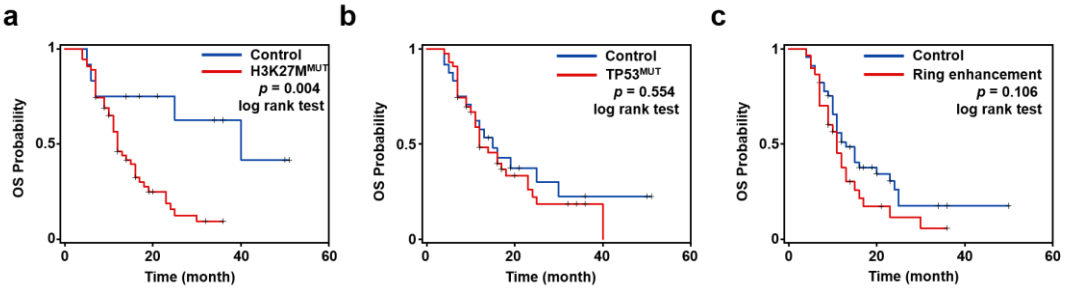

Fig. R5. Prognostic evaluation. Kaplan-Meier curves generated to evaluate the prognostic prediction efficiency of the (a) H3K27M mutation, (b) TP53 mutation, and (c) magnetic resonance imaging (MRI) ring enhancement.

We have added the related results (Supplementary Fig. 12) and discussion in the manuscript as follows.

Revision:

"In this study, we also collected the information of molecular subtypes and MRI imaging, and further explored the prognostic effectiveness of H3K27M mutation ($p = 0.004$, log-rank test, Supplementary Fig. 12a), TP53 mutation ($p = 0.554$, log-rank test, Supplementary Fig. 12b), and ring enhancement ($p = 0.106$, log-rank test, Supplementary Fig. 12c)." (Manuscript, Page 13)

"Significantly, the H3K27M mutation demonstrated superior distinguishing ability between high- and low-risk groups compared to the risk scores via static metabolic

snapshots ($p = 0.031$, log-rank test, Fig. 3d). Unlike molecular testing on tissue biopsies, risk scores from static metabolic snapshots were derived from serum samples, facilitating treatment monitoring through serial liquid biopsy. Furthermore, metabolic profiling using NPELDI MS technology offers rapid and cost-effective analysis compared to sequencing methodologies. Overall, regular monitoring of metabolic snapshots allows for prompt assessment of the patients' treatment effectiveness and provide valuable support in clinical decision-making processes." (Manuscript, Page 17)

Comment 9: *Is there any paired samples data such as patient tumor biopsy samples and patient serum? To verify the findings, authors would perform preclinical animal study using either patient-derived xenograft or genetically engineered mouse models to acquire paired samples (i.e., mice brain tumor and mice serum before and after radiation) with same analysis from discovery set. It is important to know these metabolite change including lactate in high-grade gliomas treatment course in brainstem tumor itself. These animal models experiment will increase scientific rigorously and generalizability for this method.*

Response: We thank the reviewer for the deep concern. We regret that we were unable to collect any paired samples, such as patient tumor biopsy samples and patient serum, due to the limited tissue volume available from pediatric patients. Nevertheless, we performed preclinical animal study using mouse models to acquire paired samples (*i.e.*, mice brain tumor and mice serum before and after radiation) with same analysis from discovery set. We demonstrated consistent metabolite changes, including lactic acid, in high-grade gliomas treatment course in brainstem tumor itself, as in the paired serum samples.

Specially, SPF-grade female BALB/c nude mice, aged 5-6 weeks and weighing 18-20 g, were used as experimental subjects in this study, following refinement of the experimental methods based on previous study (Supplementary Ref. 19: Kim S S, et al., A nanoparticle carrying the p53 gene targets tumors including cancer stem cells, sensitizes glioblastoma to chemotherapy and improves survival. ACS Nano. 2014. 8.

5494). All animal care and experiments were approved (#XHEC-F-2023-031) by the Animal Ethics Committee of Xinhua Hospital, School of Medicine, Shanghai Jiao Tong University.

To establish the subcutaneous tumor model, mice were inoculated with U87MG-luc cells (3.0×10^6 cells/site) suspended in Matrigel, and were injected into the axillary region of the right forelimb. Tumor volume was measured using a vernier caliper, and radiotherapy was initiated once the average tumor size exceeded 100 mm^3. Mice in the radiotherapy group were administered a daily radiation dose of 2 Gy at the tumor site for five consecutive days. Paired serum and brain tumor samples were collected before and five days after radiotherapy, and then subjected to metabolic analysis by NPELDI MS.

The preclinical animal study also indicated significant alterations in metabolite levels before and after radiotherapy treatment in brainstem tumors, aligning with observations in paired serum samples (Fig. R6, corresponding to Supplementary Fig. 14 in Supplementary Information).

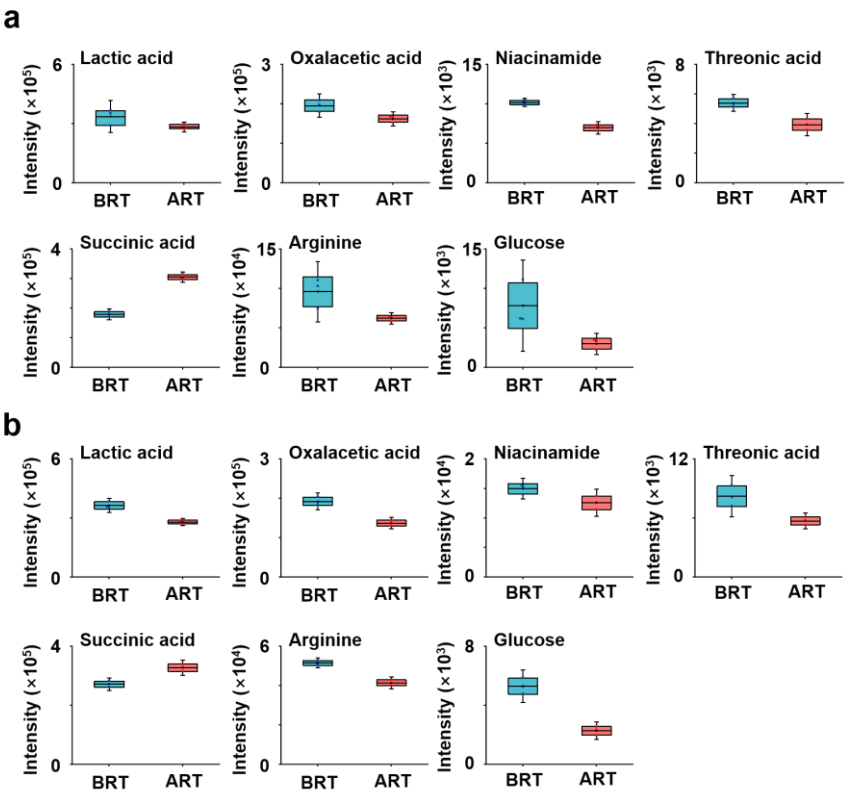

Fig. R6. Metabolic alterations throughout the treatment course of brainstem tumors. Metabolite levels before and after radiotherapy treatment in (a) paired serum samples (n = 3 vs. 3) and (b) BSG

tumors themselves (n = 3 vs. 3) from subcutaneous tumor models. Data are presented as mean ± s.d.

We have added the related results (Supplementary Fig. 14), experimental details, and discussion in the manuscript and Supplementary Information as follows.

Revision:

"We further performed preclinical animal study using mouse tumor models to acquire paired samples (i.e., mice brain tumor and mice serum before and after radiation) with same analysis from discovery set. The preclinical animal study also indicated significant alterations in metabolite levels before and after radiotherapy treatment in BSG, aligning with observations in paired serum samples (Supplementary Fig. 14)." (Manuscript, Page 15)

"**1.7 Cell culture**

U87MG-Luc (a human glioblastoma cell line with luciferase fluorescent labeling) and U251MG (a human glioblastoma cell line) cells were cultured in Dulbecco's Modified Eagle Medium (DMEM, Gibco) supplemented with 10% fetal bovine serum (Corning) and 1% penicillin-streptomycin (Gibco) at 37°C in a 5% CO_2 humidified incubator. Cells in the logarithmic growth phase were selected for subsequent experiments." (Supplementary Information, Page 6)

"**1.9 *In vivo* mouse experiments**

SPF-grade female BALB/c nude mice, aged 5-6 weeks and weighing 18-20 g, were used as experimental subjects in this study, following refinement of the experimental methods based on previous study[19]. All animal care and experiments were approved by the Animal Ethics Committee of Xinhua Hospital, School of Medicine, Shanghai Jiao Tong University (#XHEC-F-2023-031)." (Supplementary Information, Page 8)

"To establish the subcutaneous tumor model, mice were inoculated with U87MG-Luc cells (3.0×10^6 cells/site) suspended in Matrigel, and were injected into the axillary region of the right forelimb. Tumor volume was measured using a vernier caliper, and radiotherapy was initiated once the average tumor size exceeded 100 mm^3. Mice in the

radiotherapy group were administered a daily radiation dose of 2 Gy at the tumor site for five consecutive days. Serum and brain tumor samples were collected before and five days after radiotherapy, and then subjected to metabolic analysis by NPELDI-MS and RNA sequencing, respectively." (Supplementary Information, Page 8)

Comment 10: *In Figure 4c, the ability of BRT metabolic profiles to predict tumor volume changes is intriguing. Elaborating on the biological mechanisms underlying this predictive capability and discussing its clinical significance might add more value.*

Response: We thank the reviewer for the helpful advice. We have added the elaboration on the biological mechanisms underlying the predictive capability of BRT metabolic profiles to predict tumor volume changes and discussing its clinical significance.

The alteration in tumor volume directly reflects the growth and progression of the tumor. Metabolic reprogramming of tumor cells plays a critical role in the initiation, proliferation, and advancement of cancer. The behavior of cancer cells is regulated by both intrinsic cellular metabolism and the availability of metabolites in the tumor microenvironment (Ref. 69: Elia I, et al., Metabolites and the tumour microenvironment: from cellular mechanisms to systemic metabolism. Nature Metabolism. 2021. 3. 21). Therefore, BRT metabolic profiles can serve as indicators of the growth and development status of tumor, enabling the prediction of tumor volume changes, a concept that is further supported by existing literature (Ref. 70&71: Qu N, et al., Integrated proteogenomic and metabolomic characterization of papillary thyroid cancer with different recurrence risks. Nature Communications. 2024. 15. 3175; Chen Y, et al. Metabolomic machine learning predictor for diagnosis and prognosis of gastric cancer. Nature Communications. 2024. 15. 1657).

We have added the related references (Ref. 69-71) and discussion in the manuscript as follows.

Revision:

"The alteration in tumor volume directly reflects the growth and progression of the

tumor. Metabolic reprogramming of tumor cells plays a critical role in the initiation, proliferation, and advancement of cancer. The behavior of cancer cells is regulated by both intrinsic cellular metabolism and the availability of metabolites in the tumor microenvironment[69]. Therefore, BRT metabolic profiles can serve as indicators of the growth and development status of tumor, enabling the prediction of tumor volume changes (Fig. 4c), a concept that is further supported by existing literature[70,71]." (Manuscript, Page 18)

Comment 11: *In the Discussion, consider addressing the potential clinical challenges and practicality of implementing NPELDI-MS for routine BSG diagnosis and monitoring. Are there any technical or logistical hurdles to consider?*

Response: We thank the reviewer for the useful advice. We have addressed potential clinical challenges and practicality of implementing NPELDI-MS for routine BSG diagnosis and monitoring in the Discussion. The technical or logistical hurdles that warrant consideration include the accessibility of mass spectrometers and the simplification of NPELDI-MS workflow in clinical settings.

When implementing NPELDI-MS for routine BSG diagnosis and monitoring, size- and cost-effective mass spectrometers with adequate analytical performance for metabolic profiling are needed in dedicated clinical environments, particularly in remote locations. The exploration of miniaturization within mass spectrometer presents an opportunity for further advancements in this area. Additionally, simplifying the sample collection process, such as utilizing dried blood spots for patient blood samples, could facilitate the transition towards point-of-care testing in laboratory settings.

We added the related discussion in the manuscript as follows.

Revision:

"When implementing NPELDI-MS for routine BSG diagnosis and monitoring, size- and cost-effective mass spectrometers with adequate analytical performance for metabolic profiling are needed in dedicated clinical environments, particularly in

remote locations. The exploration of miniaturization within mass spectrometer presents an opportunity for further advancements in this area. Additionally, simplifying the sample collection process, such as utilizing dried blood spots for patient blood samples, could facilitate the transition towards point-of-care testing in laboratory settings." (Manuscript, Page 20)

Minor revisions

Comment 1: *The manuscript is generally well written with some minor grammatical errors in phrasing some sentences (some examples of corrected sentences in yellow). There are others throughout the paper; please proofread the manuscript again and check using Grammarly or another software.*

1.1. "Nevertheless, imaging modalities afford an accuracy of only 65-73% in BSG detection due to the unsatisfactory image resolution (approximately 1 mm), which could lead to the misdiagnosis of minimal lesions."

1.2. "In particular, tailored inorganic nanoparticles have been introduced as chromatography alternatives prior to MS to selectively enrich metabolites, which makes it better suited for bioanalysis toward biofluid detection. "

Rephrase the "bioanalysis toward biofluid detection&" to improve clarity.

1.3. "We monitored the dynamic disturbances of key metabolites during the course of therapy. "

Response: We thank the reviewer for the valuable feedback. Following the suggestion, we have carefully proofread the manuscript again and utilized Grammarly software for further validation. We have revised all grammatical errors present throughout the paper and ensured comprehensive corrections were made.

Typical revisions in the manuscript have been listed as follows.

Revision:

"Brainstem gliomas (BSG), accounting for 10%-15% of all childhood brain tumors, exhibit a peak incidence of 0.6 cases per million population annually within the

age range of 6-9 years[1-3]." (Manuscript, Page 3)

"Radiotherapy is a standard BSG treatment in the clinical settings, capable of alleviating symptom progression and prolonging progression-free survival by a few months[6-9]. Patients who undergo early and timely surgery exhibit prolonged overall survival (OS) time compared to those in late surgery group (median: 28.4 vs. 18.7 months)[10-12]. Accurate diagnosis, precise prognosis, and timely monitoring during radiotherapy are crucial in managing BSG patients. However, there are certain risks associated with biopsies, which involve sampling tissue for analysis, especially when dealing with tumors located in eloquent regions of the brain." (Manuscript, Page 3)

"Non-invasive radiologic imaging is the "one and only" technique to discover cancerous region before surgical intervention and evaluate tumor prognosis through timely monitoring." (Manuscript, Page 3)

"Nevertheless, imaging modalities afford an accuracy of only 65-73% in BSG detection due to the unsatisfactory image resolution (approximately 1 mm), which could lead to the misdiagnosis of minimal lesions[15,16]." (Manuscript, Page 3)

"Our previous study has validated the function of BBB in separating blood and brain/cerebrospinal fluid (CSF) systems, as well as in regulating the permeability that allows for metabolite transport under disease status[25]." (Manuscript, Page 4)

"Serum metabolite profiles, including static and dynamic metabolic snapshots, may provide an alternative for capturing critical metabolic information about BSG and enable the tracking of tumor dynamics via metabolic endpoints throughout the complete course of a patient's radiotherapy." (Manuscript, Page 4)

"This technique features few pretreatment operation, fast detection speed, and trace sample consumption[28-30], making it ideal for scenarios where expeditious reporting is critical[31-33]. In particular, tailored inorganic nanoparticles have been introduced as chromatography alternatives prior to MS analysis to selectively enrich metabolites, which enhances its applicability for biofluid analysis and biomarker detection." (Manuscript, Page 4)

"In particular, tailored inorganic nanoparticles have been introduced as chromatography alternatives prior to MS analysis to selectively enrich metabolites,

which enhances its applicability for biofluid analysis and biomarker detection." (Manuscript, Page 4)

"We monitored the dynamic disturbances of key metabolites during the course of therapy." (Manuscript, Page 5)

Comment 2: *Rephrase this sentence to improve clarity.*

2.1. "In the context of BSG, metabolism alteration disrupts homeostatic processes from tumor stress in blood, causing bioenergetic perturbation, endocrine disruption, and oxidative stress."

Response: We thank the reviewer for the comment. We have rephrased the sentence to improve clarity as follows.

Revision:

"Metabolic alterations in BSG disrupt normal homeostatic processes due to tumor-related stress in the blood, leading to bioenergetic disturbances, endocrine imbalances, and oxidative stress." (Manuscript, Page 4)

Comment 3: *Do not present "Results&" in the Introduction section.*

3.1. "Based on the static metabolic snapshots, we distinguished BSG patients against healthy donors (HDs) with an area under the curve of 0.923."

3.2. "We further predicted patient survival and stratified them into high-risk and low-risk groups with significant differences in prognostic outcomes ($p < 0.05$). "

Response: We thank the reviewer for the comment. We deleted the related results in the Introduction section.

Revision:

"Based on the static metabolic snapshots, we distinguished BSG patients against healthy donors (HDs) and further predicted patient survival." (Manuscript, Page 4)

Reviewer #2 (Remarks to the Author): expert in computational glioma metabolomics

***Comment**: The study by Li and colleagues shows the potential diagnostic and prognostic value of circulating metabolites in distinguishing BSG patients from healthy donors, as well as predicting patient survival and radiotherapy response. The manuscript is generally well-written and well-structured, making it easy to follow the research methodology and results. Overall, the manuscript is well-structured and presents a valuable contribution to the field; however, the study would benefit from additional experiments to help strengthen the main conclusions.*

Response: We thank the reviewer for his/her time and careful consideration. In response to the feedback provided, we have revised the manuscript to enhance its quality and address the concerns raised. Detailed revisions and responses to each point can be found below.

Major Comments:

***Comment 1:** The authors' analysis suggests that a unique metabolic signature exists in BSG and correlates these data with pathway-based topology analysis. However, it is not clear if the signature arises from systemic metabolic changes or if it is part of the metabolic rewiring of the tumors. To clarify this point, the authors should correlate the metabolic signature in BSG with RNAseq or expression data from patients.*

Response: We thank the reviewer for the valuable suggestion. We are very sorry that we failed to collect any tissue samples such as patient tumor biopsy samples, due to the limited tissue volume obtainable from pediatric patients. However, we performed preclinical animal study using mouse models to acquire the tumor samples. Subsequently, we conducted additional RNAseq experiments on the mouse tumor tissue and correlated the identified metabolic signature in BSG with the RNAseq data. We also validated this correlation through the analysis of public databases (Chinese Glioma

Genome Atlas, (CGGA)). We speculated that the unique metabolic signature arises from the metabolic rewiring of the tumors.

To further investigate the biological mechanisms underlying the differences between BSG and HDs, we performed differential expression analysis using RNAseq data obtained from tumor biopsies of mouse brain tumor tissues (n=5) and adjacent non-cancerous tissue (n=4) (Fig. R7a, corresponding to Supplementary Fig. 9a in Supplementary Information). We also validated the correlation based on the analysis of public CGGA database (Fig. R7b). As a result, we detected notable variances in gene expression within the perturbed metabolic pathways, consistently reflected in the RNAseq expression data obtained in this study, further supported by the results obtained from the CGGA database.

Moreover, our exploration revealed the regulation of specific genes associated with the adaptive reprogramming of tumor cells. Interestingly, genes HIF-1 and HIF-2 upregulated LAT1 protein in GBM cells, whereas HIF-1 bound to the HRE of the BCAT1 gene to induce its gene transcription, leading to reprogramming of leucine, isoleucine, and valine metabolism and impacting GBM cell growth (Ref. 45: Zhang B, et al., Regulation of branched-chain amino acid metabolism by hypoxia-inducible factor in glioblastoma. Cellular and Molecular Life Sciences. 2021. 78. 195). Additionally, genes ASS1 and ASL, encoding the two key enzymatic components of the arginine biosynthetic pathway, are epigenetically regulated in glial brain tumors (Ref. 46: Syed N, et al., Epigenetic status of argininosuccinate synthetase and argininosuccinate lyase modulates autophagy and cell death in glioblastoma. Cell Death & Disease. 2013. 4. e458). Therefore, we speculated that the unique metabolic signature arises from the metabolic rewiring of the tumors.

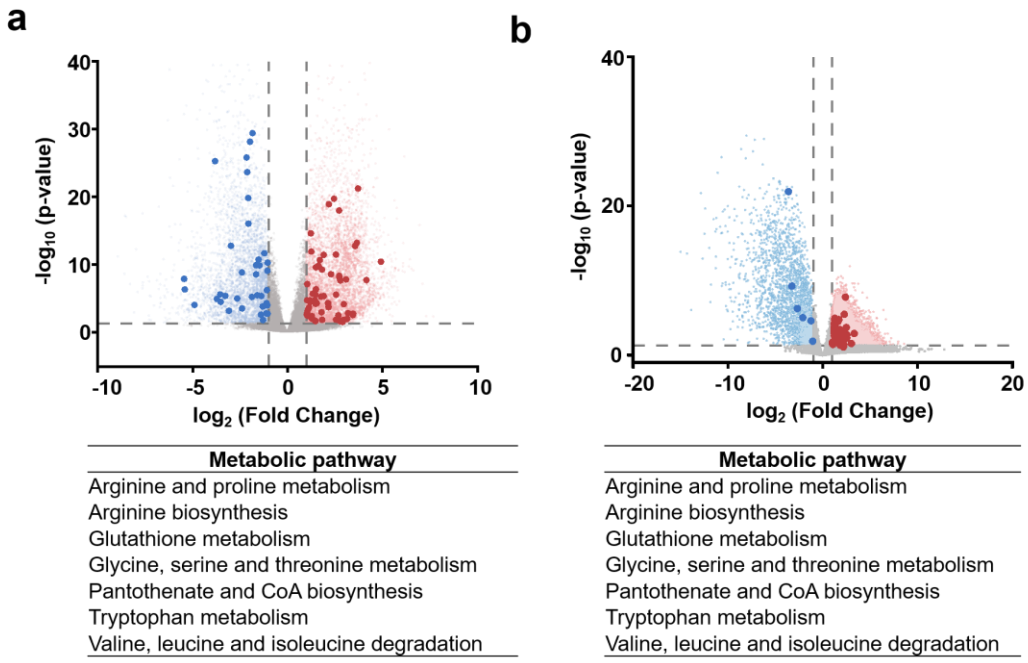

Fig. R7. Significantly differential expression genes revealed through RNAseq data. (a) RNA-seq differential expression analysis using RNAseq data obtained from tumor biopsies of mouse brain tumor tissues and adjacent non-cancerous tissue (n= 5 vs. 4). (b) RNA-seq differential expression analysis based on public Chinese Glioma Genome Atlas database.

We have added the related results (Supplementary Fig. 9), experimental details, references (Ref. 45, 46), and discussion in the manuscript and Supplementary Information as follows.

Revision:

"To further investigate the biological mechanisms underlying the differences between BSG and HDs, we performed differential expression analysis using RNAseq data obtained from tumor biopsies of mouse brain tumor tissues (n=5) and adjacent non-cancerous tissue (n=4, Supplementary Fig. 9a). We also validated the correlation based on the analysis of public Chinese Glioma Genome Atlas (CGGA) database (Supplementary Fig. 9b). As a result, we detected notable variances in gene expression within the perturbed metabolic pathways, which were consistently reflected in the RNAseq expression data obtained in this study and further supported by the results obtained from the CGGA database.

Moreover, our exploration revealed the regulation of specific genes associated

with the adaptive reprogramming of tumor cells. Interestingly, genes HIF-1 and HIF-2 upregulated LAT1 protein in glioblastoma multiforme (GBM) cells, whereas HIF-1 bound to the HRE of the BCAT1 gene to induce its gene transcription, leading to reprogramming of leucine, isoleucine, and valine metabolism and impacting GBM cell growth[45]. Additionally, genes ASS1 and ASL, encoding the two key enzymatic components of the arginine biosynthetic pathway, are epigenetically regulated in glial brain tumors[46]. Therefore, we speculated that the unique metabolic signature arises from the metabolic rewiring of the tumors." (Manuscript, page 10)

"**1.7 Cell culture**

U87MG-Luc (a human glioblastoma cell line with luciferase fluorescent labeling) and U251MG (a human glioblastoma cell line) cells were cultured in Dulbecco's Modified Eagle Medium (DMEM, Gibco) supplemented with 10% fetal bovine serum (Corning) and 1% penicillin-streptomycin (Gibco) at 37°C in a 5% CO_2 humidified incubator. Cells in the logarithmic growth phase were selected for subsequent experiments." (Supplementary Information, Page 6)

"1.9 *In vivo* mouse experiments

SPF-grade female BALB/c nude mice, aged 5-6 weeks and weighing 18-20 g, were used as experimental subjects in this study, following refinement of the experimental methods based on previous study[19]. All animal care and experiments were approved by the Animal Ethics Committee of Xinhua Hospital, School of Medicine, Shanghai Jiao Tong University (#XHEC-F-2023-031).

In the case of the orthotopic tumor model, the inoculation site was the right caudate nucleus of the mouse brain. When anesthetizing mice with isoflurane, a concentration of 1-2% was maintained once the mice are confirmed to have entered the anesthetized state, in order to sustain the anesthetic effect throughout the experiment. The trypsinized U87MG-Luc cells were resuspended in cold phosphate-buffered saline at 1.0×10^5 cells/μL. A 10 μL microsyringe was used to inject 5 μL of the cell suspension into the right hemisphere of the mouse brain (0.5 mm anterior to the bregma, 2 mm lateral to the midline, and 3.5 mm depth from the skull) at a rate of 1 μL/min. Following the injection, the bone hole was sealed with bone wax, and the incision was sutured. The

mice were placed on thermostatic electric blankets and closely monitored until fully resuscitated. Three days post tumor cell injection, tumor implantation and growth were evaluated using the IVIS Lumina Series III *in vivo* imaging system (PerkinElmer, USA). At the humane endpoint, mice were euthanized. Brain tumor tissue and adjacent non-cancerous tissue were collected and subjected to RNA sequencing." (Supplementary Information, Page 8)

"**1.10 RNA sequencing and analyses**

Total RNA was extracted using the TRIzol reagent (Invitrogen, CA, USA) according to the manufacturer's protocol. RNA purity and quantification were evaluated using the NanoDrop 2000 spectrophotometer (Thermo Scientific, USA). RNA integrity was assessed using the Agilent 2100 Bioanalyzer (Agilent Technologies, Santa Clara, CA, USA). Then the libraries were constructed using VAHTS Universal V6 RNA-seq Library Prep Kit.

The libraries were sequenced on an Illumina Novaseq 6000 platform and 150 bp paired-end reads were generated. About 44.01-50.97 M raw reads for each sample were generated. Raw reads of FASTQ format were firstly processed using fastp and the low-quality reads were removed to obtain the clean reads. Then, about 41.39-48.48 M clean reads for each sample were retained for subsequent analyses. The clean reads were mapped to the reference genome using HISAT2. FPKM of each gene was calculated and the read counts of each gene were obtained by HTSeq-count.

Differential expression analysis was performed using the DESeq2. p value < 0.05 and fold change > 2 or fold change < 0.5 was set as the threshold for significantly differential expression gene (DEGs). Based on the hypergeometric distribution, Kyoto Encyclopedia of Genes and Genomes (KEGG) pathway enrichment analysis of DEGs was performed to screen the significant enriched term using R (v 3.2.0)." (Supplementary Information, Page 10)

Comment 2: *A key missing point in the paper is the lack of experimental validation. The metabolic signature or expression signature should be validated in cell lines (e.g., CHLA-07-BSGBM).*

Response: We thank the reviewer for the helpful advice. The CHLA-07-BSGBM cell line, originating from Dr. Anat Erdreich-Epstein's laboratory at Children's Hospital Los Angeles, holds significant value in biomedical research as a unique and proprietary human-derived cell line (Ref. 41: Erdreich-Epstein A, et al., PID1 (NYGGF4), a new growth-inhibitory gene in embryonal brain tumors and gliomas. Clinical Cancer Research. 2014. 20. 827). However, obtaining these cells poses challenges due to the inherent risks associated with their transportation across borders, compliance with customs regulations, and adherence to strict ethical standards. Instead, we performed additional experimental validation of metabolic signature on a different but representative BSG cell line (U251MG).

We conducted functional studies of diagnostic biomarkers to validate the biological function of metabolite biomarkers in human glioblastoma multiforme cell line (U251MG). Reprogrammed metabolic activities such as glycolysis and amino acid metabolism play important roles in cell growth and proliferation in culture or locally aggressive tumors (Ref 38: Faubert B, et al. Metabolic reprogramming and cancer progression. Science. 2020. 368. eaaw5473). We validated the proliferative effect of lactate and ornithine on glioma cells at specific concentrations via cell counting kit-8 assay ($p < 0.05$, Fig. R1a, b, corresponding to Supplementary Fig. 4a, b in Supplementary Information). Moreover, we observed a lactic acid-induced increase in mRNA expression of hypoxia-inducible transcription factor-1-α (HIF1α) and nuclear factor kappa-B (NF-κB) in tumor cells after 12 h and 24 h treatments as determined by quantitative PCR (Fig. R1c, d). This finding confirms that lactic acid is a common byproduct of the glycolytic pathway in the tumor microenvironment (Ref. 42: Baltazar F, et al., Lactate beyond a waste metabolite: metabolic affairs and signaling in malignancy. Frontiers in Oncology. 2020. 10. 231).

To investigate the impact of leucine, valine, and threonine on tumor cells, U251MG cells were deprived of amino acids for 1.5 h and restimulated with leucine, valine, and threonine (1 mM) for another 1 h. Cell lysates were analyzed via immunoblotting for the indicated proteins and phosphorylation states. As a result, the

three amino acids positively regulated the activity of mTOR complex 1 (mTORC1), a key growth regulator in tumor cells (Ref 43: Sivanand S, et al. Emerging roles for branched-chain amino acid metabolism in cancer. Cancer Cell. 2020. 37. 147), as evidenced by the phosphorylation levels of ribosomal protein S6 kinase 1 (pPS6K) (Fig. R1e). This finding highlights the role of these amino acids in modulating critical signaling pathways involved in cancer cell metabolism and growth.

Overall, our results underscore the significant roles of lactate, ornithine, valine, leucine, and threonine in cancer cell proliferation and signaling modulation, emphasizing their potential as distinguishing factors between BSG and healthy individuals.

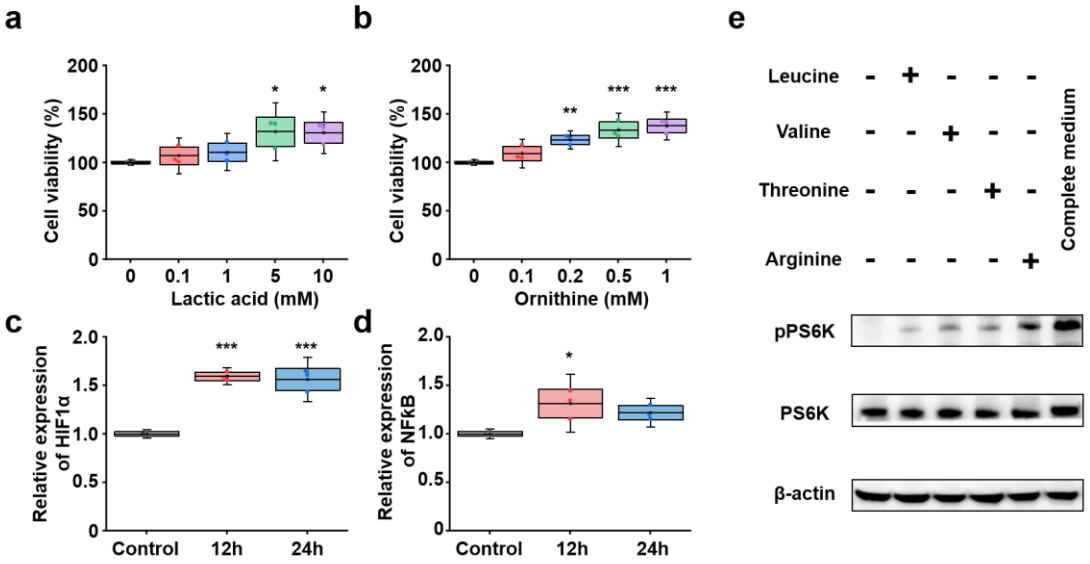

Fig. R1. Biological effects of diagnostic biomarkers on human glioblastoma multiforme (U251MG) cells. Both (a) lactic acid and (b) ornithine promoted the proliferation of tumor cells after 24 h treatment. Lactic acid induced an increase in mRNA expression of (c) HIF1α and (d) NFκB in tumor cells after 12 h and 24 h treatment, determined by quantitative polymerase chain reaction (qPCR). (e) Amino acids including leucine, valine, threonine, and arginine promoted mTOR complex 1 (mTORC1) activity, as determined by the phosphorylation of p70 ribosomal protein S6 kinase (PS6K) through western blot analysis. Cells cultured with complete medium were used as positive control sample. One-way ANOVA was used to perform statistical analyses. * $p < 0.05$, ** $p < 0.01$, *** $p < 0.001$. Experiments were repeated independently 3 times with similar results (a-d).

We have added the cell experimental results (Supplementary Fig. 4), references (Ref. 38, 41-43), and related discussion in the manuscript and Supplementary

Information as follows.

Revision:

"The metabolic signature should be validated in human-derived cell line[41]. We conducted functional studies of these biomarkers to validate the biological function of metabolite biomarkers in human glioblastoma multiforme cell line (U251MG). Reprogrammed metabolic activities such as glycolysis and amino acid metabolism play important roles in cell growth and proliferation in culture or locally aggressive tumors[38]. We validated the proliferative effect of lactic acid and ornithine on U251MG at specific concentrations via cell counting kit-8 assay ($p < 0.05$, Supplementary Fig. 4a, b). Moreover, we observed a lactic acid-induced increase in mRNA expression of hypoxia-inducible transcription factor-1-α (HIF1α) and nuclear factor kappa-B (NFκB) in tumor cells after 12 h and 24 h treatments as determined by quantitative PCR (Supplementary Fig. 4c, d). This finding confirms that lactic acid is a common byproduct of the glycolytic pathway in the tumor microenvironment[42].

To investigate the impact of leucine, valine, and threonine on tumor cells, U251MG cells were deprived of amino acids for 1.5 h and restimulated with leucine, valine, and threonine (1 mM) for another 1 h. Cell lysates were analyzed via immunoblotting for the indicated proteins and phosphorylation states. As a result, the three amino acids positively regulated the activity of mTOR complex 1 (mTORC1), a key growth regulator in tumor cells[43], as evidenced by the phosphorylation levels of ribosomal protein S6 kinase 1 (Supplementary Fig. 4e). This finding highlights the role of these amino acids in modulating critical signaling pathways involved in cancer cell metabolism and growth." (Manuscript, Page 8)

"**1.7 Cell culture**

U87MG-Luc (a human glioblastoma cell line with luciferase fluorescent labeling) and U251MG (a human glioblastoma cell line) cells were cultured in Dulbecco's Modified Eagle Medium (DMEM, Gibco) supplemented with 10% fetal bovine serum (Corning) and 1% penicillin-streptomycin (Gibco) at 37°C in a 5% CO_2 humidified incubator. Cells in the logarithmic growth phase were selected for subsequent

experiments." (Supplementary Information, Page 6)

"**1.8 *In vitro* cell experiments**

Cell proliferation assay: U251MG cells were seeded in 96-well plate at the density of 1×10^4 cells per well and incubated at 37°C for 24 h. Then the cells were treated with lactic acid (0, 0.1, 1, 5, and 10 mM) or ornithine (0, 0.1, 0.2, 0.5, and 1mM) at various concentrations in triplicate for 24 h. The cell viability was determined using an enhanced cell counting kit-8 (CCK8, Beyotime). Specifically, 10 μL of CCK8 solution was added to each well. After 1 h of cell culture, optical density (OD) value at 450 nm was detected via plate reader (BioTek Synergy H1).

Quantitative polymerase chain reaction (qPCR) assay: U251MG cells were seeded in a 12-well plate at the density of 1.5×10^5 cells per well and incubated at 37°C for 24 h. Then the cells were treated with lactic acid (10 mM) in triplicate for 12 h or 24 h. The cells were collected and subjected to RNA extraction by using SimplyP Total RNA Extraction Kit (Bioer Techology). qPCR assay was performed using HiScript III RT SuperMix Kit for qPCR (Vazyme) and ChamQ Universal SYBR qPCR Master Mix Kit (Vazyme) according to manufacturer's instructions.

Western blotting analysis: U251MG cells were seeded in culture dish (6 cm) at the density of 8×10^5 cells per dish and incubated at 37°C for 24 h. To determine the role of amino acids, the cells were starved by amino acid-depleted DMEM for 1.5 h, followed by the addition of individual amino acid (1 mM) for 1 h. Here, cells cultured with full medium for 1 h after amino acid starvation were used as positive control sample. To study the impact of glucose, the cells were treated with glucose-depleted DMEM for 24 h. Then, glucose with different concentrations (25 mM and 50 mM) were supplied for another 24 h. To assess β-nicotinamide mononucleotide (NMN), the cells were treated with NMN (0, 0.5, and 1mM) for 24 h according to literature[17]. Afterwards, the cells were collected for western blot analysis. Typically, cells were lysed in RIPA buffer (Epizyme Biotech) containing protease inhibitor (MCE) and phosphatase inhibitor cocktail (Epizyme Biotech). The concentration of protein was determined by a bicinchoninic acid (BCA) assay (Vazyme). 20 μg of cell lysate protein per sample was subjected to gel electrophoresis (Tanon). The primary antibodies include anti-phospho-

p70 S6 Kinase (Thr389) antibody (CST), anti- p70 S6 Kinase (49D7) Rabbit antibody (CST), anti-PD-L1 antibody (CST), and anti-β-Actin (8H10D10) antibody (CST), while anti-rabbit IgG HRP-linked antibody and anti-mouse IgG HRP-linked Antibody (CST) were used as the secondary antibodies. The blots were imaged by CLINX ChemiScope 6000 system." (Supplementary Information, Page 6)

Comment 3: *Along the same lines, in Fig 3, the authors identify a nine-feature panel correlated with clinical outcomes. However, there is no indication of what the biological role of these metabolites could be. Are they generated because of the rewired metabolism of tumors? Do they correlate with genetic mutations or gene expression signatures?*

Response: We thank the reviewer for the deep comment. We have conducted additional experiments on cell models to elucidate the biological role of the prognostic panel. The panel collectively predict prognosis by jointly affecting the immune escape, signal activation, and metastasis of glioma cells. Furthermore, we performed RNAseq experiments on the mouse tumor tissue before and after radiation of subcutaneous tumor model. We successfully correlated the prognostic panel with the gene expression signatures. Based on the correlation, we inferred that the prognostic panel was generated because of the rewired metabolism of tumors.

We first confirmed the biological significance of the prognostic panel using U251MG cell line. In particular, we have already validated lactic acid in the diagnostic panel. Hence, its presence in the prognostic panel does not warrant further investigation.

Programmed death-ligand 1 (PD-L1) is significantly overexpressed in various tumor types and regulates immune evasion by binding to the inhibitory receptor PD-1 on activated T cells, leading to T cell exhaustion (Ref. 48: Kornepati A, et al., Programmed death ligand 1 signals in cancer cells. Nature Reviews Cancer. 2022. 22. 174). It has been reported that glucose and niacinamide contributed to tumor immune escape via elevating expression of PD-L1 (Ref. 49&50: He H, et al., Aerobic glycolysis promotes tumor immune evasion and tumor cell stemness through the noncanonical

function of hexokinase 2. Cancer Communications. 2023. 43. 387; Lv H, et al., NAD(+) metabolism maintains inducible PD-L1 expression to drive tumor immune evasion. Cell Metabolism. 2021. 33. 110). To assess this impact on human glioblastoma multiforme cell line, U251MG cells were cultured in glucose-depleted dulbecco's modified eagle medium (DMEM) supplemented with varying glucose concentrations (0, 25, and 50 mM) for 24 h. In case of niacinamide, cells were cultured in complete medium with the addition of β-nicotinamide mononucleotide (an analog of niacinamide and a precursor to NAD^+) at selected concentrations (0, 0.5, and 1 mM) for 24 h. As a result, the increase of both glucose and niacinamide analog resulted in the up-regulation of PD-L1 expression in tumor cells (Fig. R2a, corresponding to Supplementary Fig. 10a in Supplementary Information).

We also demonstrated that arginine promoted mTORC1 activation in tumor cells through western blotting analysis, following the same protocol in exploring the biofunctions of amino acids in the diagnostic panel (Fig. R1e, corresponding to Supplementary Fig. 4e in Supplementary Information).

Succinic acid was secreted by tumor to promote metastasis via phosphoinositide 3-kinase (PI3K)-HIF1αaxis (Ref. 51: Wu J Y, et al., Cancer-derived succinate promotes macrophage polarization and cancer metastasis via succinate receptor. Molecular Cell. 2020. 77. 213-227.e5). To verify the effect of succinic acid in human glioblastoma multiforme cell line, we conducted a cell migration experiment and observed a rise in cell migration as the concentration of succinic acid increased from 0-0.1 mM (Fig. R2b). The result supported succinic acid-promoted metastasis of U251MG cells.

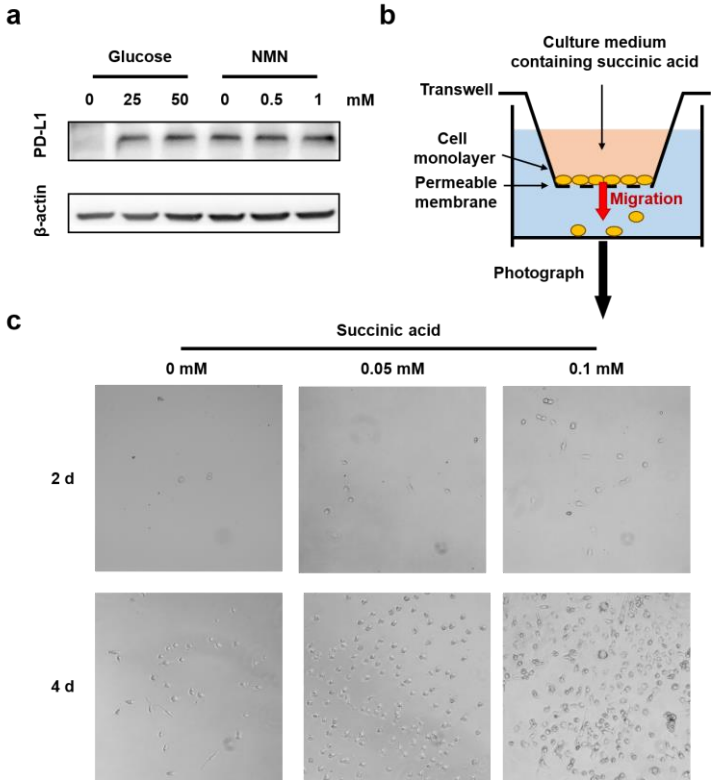

Fig. R2. Biological effects of prognostic biomarkers on human glioblastoma multiforme cells. (a) Both glucose and nicotinamide mononucleotide (NMN) improved the PD-L1 expression in U251MG cells, verified by western blot analysis. (b) U251MG cells in the upper chamber of transwell were treated with succinic acid (0.05 mM and 0.1 mM). (c) At selected time point (2 d and 4 d), migrated U251MG cells in the lower chamber were photographed under an inverted microscope using a 10× objective lens.

The prognostic panel consisted of differentially regulated metabolites together identified 14 potentially altered metabolic pathways (Fig. R8a, corresponding to Supplementary Fig. 11a in Supplementary Information). We thus conducted RNAseq experiments on mouse tumor tissue before and after radiation of subcutaneous tumor models (n= 4 vs. 4). We found five differentially expressed genes (ALDOC, ATP6V0D2, ACY1, AMDHD1, and DDC), associated with the metabolic pathways identified in the prognostic panel and expression data (Fig. R8b). In particular, glycolysis/gluconeogenesis appeared enriched in tumor cells. Tumor growth is characterized by the upregulation of ALDOC, correlated with increased glucose and fructose consumption and lactate production (Ref. 52: De Vitis C, et al., ALDOC- and ENO2- driven glucose metabolism sustains 3D tumor spheroids growth regardless of

nutrient environmental conditions: a multi-omics analysis. Journal of Experimental & Clinical Cancer Research. 2023. 42. 69). Gene ATP6V0D2 plays a role in energy metabolism, which is a highly active cellular pathway in GBM. The maintenance of redox homeostasis is vital for cellular function and survival, with oxidative processes intensified in tumor cells compared to normal cells. Recent studies have highlighted the regulatory impact of oxidative phosphorylation on GBM progression (Ref. 53: Liu P, et al., Unraveling the intricacies of glioblastoma progression and recurrence: insights into the role of NFYB and oxidative phosphorylation at the single-cell level. Frontiers in Immunology. 2024. 15. 1368685). Similarly, amino acid metabolism, a significant hallmark of glioblastoma impacting patient prognosis, has been confirmed through our metabolic and sequencing results and supported by existing literature (Ref. 54: Chinnaiyan P, et al., The metabolomic signature of malignant glioma reflects accelerated anabolic metabolism. Cancer Research. 2012. 72. 5878). Thus, we conclude that the prognostic panel reflects the rewired metabolism of tumors.

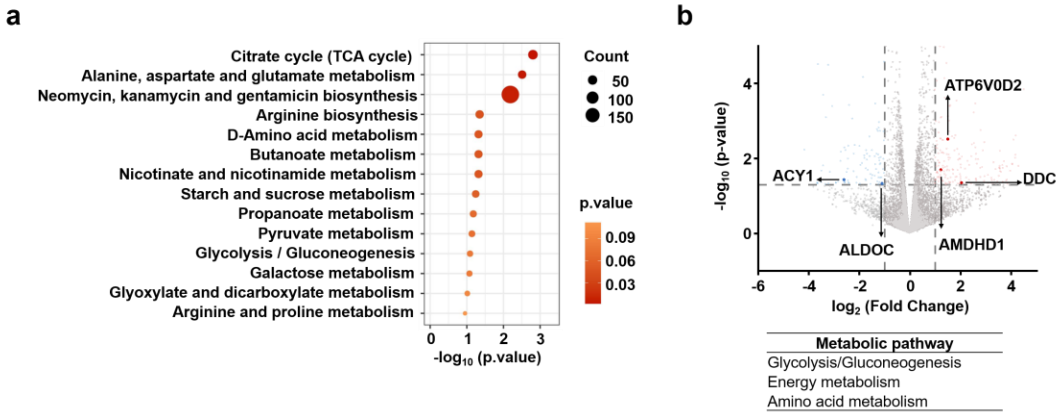

Fig. R8. *In vivo* validation of the prognostic panel. (a) Metabolite set enrichment analysis of metabolite biomarkers from the prognostic panel using Kyoto Encyclopedia of Genes and Genomes (KEGG) dataset. (b) RNA-seq differential expression analysis using RNAseq data obtained from mouse tumor tissue before and after radiation of subcutaneous tumor models (n= 4 vs. 4).

We have added the cell experimental results (Supplementary Fig. 4, 10, and 11), references (Ref. 48-54), and related discussion in the manuscript and Supplementary Information as follows.

Revision:

"We confirmed the biological significance of the prognostic panel using U251MG cell line. In particular, we have already validated lactic acid in the diagnostic panel. Hence, its presence in the prognostic panel does not warrant further investigation.

Programmed death-ligand 1 (PD-L1) is significantly overexpressed in various tumor types and regulates immune evasion by binding to the inhibitory receptor PD-1 on activated T cells, leading to T cell exhaustion[48]. It has been reported that glucose and niacinamide contributed to tumor immune escape via elevating expression of PD-L1[49,50]. To assess this impact on human glioblastoma multiforme cell line, U251MG cells were cultured in glucose-depleted dulbecco's modified eagle medium (DMEM) supplemented with varying glucose concentrations (0, 25, and 50 mM) for 24 h. In case of niacinamide, cells were cultured in complete medium with the addition of β-nicotinamide mononucleotide (an analog of niacinamide and a precursor to NAD^+) at selected concentrations (0, 0.5, and 1 mM) for 24 h. As a result, the increase of both glucose and niacinamide analog resulted in the up-regulation of PD-L1 expression in tumor cells (Supplementary Fig. 10a).

We also demonstrated that arginine promoted mTORC1 activation in tumor cells through western blotting analysis, following the same protocol in exploring the biofunctions of amino acids in the diagnostic panel (Supplementary Fig. 4e).

Succinic acid was secreted by tumor to promote metastasis via phosphoinositide 3-kinase-HIF1α axis[51]. To verify the effect of succinic acid in human glioblastoma multiforme cell line, we conducted a cell migration experiment and observed a rise in cell migration as the concentration of succinic acid increased from 0-0.1 mM (Supplementary Fig. 10b, c). The result supported succinic acid-promoted metastasis of U251MG cells.

The prognostic panel consisted of differentially regulated metabolites together identified 14 potentially altered metabolic pathways (Supplementary Fig. 11a). We thus conducted RNAseq experiments on mouse tumor tissue before and after radiation of subcutaneous tumor models (n= 4 vs. 4). We found five differentially expressed genes (ALDOC, ATP6V0D2, ACY1, AMDHD1, and DDC), associated with the metabolic

pathways identified in the prognostic panel and expression data (Supplementary Fig. 11b). In particular, glycolysis/gluconeogenesis appeared enriched in tumor cells. Tumor growth is characterized by the upregulation of ALDOC, correlated with increased glucose and fructose consumption and lactate production[52]. Gene ATP6V0D2 plays a role in energy metabolism, which is a highly active cellular pathway in GBM. The maintenance of redox homeostasis is vital for cellular function and survival, with oxidative processes intensified in tumor cells compared to normal cells. Recent studies have highlighted the regulatory impact of oxidative phosphorylation on GBM progression[53]. Similarly, amino acid metabolism, a significant hallmark of glioblastoma impacting patient prognosis, has been confirmed through our metabolic and sequencing results and supported by existing literature[54]. Thus, we conclude that the prognostic panel reflects the rewired metabolism of tumors." (Manuscript, Page 11)

"**1.7 Cell culture**

U87MG-Luc (a human glioblastoma cell line with luciferase fluorescent labeling) and U251MG (a human glioblastoma cell line) cells were cultured in Dulbecco's Modified Eagle Medium (DMEM, Gibco) supplemented with 10% fetal bovine serum (Corning) and 1% penicillin-streptomycin (Gibco) at 37°C in a 5% CO_2 humidified incubator. Cells in the logarithmic growth phase were selected for subsequent experiments.

1.8 *In vitro* cell experiments

Cell proliferation assay: U251MG cells were seeded in 96-well plate at the density of 1×10^4 cells per well and incubated at 37°C for 24 h. Then the cells were treated with lactic acid (0, 0.1, 1, 5, and 10 mM) or ornithine (0, 0.1, 0.2, 0.5, and 1mM) at various concentrations in triplicate for 24 h. The cell viability was determined using an enhanced cell counting kit-8 (CCK8, Beyotime). Specifically, 10 μL of CCK8 solution was added to each well. After 1 h of cell culture, optical density (OD) value at 450 nm was detected via plate reader (BioTek Synergy H1).

Quantitative polymerase chain reaction (qPCR) assay: U251MG cells were seeded in a 12-well plate at the density of 1.5×10^5 cells per well and incubated at 37°C for 24 h. Then the cells were treated with lactic acid (10 mM) in triplicate for 12 h or

24 h. The cells were collected and subjected to RNA extraction by using SimplyP Total RNA Extraction Kit (Bioer Techology). qPCR assay was performed using HiScript III RT SuperMix Kit for qPCR (Vazyme) and ChamQ Universal SYBR qPCR Master Mix Kit (Vazyme) according to manufacturer's instructions.

Western blotting analysis: U251MG cells were seeded in culture dish (6 cm) at the density of 8×10^5 cells per dish and incubated at 37°C for 24 h. To determine the role of amino acids, the cells were starved by amino acid-depleted DMEM for 1.5 h, followed by the addition of individual amino acid (1 mM) for 1 h. Here, cells cultured with full medium for 1 h after amino acid starvation were used as positive control sample. To study the impact of glucose, the cells were treated with glucose-depleted DMEM for 24 h. Then, glucose with different concentrations (25 mM and 50 mM) were supplied for another 24 h. To assess β-nicotinamide mononucleotide (NMN), the cells were treated with NMN (0, 0.5, and 1mM) for 24 h according to literature[17]. Afterwards, the cells were collected for western blot analysis. Typically, cells were lysed in RIPA buffer (Epizyme Biotech) containing protease inhibitor (MCE) and phosphatase inhibitor cocktail (Epizyme Biotech). The concentration of protein was determined by a bicinchoninic acid (BCA) assay (Vazyme). 20 μg of cell lysate protein per sample was subjected to gel electrophoresis (Tanon). The primary antibodies include anti-phospho-p70 S6 Kinase (Thr389) antibody (CST), anti- p70 S6 Kinase (49D7) Rabbit antibody (CST), anti-PD-L1 antibody (CST), and anti-β-Actin (8H10D10) antibody (CST), while anti-rabbit IgG HRP-linked antibody and anti-mouse IgG HRP-linked Antibody (CST) were used as the secondary antibodies. The blots were imaged by CLINX ChemiScope 6000 system.

Cell migration: U251MG cells were seeded on the upper chamber of a 24-well transwell plate at the density of 2×10^4 cells per well and treated with succinic acid of different concentrations (0.05 mM and 1 mM) according to literature[18]. After 2 d or 4 d simulation, cells migrated to the lower chamber and were photographed under an inverted microscope using a 10× objective lens.

1.9 *In vivo* mouse experiments

SPF-grade female BALB/c nude mice, aged 5-6 weeks and weighing 18-20 g,

were used as experimental subjects in this study, following refinement of the experimental methods based on previous study[19]. All animal care and experiments were approved by the Animal Ethics Committee of Xinhua Hospital, School of Medicine, Shanghai Jiao Tong University (#XHEC-F-2023-031).

In the case of the orthotopic tumor model, the inoculation site was the right caudate nucleus of the mouse brain. When anesthetizing mice with isoflurane, a concentration of 1-2% was maintained once the mice are confirmed to have entered the anesthetized state, in order to sustain the anesthetic effect throughout the experiment. The trypsinized U87MG-Luc cells were resuspended in cold phosphate-buffered saline at 1.0×10^5 cells/μL. A 10 μL microsyringe was used to inject 5 μL of the cell suspension into the right hemisphere of the mouse brain (0.5 mm anterior to the bregma, 2 mm lateral to the midline, and 3.5 mm depth from the skull) at a rate of 1 μL/min. Following the injection, the bone hole was sealed with bone wax, and the incision was sutured. The mice were placed on thermostatic electric blankets and closely monitored until fully resuscitated. Three days post tumor cell injection, tumor implantation and growth were evaluated using the IVIS Lumina Series III *in vivo* imaging system (PerkinElmer, USA). At the humane endpoint, mice were euthanized. Brain tumor tissue and adjacent non-cancerous tissue were collected and subjected to RNA sequencing.

To establish the subcutaneous tumor model, mice were inoculated with U87MG-Luc cells (3.0×10^6 cells/site) suspended in Matrigel, and were injected into the axillary region of the right forelimb. Tumor volume was measured using a vernier caliper, and radiotherapy was initiated once the average tumor size exceeded 100 mm^3. Mice in the radiotherapy group were administered a daily radiation dose of 2 Gy at the tumor site for five consecutive days. Serum and brain tumor samples were collected before and five days after radiotherapy, and then subjected to metabolic analysis by NPELDI-MS and RNA sequencing, respectively.

1.10 RNA sequencing and analyses

Total RNA was extracted using the TRIzol reagent (Invitrogen, CA, USA) according to the manufacturer's protocol. RNA purity and quantification were evaluated using the NanoDrop 2000 spectrophotometer (Thermo Scientific, USA). RNA integrity

was assessed using the Agilent 2100 Bioanalyzer (Agilent Technologies, Santa Clara, CA, USA). Then the libraries were constructed using VAHTS Universal V6 RNA-seq Library Prep Kit.

The libraries were sequenced on an Illumina Novaseq 6000 platform and 150 bp paired-end reads were generated. About 44.01-50.97 M raw reads for each sample were generated. Raw reads of FASTQ format were firstly processed using fastp and the low-quality reads were removed to obtain the clean reads. Then, about 41.39-48.48 M clean reads for each sample were retained for subsequent analyses. The clean reads were mapped to the reference genome using HISAT2. FPKM of each gene was calculated and the read counts of each gene were obtained by HTSeq-count.

Differential expression analysis was performed using the DESeq2. p value < 0.05 and fold change > 2 or fold change < 0.5 was set as the threshold for significantly differential expression gene (DEGs). Based on the hypergeometric distribution, Kyoto Encyclopedia of Genes and Genomes (KEGG) pathway enrichment analysis of DEGs was performed to screen the significant enriched term using R (v 3.2.0)." (Supplementary Information, Page 6)

Minor Comment:

Comment 1: *Elaborate on the clinical implications of the findings, discussing how this research could impact patient care, treatment strategies, and potential future studies*

Response: We thank the reviewer for the insightful comment. We have included an expanded discussion on the clinical implications of the findings.

The use of serum samples as a less invasive alternative to traditional pathological molecular testing offers promising implications for the diagnosis and prognosis of tumors, particularly in challenging-to-biopsy brain tumors such as BSG. The non-invasive nature of serum metabolic testing yields benefit such as reduced patient anxiety, fewer postoperative complications, and decreased physical and mental burdens, fostering a positive doctor-patient relationship. Regular monitoring of metabolite levels enables a timely assessment of the patient's condition and treatment efficacy. This

approach allows for personalized treatment adjustments and the development of individualized dietary plans, leading to improved patient care and outcomes.

We have added the related discussion in the manuscript as follows.

Revision:

"The use of serum samples as a less invasive alternative to traditional pathological molecular testing offers promising implications for the diagnosis and prognosis of tumors, particularly in challenging-to-biopsy brain tumors such as BSG. The non-invasive nature of serum metabolic testing yields benefits such as reduced patient anxiety, fewer postoperative complications, and decreased physical and mental burdens, fostering a positive doctor-patient relationship. Regular monitoring of metabolite levels enables a timely assessment of the patient's condition and treatment efficacy. This approach allows for personalized treatment adjustments and the development of individualized dietary plans, leading to improved patient care and outcomes." (Manuscript, Page 18)

Reviewer #3 (Remarks to the Author): technical expertise in mass spectrometry methods

Comment: *Li et al., apply a MALDI-based metabolomics platform to identify serum metabolites in pediatric brainstem gliomas that could be used for diagnosis and determination of patient responses to therapy. They find metabolites that could distinguish brainstem glioma from healthy controls and predict outcomes. Additionally, using longitudinally-collected samples they identify metabolites, including lactic acid, associated with response to radiotherapy.*

Brainstem gliomas represent a significant portion of CNS tumors that arise in pediatric populations and we have limited knowledge of the molecular underpinnings of this tumor type. This limits therapeutic development for these cancers. As such, studies that identify metabolic alterations associated with this tumor type are important for expanding our understanding of how these tumors develop. In this referee’s opinion, a strength of the study is the development of a patient cohort that is followed longitudinally with serial sampling of serum. Additionally, the use of their nanoparticle-based MS platform (NPELDI MS) had the potential to scale to larger patient populations. However, there are several there are key experiments missing as well as broader details on their MS platform that make it difficult to substantiate their claims.

Response: We thank the reviewer for his/her time and careful consideration. We have performed additional key experiments following the reviewer's valuable suggestions and comments. We also provided broader details on the MS platform to substantiate our claims. Detailed point-by-point responses and revisions can be found below.

Comment 1: *There are major details/data lacking for their NPELDI-MS platform. In total they detected 402 metabolic features with 287 metabolic features changed from BSG and healthy controls. This language is confusing. Typically features refers to MS peaks that haven't been identified. Did they identify 402 metabolites from their method?*

It appears that metabolite identification was determined by mass. How were these IDs verified? Were authentic standards used? If so they should show their data (MS/MS, match to standards). Additionally, the level of metabolite IDs should be stated according to the Metabolomics Standards Initiative (PMID: 24039616). The number of predictor metabolites is low, for example only seven metabolites were used to determine BSG diagnosis. This makes it essential that IDs are correct.

Response: We thank the reviewer for the careful comment. We apologize for the confusing language used in the original manuscript. We have carefully revised the language to address any potential confusion, both in the main text and in Fig. R9c-f (corresponding to Fig. 2c-f in manuscript).

To clarify, we did not identify 402 metabolites from the MS method. After quality control and data filtering, we obtained 402 metabolic features (defined as the localized highest intensity of the raw MS data) across different samples. It should be noted that the metabolic features here refer to MS peaks that haven't been identified.

Verification of the metabolite identities was conducted by comparing the exact mass in serum to the obtained mass of standard molecules, acquired by high resolution MALDI-Fourier transform ion cyclotron resonance (FTICR) mass spectrometry (Table R1&2, corresponding to Supplementary Table 5&7). The elemental composition of MS peak was determined by the exact accurate mass at an m/z tolerance of 10 ppm.

Authentic standards were used in this study. Following the guidelines of the Metabolomics Standards Initiative (Supplementary Ref. 12: Sumner L W, et al., Proposed minimum reporting standards for chemical analysis Chemical Analysis Working Group (CAWG) Metabolomics Standards Initiative (MSI). Metabolomics. 2007. 3. 211), the level of metabolite IDs should be stated as Level 1 (Annotated compounds: accurate mass confirmation and real-case serum sample validation relative to an authentic compound analyzed under identical experimental conditions). This level of identification covered all identified metabolite biomarkers except for 2-AAS, oxalacetic acid, and threonic acid, which we failed to obtain the chemical standards.

We have included the related results (Fig. 2c-f, Supplementary Table 5&7),

references (Supplementary Ref. 12), and experimental details in manuscript as follows.

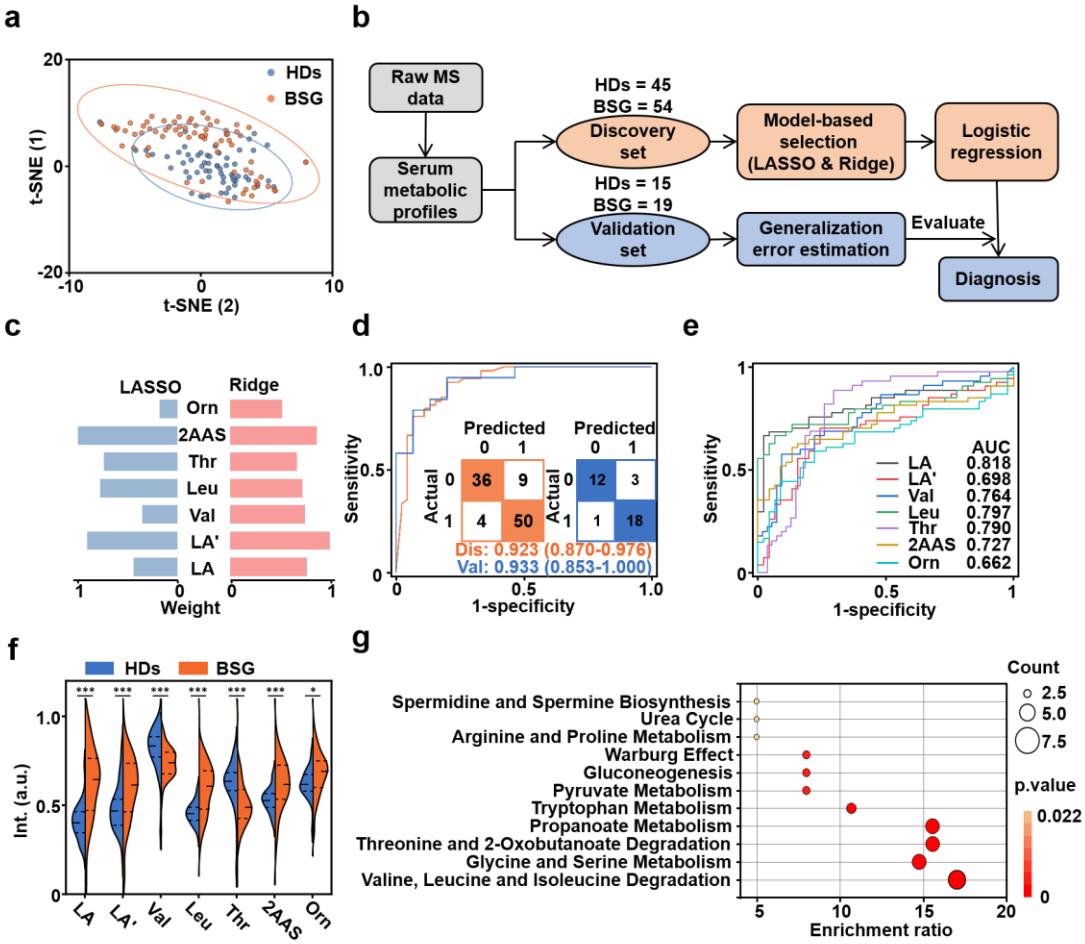

Fig. R9. Diagnostic value of circulating metabolites in BSG patients. (a) t-distributed stochastic neighbor embedding of serum metabolic profiles for 60 HDs and 73 BSG patients was plotted using 402 m/z features after data processing. (b) Study design for BSG diagnosis using machine learning. Static metabolic snapshots from 99 participants (45/54, HDs/BSG) in the discovery set for feature selection and model building. The optimized model was tested in an independent validation set (15/19, HDs/BSG). (c) Coefficients of the least absolute shrinkage and selection operator (LASSO) and Ridge algorithms were shown as the evaluation index for six metabolic biomarkers. (d) Receiver operating characteristic (ROC) curves of the discovery set and validation set to distinguish HDs and BSG patients within the metabolic panel. The corresponding confusion matrices were shown as the inset. (e) ROC curves analysis was shown with each single feature (AUC of 0.662-0.818). (f) Violin-plot illustrated the differential regulation of normalized intensities for metabolic biomarkers in HDs and BSG. (g) Potential pathways were differentially regulated in HDs and BSG patients. Color and size of each circle were correlated to the p value and enrichment ratio. *** represented $p < 0.005$, * represented $p < 0.05$. LA and LA': lactic acid; Val: valine; Leu: leucine; Thr: threonine; 2AAS: 2-Aminomuconic acid semialdehyde; Orn: ornithine.

Table R1. Metabolic panel for BSG diagnosis.

Compound name	HMDB ID	Measured m/z in serum [a)]	Measured m/z in standards [a)]	Theoretical m/z	ppm [b)]	AUC (95% CI)
Lactic acid	HMDB0000190	135.0027	135.0024	135.0029	2	0.818 (0.730-0.906)
		150.9766	150.9764	150.9768	1	0.698 (0.592-0.804)
Valine	HMDB0000883	162.0502	162.0496	162.0501	4	0.764 (0.667-0.860)
Leucine	HMDB0000687	170.0571	170.0571	170.0578	0	0.797 (0.705-0.889)
Threonine	HMDB0000167	180.0037	180.0028	180.0033	5	0.790 (0.696-0.884)
2-Aminomuconic acid semialdehyde	HMDB0001280	186.0148	/	186.0138	5[c)]	0.727 (0.624-0.829)
Ornithine	HMDB0000214	193.0350	193.0345	193.035	3	0.662 (0.552-0.771)

[a)] The m/z values were measured by high resolution MALDI-Fourier transform ion cyclotron resonance (FTICR) mass spectrometry.

[b)] ppm values were calculated by comparing the measured m/z in serum with that of the corresponding chemical standards.

[c)] For 2-AAS, ppm values were calculated by comparing the measured m/z in serum with that of the theoretical mass of adducts.

Table R2. Metabolic panel for BSG prognosis.

Compound name	HMDB ID	Measured m/z in serum[a)]	Measured m/z in standards[a)]	Theoretical m/z	ppm[b)]	$\text{Weight}_{\text{feature}}$
Lactic acid	HMDB0000190	113.0207	113.0206	113.0209	1	0.001501
Oxalacetic acid	HMDB0000223	115.0028	/	115.0032	3[c)]	-0.00357
Niacinamide	HMDB0001406	123.0557	123.0550	123.0553	6	-0.00343
Threonic acid	HMDB0000943	137.0455	/	137.0444	8[c)]	0.003158
Succinic acid	HMDB0000254	156.9889	156.9894	156.9898	3	-0.00048
Arginine	HMDB0000517	197.1009	197.1005	197.1009	2	-0.00131
Glucose	HMDB0000122	219.0268	219.0265	219.0265	1	0.007082
Formula			$\boldsymbol{Score = \sum \text{Weight}_{\text{featuer}} \times \text{Intensity}_{\text{feature}}}$			

[a)] The m/z values were measured by high resolution MALDI-FTICR mass spectrometry.

[b)] ppm values were calculated by comparing the measured m/z in serum with that of the corresponding chemical standards.

[c)] For oxalacetic acid and threonic acid, ppm values were calculated by comparing the measured m/z in serum with that of the theoretical mass of adducts.

Revision:

"After quality control and data filtering (see details in Supporting Information), we obtained 402 metabolic features (defined as the localized highest intensity of the raw MS data) across different samples (Supplementary Fig. 1c)." (Manuscript, Page 6)

"**1.5 Metabolite identification**

Verification of the metabolite identities was conducted by comparing the exact mass in serum to the obtained mass of standard molecules, acquired by high resolution MALDI-Fourier transform ion cyclotron resonance (FTICR) mass spectrometry (Supplementary Table 5 & 7). The elemental composition of MS peak was determined by the exact accurate mass at an m/z tolerance of 10 ppm.

Authentic standards were used in this study. Following the guidelines of the Metabolomics Standards Initiative[12], the level of metabolite IDs should be stated as Level 1 (Annotated compounds: accurate mass confirmation and real-case serum sample validation relative to an authentic compound analyzed under identical experimental conditions). This level of identification covered all identified metabolite biomarkers except for 2-AAS, oxalacetic acid, and threonic acid, which we failed to obtain the chemical standard. For 2-AAS, oxalacetic acid, and threonic acid, theoretical mass of adducts was compared at an m/z tolerance of 10 ppm." (Supplementary Information, Page 5)

Comment 2: *While this referee appreciates that this study is performed on pediatric patients, making recruitment challenging. The low number of patients that were used for this study is problematic, especially for validation of biomarkers. A clear strength of their NPELDI-MS platform would be sample throughput, yet the authors don't take advantage of that. Instead evaluating 73 patients (40 patients for longitudinal sampling). These low numbers are likely to make translation of the biomarkers to larger patient populations difficult. Are there historical samples that the authors could use for validation?*

Response: We thank the reviewer for the valuable suggestion. We tried our best to increase the sample size from 244 to 405, and updated the study design of participant enrollment and longitudinal sample collection in Fig. R10a-b (corresponding to Fig. 1a-b in manuscript). We constructed an external set based on the increased samples for further validation of biomarkers.

Importantly, we recruited a new cohort (Table R3, corresponding to Supplementary Table 2 in Supplementary Information) from Shanghai Xinhua Hospital, with an independent set of 161 samples (96/65, brainstem gliomas (BSG)/healthy donors (HDs)) as the external set. Notably, the external set was independent from the discovery and validation subjects in model construction stage and blinding to the as-built model (Fig. R11a, corresponding to Supplementary Fig. 6a in Supplementary Information). The situations for blood drawn were the same for all sample sets

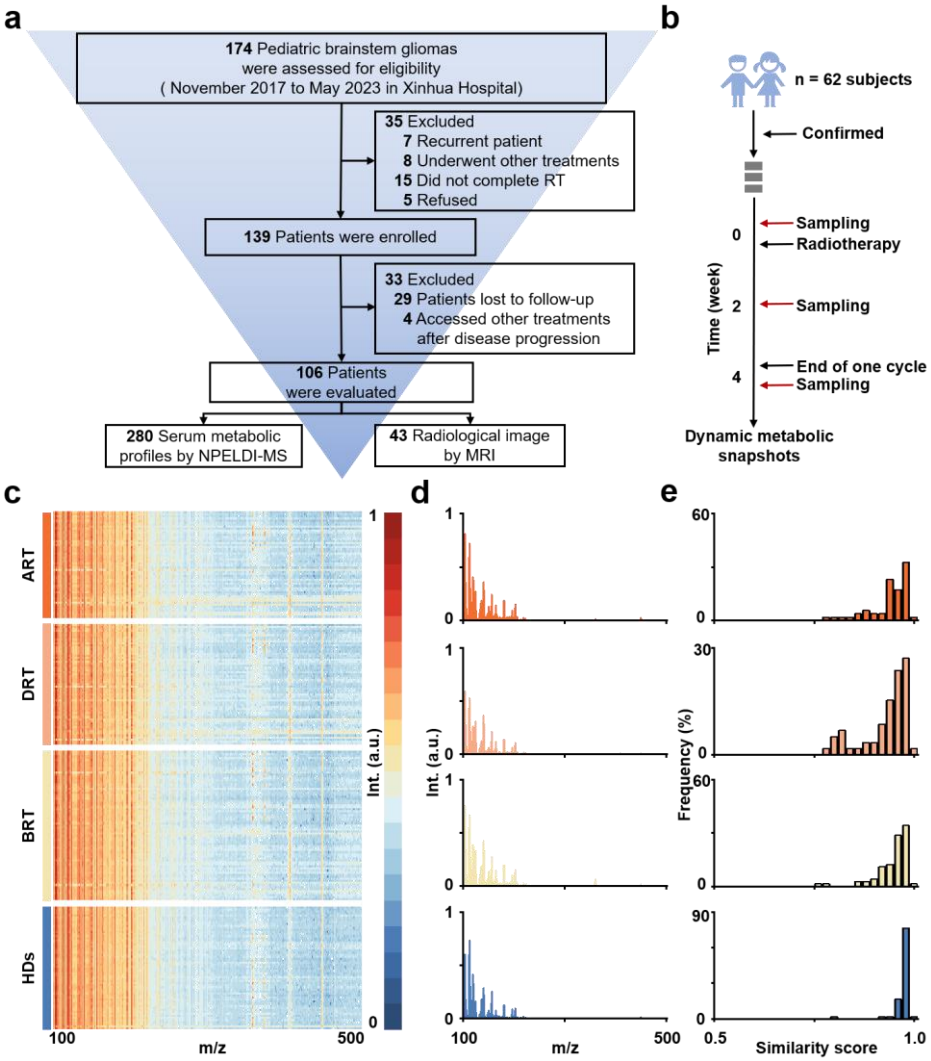

Fig. R10. Study design and patient cohort characteristics. (a) Study design of participant enrollment, including 125 HDs and 106 BSG patients. (b) Longitudinal sample collection of 62 BSG patients at three time points as the dynamic metabolic snapshots. (c) Heatmap of serum metabolic profiles from 60 HDs and 184 BSG patients, including 73 serum samples collected before radiotherapy (BRT), 59 samples collected during radiotherapy (DRT), and 52 samples collected after radiotherapy (ART), using 402 m/z features through data processing. The color scale was processed by normalized correction. (d) Typical mass spectra of serum metabolic profiles among four groups. (e) Frequency distribution of similarity scores was calculated for HDs, BRT, DRT, and ART, regarding serum metabolic profiles within the same group.

.

Table R3. Clinical characteristics of newly recruited 161 samples for external set.

Characteristics		HDs (n=65)	BSG		
			BRT (n=33)	DRT (n = 28)	ART (n =35)
Gender (female/male)		30/35	20/13	15/13	21/14
Age (years)		7.78 (1-13)	7.21 (2-14)	7 (2-14)	6.68 (2-14)
Height (cm)		-	123.74 (90-173)	-	-
Weight (kg)		-	27.12 (11-70)	-	-
BMI (kg m^{-2})		-	16.89 (12.43-24.79)	-	-
Lansky score		-	62.73 (30-80)	-	-
CNS WHO grade	1	-	2	-	-
	4	-	25	-	-
	NOS	-	6	-	-
Tumor size (mL)	Unknown	-	0	-	-
	Mean ± SD (range)	-	52.71 ± 24.71 (14.8-131.1)	-	-
Enhancement	Ring enhancement	-	17	-	-

	Non-enhancement	-	16	-	-
Gene mutation	Unknown	-	6	-	-
	$H3K27M^{WT}$ /$H3K27M^{MUT}$	-	3/24	-	-
	$TP53^{WT}$ /$TP53^{MUT}$	-	10/17	-	-

We obtained the area under the curve (AUC) of 0.847-0.852 (Fig. R11b), consistent with the previous results in the methodology development. The consistent diagnostic results validated the robustness of the biomarkers, facilitating translation of the biomarkers to larger patient populations.

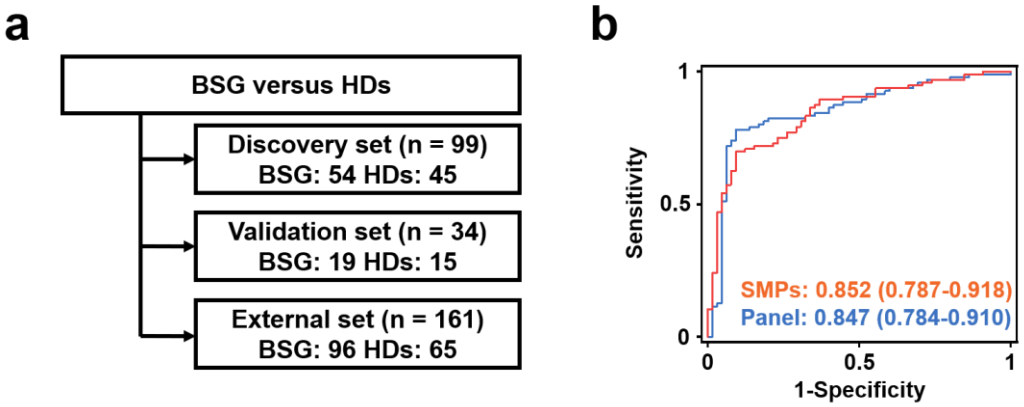

Fig. R11. Performance of BSGs versus HDs. (a) Study design for classifying BSG versus HDs. (b) Receiver operating characteristic (ROC) curves for 96 BSG versus 65 HDs in external set via serum metabolic profiles and the diagnostic panel.

We have added the related results (Fig. 1, Supplementary Fig. 6, and Supplementary Table 2), experimental details, and discussion in the manuscript and Supplementary Information as follows.

Revision:

"Here, we for the first time construct diagnostic and prognostic assays of BSG via circulating metabolites based on both cross-sectional study and longitudinal cohort study with 106 BSG patients." (Manuscript, Page 2)

"Demographic and clinical characteristics of the enrolled participants are presented in Supplementary Table 1 and Supplementary Table 2." (Manuscript, Page 5)

"As a result, detection process of 405 serum samples in this project was completed within ~3 hours." (Manuscript, Page 6)

"We recruited a new cohort (Supplementary Table 2) from Shanghai Xinhua Hospital, with 161 samples collected (96/65, BSG/HDs) as the external set. Notably, the external set was independent from the discovery and validation sets in model

construction stage and blinding to the as-built model (Supplementary Fig. 6a). The situations for blood drawn were the same for all sample sets. We obtained the AUC of 0.847-0.852 (Supplementary Fig. 6a), consistent with the previous results in the methodology development. The consistent diagnostic results validated the robustness of the biomarkers, facilitating translation of the biomarkers to larger patient populations." (Manuscript, Page 9)

"We designed a cross-sectional study for BSG diagnosis and prognosis, as well as a longitudinal study to monitor responses to radiotherapy. We first collected 244 serum samples from 60 HDs and 73 BSG patients (HDs/BRT/DRT/ART = 60/73/59/52, Supplementary Table 1), as the discovery and validation cohort. Following the same process, we newly collected 161 serum samples, including 65 HDs, 33 BRT, 28 DRT, and 35 ART (Supplementary Table 2), as the external cohort." (Supplementary Information, Page 2)

Comment 3: *The small number of serum metabolites that are used as predictors is problematic. Performing pathway analysis on such a small set is not meaningful especially since metabolites often participate in multiple pathways. For example, ornithine participates in proline metabolism, urea cycle, and polyamine metabolism. With the single ID of ornithine, pathway assignment is not possible. Looking at the metabolite predictors, the majority of significant metabolites are amino acids. This might be due to diet (or illness impacting eating) rather than glioma. Information should be given for medication and diet if possible. I also recommend authors search for other public datasets that might correlate biological responses to their small number of metabolite changes (other cancers perhaps).*

Response: We thank the reviewer for the deep concern. We have performed additional experiments and literature research to address the concerns raised. Most importantly, we have substantiated the biological relevance of the serum metabolites through complementary **(1)** in vivo cell experiments and **(2)** in vitro sequencing analyses. **(3)** While we regret the unavailability of medication and diet information for all samples

in our historical dataset spanning from 2017 to 2023, strict enrollment criteria were implemented during sample collection to mitigate potential influences from external factors, such as medication and diet. **(4)** We acknowledge the complexity associated with pathway analysis on a limited set of metabolites, particularly when metabolites participate in multiple pathways. Thus, we provided the mechanism details in enrichment analysis to validate our pathway assignments. **(5)** Lastly, we have searched for other public datasets that might correlate biological responses to their small number of metabolite changes.

(1) We conducted functional studies of diagnostic biomarkers to validate the biological function of metabolite biomarkers in human glioblastoma multiforme cell line (U251MG). Reprogrammed metabolic activities such as glycolysis and amino acid metabolism play important roles in cell growth and proliferation in culture or locally aggressive tumors (Ref 38: Faubert B, et al. Metabolic reprogramming and cancer progression. Science. 2020. 368. 152). We validated the proliferative effect of lactic acid and ornithine on glioma cells at specific concentrations via cell counting kit-8 assay ($p < 0.05$, Fig. R1a, b, corresponding to Supplementary Fig. 4a, b in Supplementary Information). Moreover, we observed a lactic acid-induced increase in mRNA expression of hypoxia-inducible transcription factor-1-α (HIF1α) and nuclear factor kappa-B (NF-κB) in tumor cells after 12 h and 24 h treatments as determined by quantitative PCR (Fig. R1c, d). This finding confirms that lactic acid is a common byproduct of the glycolytic pathway in the tumor microenvironment (Ref. 42: Baltazar F, et al. Lactate beyond a waste metabolite: metabolic affairs and signaling in malignancy. Frontiers in Oncology. 2020. 10. 231).

To investigate the impact of leucine, valine, and threonine on tumor cells, U251MG cells were deprived of amino acids for 1.5 h and restimulated with leucine, valine, and threonine (1 mM) for another 1 h. Cell lysates were analyzed via immunoblotting for the indicated proteins and phosphorylation states. As a result, the three amino acids positively regulated the activity of mTOR complex 1 (mTORC1), a key growth regulator in tumor cells (Ref 43: Sivanand S, et al. Emerging roles for branched-chain amino acid metabolism in cancer. Cancer Cell. 2020. 37. 147), as

evidenced by the phosphorylation levels of ribosomal protein S6 kinase 1 (pPS6K) (Fig. R1e). This finding highlights the role of these amino acids in modulating critical signaling pathways involved in cancer cell metabolism and growth.

Overall, our results underscore the significant roles of lactate, ornithine, valine, leucine, and threonine in cancer cell proliferation and signaling modulation, emphasizing their potential as distinguishing factors between BSG and healthy individuals.

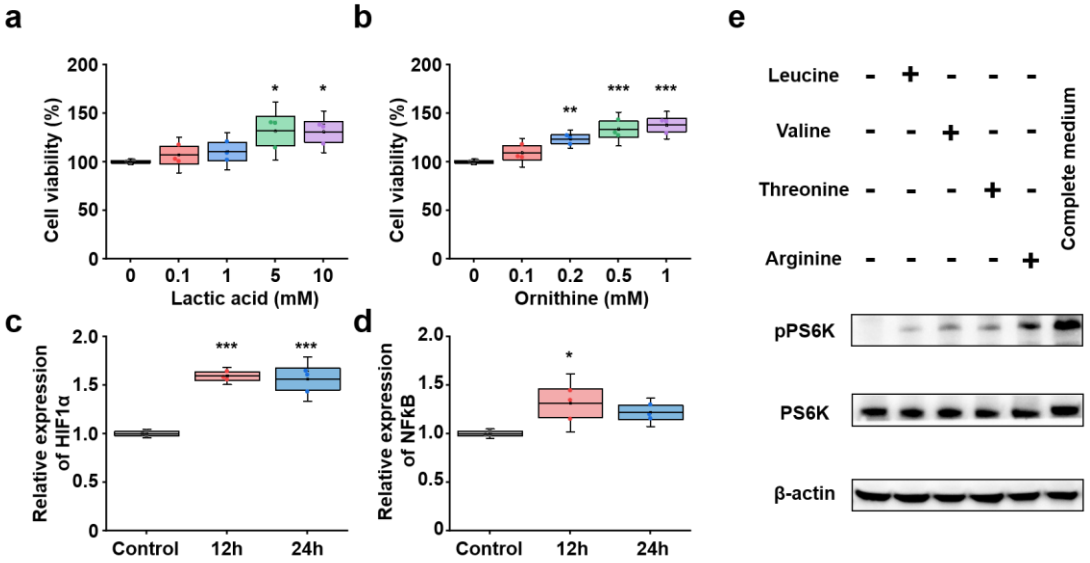

Fig. R1. Biological effects of diagnostic biomarkers on human glioblastoma multiforme (U251MG) cells. Both (a) lactic acid and (b) ornithine promoted the proliferation of tumor cells after 24 h treatment. Lactic acid induced an increase in mRNA expression of (c) HIF1α and (d) NFκB in tumor cells after 12 h and 24 h treatment, determined by quantitative polymerase chain reaction (qPCR). (e) Amino acids including leucine, valine, threonine, and arginine promoted mTOR complex 1 (mTORC1) activity, as determined by the phosphorylation of p70 ribosomal protein S6 kinase (PS6K) through western blot analysis. Cells cultured with complete medium were used as positive control sample. One-way ANOVA was used to perform statistical analyses. * $p < 0.05$, ** $p < 0.01$, *** $p < 0.001$. Experiments were repeated independently 3 times with similar results (a-d).

(2) To further investigate the biological mechanisms underlying the differences between BSG and HD, we performed differential expression analysis using RNAseq data obtained from tumor biopsies of mouse brain tumor tissues (n=5) and adjacent non-cancerous tissue (n=4) (Fig. R7a, corresponding to Supplementary Fig. 9a in Supplementary Information). We also validated the correlation based on the analysis of

public CGGA database (Fig. R7b). As a result, we detected notable variances in gene expression within the perturbed metabolic pathways, consistently reflected in the RNAseq expression data obtained in this study, further supported by the results obtained from the CGGA database.

Moreover, our exploration revealed the regulation of specific genes associated with the adaptive reprogramming of tumor cells. Interestingly, genes HIF-1 and HIF-2 upregulated LAT1 protein in GBM cells, whereas HIF-1 bound to the HRE of the BCAT1 gene to induce its gene transcription, leading to reprogramming of leucine, isoleucine, and valine metabolism and impacting GBM cell growth (Ref. 45: Zhang B, et al. Regulation of branched-chain amino acid metabolism by hypoxia-inducible factor in glioblastoma. Cellular and Molecular Life Sciences. 2021. 78. 195). Additionally, genes ASS1 and ASL, encoding the two key enzymatic components of the arginine biosynthetic pathway, are epigenetically regulated in glial brain tumors (Ref. 46: Syed N, et al. Epigenetic status of argininosuccinate synthetase and argininosuccinate lyase modulates autophagy and cell death in glioblastoma. Cell Death & Disease. 2013. 4. e458). Therefore, we speculated that the unique metabolic signature arises from the metabolic rewiring of the tumors.

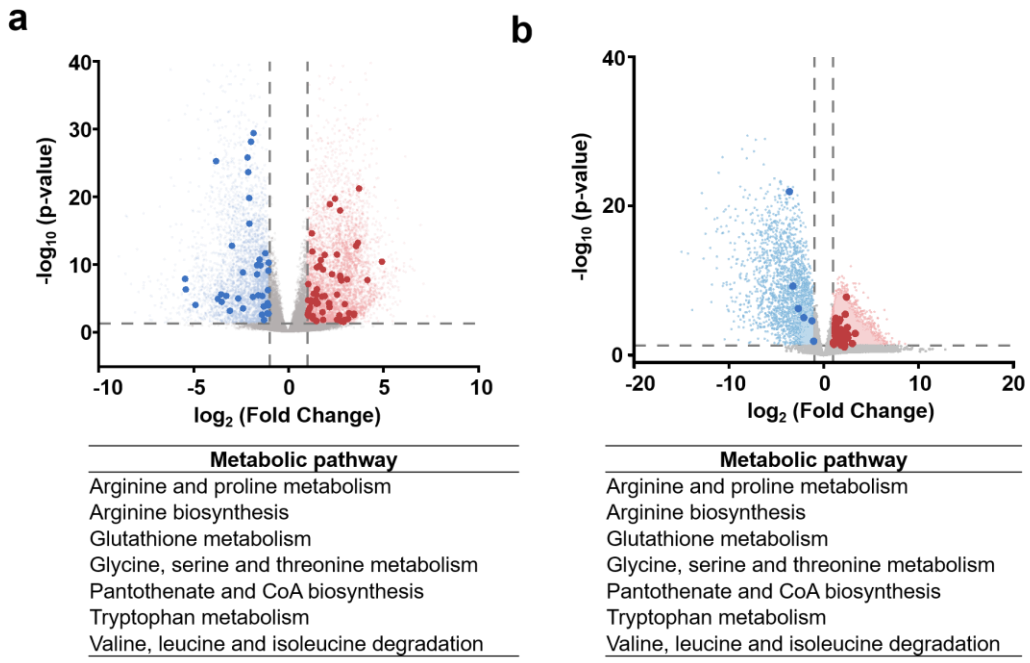

Fig. R7. Significantly differential expression genes revealed through RNAseq data. (a) RNA-seq differential expression analysis using RNAseq data obtained from tumor biopsies of mouse brain

tumor tissues and adjacent non-cancerous tissue (n= 5 vs. 4). (b) RNA-seq differential expression analysis based on public Chinese Glioma Genome Atlas database.

(3) During the treatment, all patients maintain the same hospital-provided diet without additional nutritional food or drugs. Blood samples were collected from participants fasting for at least 8 h. Such strict enrollment criteria were implemented during sample collection to mitigate potential influences from external factors, such as medication and diet according to existing literature (Supplementary Ref. 7: Simundic A M, et al., Joint EFLM-COLABIOCLI recommendation for venous blood sampling. Clinical Chemistry and Laboratory Medicine. 2018. 56. 2015).

(4) We conducted overrepresentation analysis using Metaboanalyst to perform metabolite set enrichment analysis (MSEA) on the seven identified metabolite biomarkers. The enrichment analysis was based on the metabolic network in the SMPDB dataset, comprising 99 metabolite sets representing normal human metabolic pathways. Pathways with an enrichment ratio greater than 5 (calculated by observed hits/expected hits) and a significance level of $p < 0.05$ were considered relevant, aligning with established practices in the field (Supplementary Ref. 13-15: Wang X, et al., Targeting pyrimidine synthesis accentuates molecular therapy response in glioblastoma stem cells. Science Translational Medicine. 2019. 11. eaau4972; Deng L, et al., Sparse PLS-based method for overlapping metabolite set enrichment analysis. Journal of Proteome Research. 2021. 20. 3204; Morel J D, et al., The mouse metallomic landscape of aging and metabolism. Nature Communications. 2022. 13. 607). Importantly, MSEA enables the investigation of functionally related metabolite groups rather than individual metabolites, helping to identify pathways that may be involved in the observed metabolic changes. This approach is advantageous as it avoids bias that could arise from pre-selecting metabolites based on an arbitrary threshold (Supplementary Ref. 16: Xia J, et al. MSEA: a web-based tool to identify biologically meaningful patterns in quantitative metabolomic data. Nucleic Acids Research. 2010. 38. 71).

(5) Subsequently, we conducted MSEA analysis using Kyoto Encyclopedia of Genes and Genomes (KEGG) dataset (80 metabolite sets based on KEGG human metabolic pathways) to identify the most strongly influenced metabolic pathways using the identified metabolites. Our findings revealed that the metabolites were notably enriched in six distinct metabolic pathways, aligning with the results obtained from the SMPDB dataset. These pathways included valine, leucine, and isoleucine degradation, glycine and serine-related metabolism, tryptophan metabolism, and arginine and proline metabolism (Fig. R12, corresponding to Supplementary Fig. 8). By employing pathway analyses such as MSEA, we were able to gain insights into the significant metabolic pathways influenced by the identified metabolites. This approach served as a valuable tool for knowledge-based dimensionality reduction, allowing us to focus on essential pathways while excluding redundant or less influential ones. Through this analysis, we aimed to provide a more streamlined interpretation of the metabolic pathways and their associations with the identified metabolites, without oversimplifying the dataset.

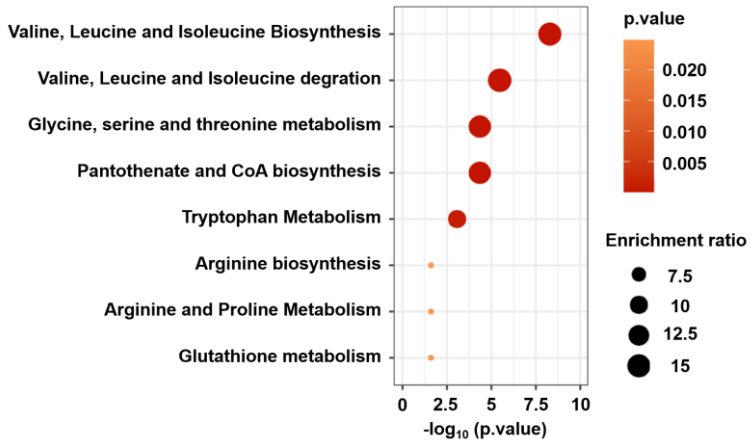

Fig. R12. Metabolite set enrichment analysis of metabolite biomarkers from the diagnostic panel using Kyoto Encyclopedia of Genes and Genomes (KEGG) dataset.

We have added the related results (Supplementary Fig. 4, 8, 9), experimental details, references (Ref. 38, 42-46 and Supplementary Ref. 7, 13-16), and discussion in the manuscript and Supplementary Information as follows.

Revision:

"The metabolic signature should be validated in human-derived cell line[41]. We conducted functional studies of these biomarkers to validate the biological function of metabolite biomarkers in human glioblastoma multiforme cell line (U251MG). Reprogrammed metabolic activities such as glycolysis and amino acid metabolism play important roles in cell growth and proliferation in culture or locally aggressive tumors[38]. We validated the proliferative effect of lactic acid and ornithine on U251MG at specific concentrations via cell counting kit-8 assay ($p < 0.05$, Supplementary Fig. 4a, b). Moreover, we observed a lactic acid-induced increase in mRNA expression of hypoxia-inducible transcription factor-1-α (HIF1α) and nuclear factor kappa-B (NFκB) in tumor cells after 12 h and 24 h treatments as determined by quantitative PCR (Supplementary Fig. 4c, d). This finding confirms that lactic acid is a common byproduct of the glycolytic pathway in the tumor microenvironment[42].

To investigate the impact of leucine, valine, and threonine on tumor cells, U251MG cells were deprived of amino acids for 1.5 h and restimulated with leucine, valine, and threonine (1 mM) for another 1 h. Cell lysates were analyzed via immunoblotting for the indicated proteins and phosphorylation states. As a result, the three amino acids positively regulated the activity of mTOR complex 1 (mTORC1), a key growth regulator in tumor cells[43], as evidenced by the phosphorylation levels of ribosomal protein S6 kinase 1 (Supplementary Fig. 4e). This finding highlights the role of these amino acids in modulating critical signaling pathways involved in cancer cell metabolism and growth." (Manuscript, Page 8)

"To further investigate the biological mechanisms underlying the differences between BSG and HDs, we performed differential expression analysis using RNAseq data obtained from tumor biopsies of mouse brain tumor tissues (n=5) and adjacent non-cancerous tissue (n=4, Supplementary Fig. 9a). We also validated the correlation based on the analysis of public Chinese Glioma Genome Atlas (CGGA) database (Supplementary Fig. 9b). As a result, we detected notable variances in gene expression within the perturbed metabolic pathways, which were consistently reflected in the RNAseq expression data obtained in this study and further supported by the results obtained from the CGGA database.

Moreover, our exploration revealed the regulation of specific genes associated with the adaptive reprogramming of tumor cells. Interestingly, genes HIF-1 and HIF-2 upregulated LAT1 protein in glioblastoma multiforme (GBM) cells, whereas HIF-1 bound to the HRE of the BCAT1 gene to induce its gene transcription, leading to reprogramming of leucine, isoleucine, and valine metabolism and impacting GBM cell growth[45]. Additionally, genes ASS1 and ASL, encoding the two key enzymatic components of the arginine biosynthetic pathway, are epigenetically regulated in glial brain tumors[46]. Therefore, we speculated that the unique metabolic signature arises from the metabolic rewiring of the tumors." (Manuscript, Page 10)

"**1.6 Pathway analysis**

We conducted overrepresentation analysis using MetaboAnalyst 5.0 (https://www.metaboanalyst.ca/) to perform metabolite set enrichment analysis (MSEA) on the identified metabolite biomarkers from both diagnostic and prognostic panel. The enrichment analysis was based on the metabolic network in the Small Molecule Pathway Database (SMPDB) dataset, comprising 99 metabolite sets representing normal human metabolic pathways. Pathways with an enrichment ratio greater than 5 (calculated by observed hits/expected hits) and a significance level of $p < 0.05$ were considered relevant, aligning with established practices in the field[13-15]. Importantly, MSEA enables the investigation of functionally related metabolite groups rather than individual metabolites, helping to identify pathways that may be involved in the observed metabolic changes.

This approach is advantageous as it avoids bias that could arise from pre-selecting metabolites based on an arbitrary threshold[16]. By employing pathway analyses such as MSEA, we were able to gain insights into the significant metabolic pathways influenced by the identified metabolites. This approach served as a valuable tool for knowledge-based dimensionality reduction, allowing us to focus on essential pathways while excluding redundant or less influential ones. Through this analysis, we aimed to provide a more streamlined interpretation of the metabolic pathways and their associations with the identified metabolites, without oversimplifying the dataset.

1.7 Cell culture

U87MG-Luc (a human glioblastoma cell line with luciferase fluorescent labeling) and U251MG (a human glioblastoma cell line) cells were cultured in Dulbecco's Modified Eagle Medium (DMEM, Gibco) supplemented with 10% fetal bovine serum (Corning) and 1% penicillin-streptomycin (Gibco) at 37°C in a 5% CO_2 humidified incubator. Cells in the logarithmic growth phase were selected for subsequent experiments.

1.8 *In vitro* cell experiments

Cell proliferation assay: U251MG cells were seeded in 96-well plate at the density of 1×10^4 cells per well and incubated at 37°C for 24 h. Then the cells were treated with lactic acid (0, 0.1, 1, 5, and 10 mM) or ornithine (0, 0.1, 0.2, 0.5, and 1mM) at various concentrations in triplicate for 24 h. The cell viability was determined using an enhanced cell counting kit-8 (CCK8, Beyotime). Specifically, 10 μL of CCK8 solution was added to each well. After 1 h of cell culture, optical density (OD) value at 450 nm was detected via plate reader (BioTek Synergy H1).

Quantitative polymerase chain reaction (qPCR) assay: U251MG cells were seeded in a 12-well plate at the density of 1.5×10^5 cells per well and incubated at 37°C for 24 h. Then the cells were treated with lactic acid (10 mM) in triplicate for 12 h or 24 h. The cells were collected and subjected to RNA extraction by using SimplyP Total RNA Extraction Kit (Bioer Techology). qPCR assay was performed using HiScript III RT SuperMix Kit for qPCR (Vazyme) and ChamQ Universal SYBR qPCR Master Mix Kit (Vazyme) according to manufacturer's instructions.

Western blotting analysis: U251MG cells were seeded in culture dish (6 cm) at the density of 8×10^5 cells per dish and incubated at 37°C for 24 h. To determine the role of amino acids, the cells were starved by amino acid-depleted DMEM for 1.5 h, followed by the addition of individual amino acid (1 mM) for 1 h. Here, cells cultured with full medium for 1 h after amino acid starvation were used as positive control sample. To study the impact of glucose, the cells were treated with glucose-depleted DMEM for 24 h. Then, glucose with different concentrations (25 mM and 50 mM) were supplied for another 24 h. To assess β-nicotinamide mononucleotide (NMN), the cells were treated with NMN (0, 0.5, and 1mM) for 24 h according to literature[17]. Afterwards, the cells

were collected for western blot analysis. Typically, cells were lysed in RIPA buffer (Epizyme Biotech) containing protease inhibitor (MCE) and phosphatase inhibitor cocktail (Epizyme Biotech). The concentration of protein was determined by a bicinchoninic acid (BCA) assay (Vazyme). 20 μg of cell lysate protein per sample was subjected to gel electrophoresis (Tanon). The primary antibodies include anti-phospho-p70 S6 Kinase (Thr389) antibody (CST), anti- p70 S6 Kinase (49D7) Rabbit antibody (CST), anti-PD-L1 antibody (CST), and anti-β-Actin (8H10D10) antibody (CST), while anti-rabbit IgG HRP-linked antibody and anti-mouse IgG HRP-linked Antibody (CST) were used as the secondary antibodies. The blots were imaged by CLINX ChemiScope 6000 system.

Cell migration: U251MG cells were seeded on the upper chamber of a 24-well transwell plate at the density of 2×10^4 cells per well and treated with succinic acid of different concentrations (0.05 mM and 1 mM) according to literature[18]. After 2 d or 4 d simulation, cells migrated to the lower chamber and were photographed under an inverted microscope using a 10× objective lens.

1.9 *In vivo* mouse experiments

SPF-grade female BALB/c nude mice, aged 5-6 weeks and weighing 18-20 g, were used as experimental subjects in this study, following refinement of the experimental methods based on previous study[19]. All animal care and experiments were approved by the Animal Ethics Committee of Xinhua Hospital, School of Medicine, Shanghai Jiao Tong University (#XHEC-F-2023-031).

In the case of the orthotopic tumor model, the inoculation site was the right caudate nucleus of the mouse brain. When anesthetizing mice with isoflurane, a concentration of 1-2% was maintained once the mice are confirmed to have entered the anesthetized state, in order to sustain the anesthetic effect throughout the experiment. The trypsinized U87MG-Luc cells were resuspended in cold phosphate-buffered saline at 1.0×10^5 cells/μL. A 10 μL microsyringe was used to inject 5 μL of the cell suspension into the right hemisphere of the mouse brain (0.5 mm anterior to the bregma, 2 mm lateral to the midline, and 3.5 mm depth from the skull) at a rate of 1 μL/min. Following the injection, the bone hole was sealed with bone wax, and the incision was sutured. The

mice were placed on thermostatic electric blankets and closely monitored until fully resuscitated. Three days post tumor cell injection, tumor implantation and growth were evaluated using the IVIS Lumina Series III *in vivo* imaging system (PerkinElmer, USA). At the humane endpoint, mice were euthanized. Brain tumor tissue and adjacent non-cancerous tissue were collected and subjected to RNA sequencing.

To establish the subcutaneous tumor model, mice were inoculated with U87MG-Luc cells (3.0×10^6 cells/site) suspended in Matrigel, and were injected into the axillary region of the right forelimb. Tumor volume was measured using a vernier caliper, and radiotherapy was initiated once the average tumor size exceeded 100 mm^3. Mice in the radiotherapy group were administered a daily radiation dose of 2 Gy at the tumor site for five consecutive days. Serum and brain tumor samples were collected before and five days after radiotherapy, and then subjected to metabolic analysis by NPELDI-MS and RNA sequencing, respectively." (Supplementary Information, Page 7)

1.10 RNA sequencing and analyses

Total RNA was extracted using the TRIzol reagent (Invitrogen, CA, USA) according to the manufacturer's protocol. RNA purity and quantification were evaluated using the NanoDrop 2000 spectrophotometer (Thermo Scientific, USA). RNA integrity was assessed using the Agilent 2100 Bioanalyzer (Agilent Technologies, Santa Clara, CA, USA). Then the libraries were constructed using VAHTS Universal V6 RNA-seq Library Prep Kit.

The libraries were sequenced on an Illumina Novaseq 6000 platform and 150 bp paired-end reads were generated. About 44.01-50.97 M raw reads for each sample were generated. Raw reads of FASTQ format were firstly processed using fastp and the low-quality reads were removed to obtain the clean reads. Then, about 41.39-48.48 M clean reads for each sample were retained for subsequent analyses. The clean reads were mapped to the reference genome using HISAT2. FPKM of each gene was calculated and the read counts of each gene were obtained by HTSeq-count.

Differential expression analysis was performed using the DESeq2. p value < 0.05 and fold change > 2 or fold change < 0.5 was set as the threshold for significantly differential expression gene (DEGs). Based on the hypergeometric distribution, Kyoto

Encyclopedia of Genes and Genomes (KEGG) pathway enrichment analysis of DEGs was performed to screen the significant enriched term using R (v 3.2.0)." (Supplementary Information, Page 6)

Comment 4: *In the panel of nine metabolites associated with clinical outcome, dialuric acid, N,N' sulfonylbisurea, caffeic acid 3-O-glucuronide, dihydroperillic acid are not endogenous metabolites and probably come from drugs the patients are receiving. Their biological significance is not clear.*

Response: We appreciate the reviewer for the insightful comment regarding the potential interference of certain metabolites. Taking this into consideration, we conducted additional analyses to address this concern. We calculated the odds ratios of the nine original metabolites associated with clinical outcome, not only in a basic logistic regression model but also after adjusting for key clinical covariates such as age, gender, BMI, and Lansky score, as suggested by previous studies (Ref. 47: Arrillaga-Romany I, et al., ACTION: a randomized phase 3 study of ONC201 (dordaviprone) in patients with newly diagnosed H3 K27M-mutant diffuse glioma. Neuro-Oncology. 2024. 26. 173). Through this analysis, we found that BMI and Lansky score emerged as a significant covariate for risk scores, leading to significantly altered odds ratios (Table R4).

Furthermore, in order to enhance the reliability of our findings, we expanded the sample size from 244 to 405. This increase allowed us to further substantiate the robustness of the prognostic panel identified in our study. Consequently, we have now identified a revised set of metabolites (including lactic acid, oxalacetic acid, niacinamide, threonic acid, succinic acid, arginine, and glucose) that constitute a new prognostic panel. Importantly, even after adjusting for BMI and Lansky score, the odds ratios of risk scores remained nearly unchanged (Table R5, corresponding to Supplementary Table 8 in Supplementary Information).

Table R4. Odds ratios of previous risk score adjusted for key clinical covariates.

	Odds ratios (95% Confidence interval (CI)) in basic model	Odds ratios (95% Confidence interval (CI) in adjusted models with covariates			
		Sex	Age	BMI	Lansky
Previous risk score	0.333 (0.150-0.742)	0.228 (0.091-0.573)	0.145 (0.050-0.420)	0.123 (0.040-0.375)	0.106 (0.034-0.326)

Table R5. Odds ratios of prognostic risk score adjusted for key clinical covariates.

	Odds ratios (95% Confidence interval (CI)) in basic model	Odds ratios (95% Confidence interval (CI) in adjusted models with covariates			
		Sex	Age	BMI	Lansky
Risk score	1.596 (0.708-3.598)	1.687 (0.738-3.856)	1.593 (0.705-3.601)	1.679 (0.739-3.814)	1.690 (0.731-3.909)

We further explored biological significance the new prognostic panel on both cell experiments and molecular expression. We first confirmed the biological significance of the prognostic panel using U251MG cell line. In particular, we have already validated lactic acid in the diagnostic panel. Hence, its presence in the prognostic panel does not warrant further investigation.

Programmed death-ligand 1 (PD-L1) is significantly overexpressed in various tumor types and regulates immune evasion by binding to the inhibitory receptor PD-1 on activated T cells, leading to T cell exhaustion (Ref. 48: Kornepati A, et al., Programmed death ligand 1 signals in cancer cells. Nature Reviews Cancer. 2022. 22. 174). It has been reported that glucose and niacinamide contributed to tumor immune escape via elevating expression of PD-L1 (Ref. 49&50: He H, et al. Aerobic glycolysis promotes tumor immune evasion and tumor cell stemness through the noncanonical function of hexokinase 2. Cancer Communications. 2023. 43. 387; Lv H, et al. NAD(+) metabolism maintains inducible PD-L1 expression to drive tumor immune evasion. Cell Metabolism. 2021. 33. 110). To assess this impact on human glioblastoma multiforme cell line, U251MG cells were cultured in glucose-depleted dulbecco's modified eagle medium (DMEM) supplemented with varying glucose concentrations (0, 25, and 50 mM) for 24 h. In case of niacinamide, cells were cultured in complete medium with the addition of β-nicotinamide mononucleotide (an analog of niacinamide and a precursor to NAD^+) at selected concentrations (0, 0.5, and 1 mM) for 24 h. As a result, the increase of both glucose and niacinamide analog resulted in the up-regulation of PD-L1 expression in tumor cells (Fig. R2a, corresponding to Supplementary Fig. 10a in Supplementary Information).

We also demonstrated that arginine promoted mTORC1 activation in tumor cells through western blotting analysis, following the same protocol in exploring the biofunctions of amino acids in the diagnostic panel (Fig. R1e, corresponding to Supplementary Fig. 4e in Supplementary Information).

Succinic acid was secreted by tumor to promote metastasis via phosphoinositide 3-kinase (PI3K)-HIF1αaxis (Ref. 51: Wu J Y, et al., Cancer-derived succinate promotes macrophage polarization and cancer metastasis via succinate receptor. Molecular Cell.

2020. 77. 213). To verify the effect of succinic acid in human glioblastoma multiforme cell line, we conducted a cell migration experiment and observed a rise in cell migration as the concentration of succinic acid increased from 0-0.1 mM (Fig. R2b). The result supported succinic acid-promoted metastasis of U251MG cells.

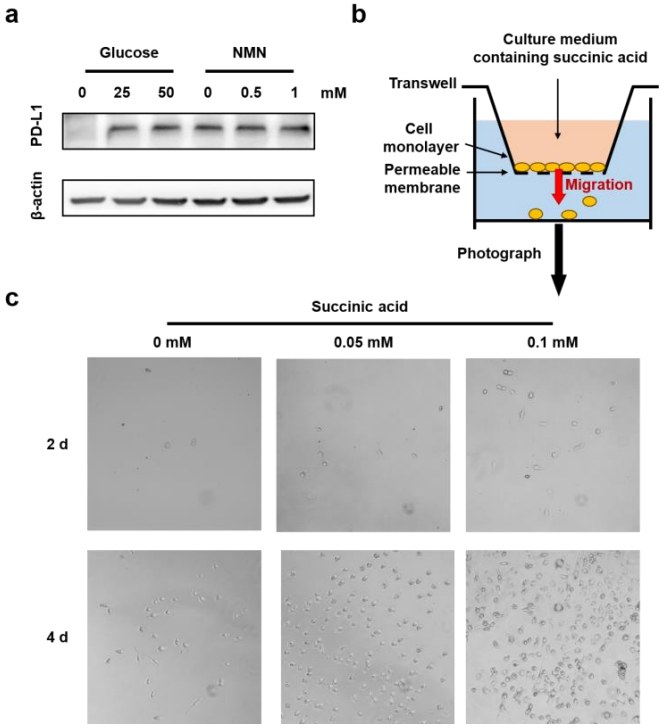

Fig. R2. Biological effects of prognostic biomarkers on human glioblastoma multiforme cells. (a) Both glucose and nicotinamide mononucleotide (NMN) improved the PD-L1 expression in U251MG cells, verified by western blot analysis. (b) U251MG cells in the upper chamber of transwell were treated with succinic acid (0.05 mM and 0.1 mM). (c) At selected time point (2 d and 4 d), migrated U251MG cells in the lower chamber were photographed under an inverted microscope using a 10× objective lens.

The prognostic panel consisted of differentially regulated metabolites together identified 14 potentially altered metabolic pathways (Fig. R8a, corresponding to Supplementary Fig. 11a in Supplementary Information). We thus conducted RNAseq experiments on mouse tumor tissue before and after radiation of subcutaneous tumor models (n= 4 vs. 4). We found five differentially expressed genes (ALDOC, ATP6V0D2, ACY1, AMDHD1, and DDC), associated with the metabolic pathways identified in the prognostic panel and expression data (Fig. R8b). In particular, glycolysis/gluconeogenesis appeared enriched in tumor cells. Tumor growth is characterized by the upregulation of ALDOC, correlated with increased glucose and

fructose consumption and lactate production (Ref. 52: De Vitis C, et al., ALDOC- and ENO2- driven glucose metabolism sustains 3D tumor spheroids growth regardless of nutrient environmental conditions: a multi-omics analysis. Journal of Experimental & Clinical Cancer Research. 2023. 42. 69). Gene ATP6V0D2 plays a role in oxidative phosphorylation, which is a highly active cellular pathway in GBM. The maintenance of redox homeostasis is vital for cellular function and survival, with oxidative processes intensified in tumor cells compared to normal cells. Recent studies have highlighted the regulatory impact of oxidative phosphorylation on GBM progression (Ref. 53: Liu P, et al. Unraveling the intricacies of glioblastoma progression and recurrence: insights into the role of NFYB and oxidative phosphorylation at the single-cell level. Frontiers in Immunology. 2024. 15. 1368685). Similarly, amino acid metabolism, a significant hallmark of glioblastoma impacting patient prognosis, has been confirmed through our metabolic and sequencing results and supported by existing literature (Ref. 54: Chinnaiyan P, et al. The metabolomic signature of malignant glioma reflects accelerated anabolic metabolism. Cancer Research. 2012. 72. 5878). Thus, we conclude that the prognostic panel reflects the rewired metabolism of tumors.

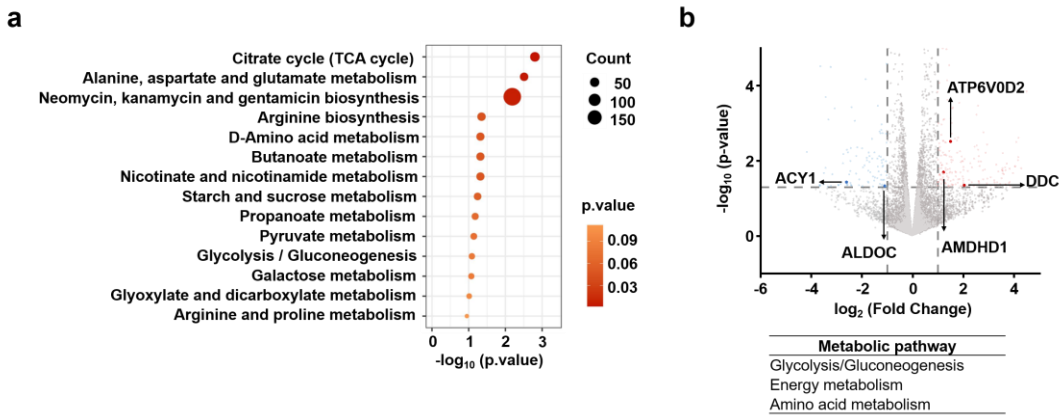

Fig. R8. *In vivo* validation of the prognostic panel. (a) Metabolite set enrichment analysis of metabolite biomarkers from the prognostic panel using Kyoto Encyclopedia of Genes and Genomes (KEGG) dataset. (b) RNA-seq differential expression analysis using RNAseq data obtained from mouse tumor tissue before and after radiation of subcutaneous tumor models (n= 4 vs. 4).

We have added the related results (Supplementary Fig. 4, 10, 11, and Supplementary Table 8), experimental details, references (Ref. 47-54), and discussion in the manuscript and Supplementary Information as follows.

Revision:

"Importantly, we identified a seven-feature panel correlated with clinical outcomes, consisting of lactic acid, oxalacetic acid, niacinamide, threonic acid, succinic acid, arginine, and glucose (Supplementary Table 7). Importantly, even after adjusting for key clinical covariates such as age, gender, BMI, and Lansky score, as suggested by previous studies[47], the odds ratios of risk scores remained nearly unchanged (Supplementary Table 8). We confirmed the biological significance of the prognostic panel using U251MG cell line. In particular, we have already validated lactic acid in the diagnostic panel. Hence, its presence in the prognostic panel does not warrant further investigation.

Programmed death-ligand 1 (PD-L1) is significantly overexpressed in various tumor types and regulates immune evasion by binding to the inhibitory receptor PD-1 on activated T cells, leading to T cell exhaustion[48]. It has been reported that glucose and niacinamide contributed to tumor immune escape via elevating expression of PD-L1[49,50]. To assess this impact on human glioblastoma multiforme cell line, U251MG cells were cultured in glucose-depleted dulbecco's modified eagle medium (DMEM) supplemented with varying glucose concentrations (0, 25, and 50 mM) for 24 h. In case of niacinamide, cells were cultured in complete medium with the addition of β-nicotinamide mononucleotide (an analog of niacinamide and a precursor to NAD^+) at selected concentrations (0, 0.5, and 1 mM) for 24 h. As a result, the increase of both glucose and niacinamide analog resulted in the up-regulation of PD-L1 expression in tumor cells (Supplementary Fig. 10a).

We also demonstrated that arginine promoted mTORC1 activation in tumor cells through western blotting analysis, following the same protocol in exploring the biofunctions of amino acids in the diagnostic panel (Supplementary Fig. 4e).

Succinic acid was secreted by tumor to promote metastasis via phosphoinositide 3-kinase-HIF1α axis[51]. To verify the effect of succinic acid in human glioblastoma multiforme cell line, we conducted a cell migration experiment and observed a rise in cell migration as the concentration of succinic acid increased from 0-0.1 mM

(Supplementary Fig. 10b, c). The result supported succinic acid-promoted metastasis of U251MG cells.

The prognostic panel consisted of differentially regulated metabolites together identified 14 potentially altered metabolic pathways (Supplementary Fig. 11a). We thus conducted RNAseq experiments on mouse tumor tissue before and after radiation of subcutaneous tumor models (n= 4 vs. 4). We found five differentially expressed genes (ALDOC, ATP6V0D2, ACY1, AMDHD1, and DDC), associated with the metabolic pathways identified in the prognostic panel and expression data (Supplementary Fig. 11b). In particular, glycolysis/gluconeogenesis appeared enriched in tumor cells. Tumor growth is characterized by the upregulation of ALDOC, correlated with increased glucose and fructose consumption and lactate production[52]. Gene ATP6V0D2 plays a role in energy metabolism, which is a highly active cellular pathway in GBM. The maintenance of redox homeostasis is vital for cellular function and survival, with oxidative processes intensified in tumor cells compared to normal cells. Recent studies have highlighted the regulatory impact of oxidative phosphorylation on GBM progression[53]. Similarly, amino acid metabolism, a significant hallmark of glioblastoma impacting patient prognosis, has been confirmed through our metabolic and sequencing results and supported by existing literature[54]. Thus, we conclude that the prognostic panel reflects the rewired metabolism of tumors." (Manuscript, Page 11)

Comment 5: *The rationale for use of serum metabolite biomarkers for diagnosis isn't strong. The samples were collected from brainstem glioma patients when disease was already present and confirmed by imaging. It doesn't make sense to compare glioma patients to healthy controls since the presence of a tumor would be confirmed by imaging anyway. A better (or more clinically useful) comparison in my opinion would be to try and look for metabolic changes associated with glioma that could distinguish pediatric tumors (or neurological conditions) with similar presentation.*

Response: We thank the reviewer for the insightful advice. The rationale for employing serum metabolite biomarkers in the diagnostic process of BSG lies in their potential to

enable precise screening before the manifestation of clinical symptoms, thereby facilitating early intervention at the initial stages of the disease and ultimately enhancing patient survival rates. While it is acknowledged that the presence of BSG would typically be confirmed by imaging modalities, such as magnetic resonance imaging, it is essential to consider the global healthcare landscape, particularly in low-income countries where imaging facilities may not be uniformly available. The World Health Organization reports that less than 30% of low-income countries have adequate imaging facilities, leading to a substantial number of undiagnosed cases and delayed interventions (Ref. 60: Wang R, et al. A sustainable approach to universal metabolic cancer diagnosis. Nature Sustainability. 2024).

BSG especially in pediatric cases, exhibits atypical clinical presentations that include subtle mental signs like emotional and behavioral changes or acquired torticollis (Ref. 61&62: Milanaccio C, et al. DIPG-27. Behavioral disturbances as underestimated presenting symptoms in children with Diffuse Intrinsic Pontine Glioma (DIPG). Neuro-Oncology. 2022. 24. 24; Baklizi N, et al. Torticollis as a presenting symptom of pediatric CNS tumors: a systematic review. Seminars in Oncology. 2022. 49. 419). These symptoms can be easily missed or misinterpreted, resulting in delays in diagnosis and treatment initiation (Ref. 63: Patel V, et al., Diagnostic delay and morbidity of central nervous system tumors in children and young adults: a pediatric hospital experience. Journal of Neuro-Oncology. 2019. 143. 297). Given the aggressive nature of BSG and their rapid progression, delays in the commencement of essential treatments, such as radiotherapy, can significantly impact patient outcomes and reduce survival periods.

To provide a better (or more clinically useful) comparison, we also newly collected 68 serum samples from patients with other neural diseases. We added the comparison between BSG and other neural diseases (28 encephalitis cases and 40 idiopathic epilepsy cases) through the static metabolic snapshots. We adopted the same protocol to detect the differences between BSG vs. other neurological diseases based on static metabolic snapshots (Fig. R3a, corresponding to Supplementary Fig. 7a in Supplementary Information). As a result, the models also achieved outstanding

performance in differentiating BSG from encephalitis and idiopathic epilepsy, with area under receiver operating characteristic of 0.929 and 0.923, respectively (Fig. R3b).

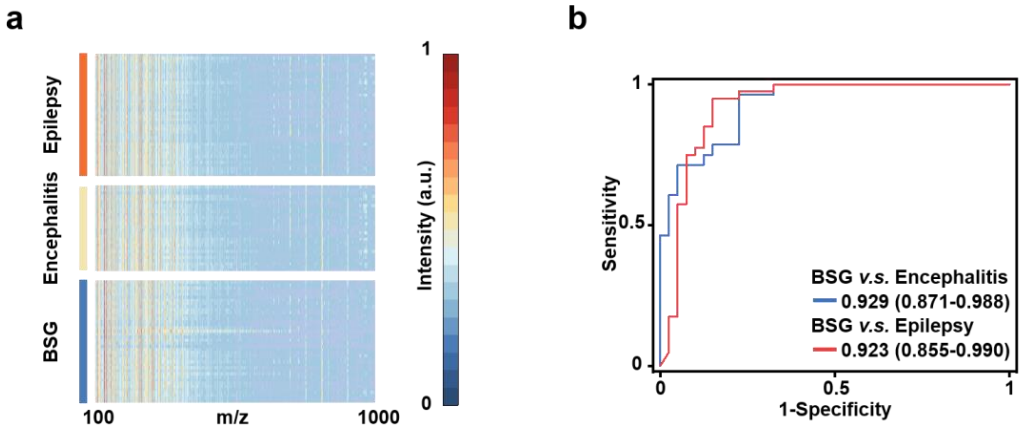

Fig. R3. Static metabolic snapshots of other neural diseases. (a) Heatmap of serum metabolic profiles from 40 BSG patients, 28 encephalitis patients, and 40 epilepsy patients. (b) ROC curves for differentiating BSG patients from encephalitis and epilepsy patients via the static metabolic snapshots, respectively.

We have added the related results (Supplementary Fig. 7), experimental details, references (Ref. 60-63), and discussion in the manuscript and Supplementary Information as follows.

Revision:

"While it is acknowledged that the presence of BSG would typically be confirmed by imaging modalities, such as MRI, it is essential to consider the global healthcare landscape, particularly in low-income countries where imaging facilities may not be uniformly available. The World Health Organization reports that less than 30% of low-income countries have adequate imaging facilities, leading to a substantial number of undiagnosed cases and delayed interventions[60]. BSG especially in pediatric cases, exhibits atypical clinical presentations that include subtle mental signs like emotional and behavioral changes or acquired torticollis[61,62]. These symptoms can be easily missed or misinterpreted, resulting in delays in diagnosis and treatment initiation[63]. Given the aggressive nature of BSG and their rapid progression, delays in the

commencement of essential treatments, such as radiotherapy, can significantly impact patient outcomes and reduce survival periods." (Manuscript, Page 16)

"Another major challenge in clinical practice is the differentiation of BSG from other neural diseases by MRI imaging[44]. We added the comparison between BSG and other neural diseases (28 encephalitis cases and 40 idiopathic epilepsy cases) through the static metabolic snapshots. We adopted the same protocol to detect the differences (Supplementary Fig. 7a). As a result, the models also achieved outstanding performance in differentiating BSG from encephalitis and idiopathic epilepsy, with AUC of 0.929 and 0.923, respectively (Supplementary Fig. 7b)." (Manuscript, Page 16)

Comment 6: *The most clinically useful and interesting part of this study is the longitudinal collection of samples to determine response to therapy. However, the small number of patients limits the robustness of their biomarkers. Could the authors expand to a larger patient population?*

Response: We thank the reviewer for the very valuable advice. We newly collected 66 serum samples from 22 patients in the process of treatment to validate the robustness of biomarkers. We expanded the longitudinal collection of samples from original 40 patients to 62 patients. Meanwhile, we updated the analysis results of dynamic metabolic snapshots during radiotherapy (Fig. R13d-g, corresponding to Fig. 4 d-g). Consistently, lactic acid involved in pyruvate metabolism still displayed different tendencies along with radiotherapy progression in low-risk and high-risk groups within the larger longitudinal cohorts (Fig. R13g).

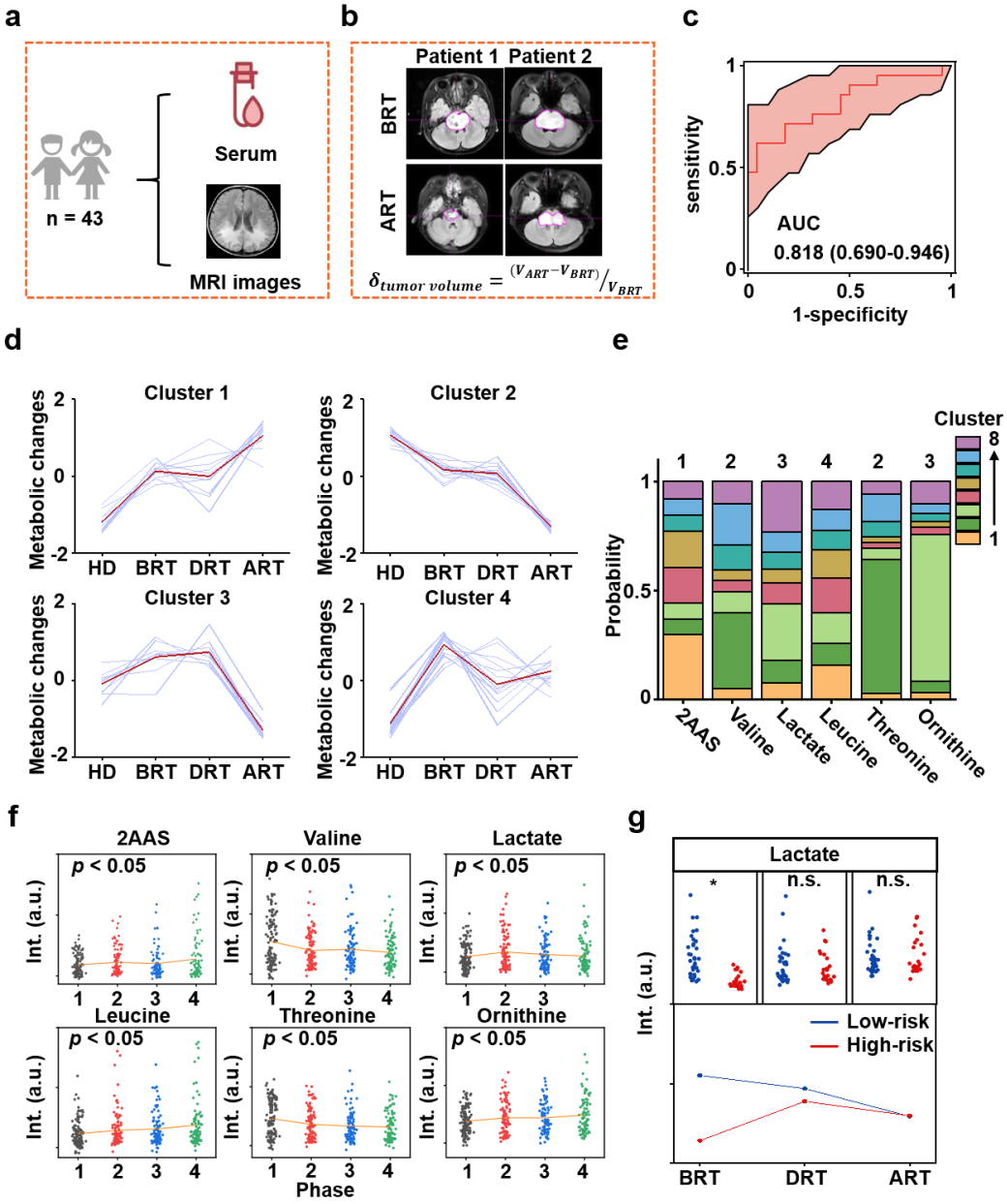

Fig. R13. **Dynamic metabolic snapshots during radiotherapy.** (a) Sample information collected for 43 BSG participants. (b) Calculation of the change in tumor size based on magnetic resonance imaging (MRI) images. (c) ROC curves to distinguish volume-decreasing participants from volume-increasing participants using the static metabolic snapshots collected BRT. (d) Clustering of metabolic trajectories using dynamic metabolic snapshots along HDs, BRT, DRT, and ART. (e) Probabilities of six biomarkers tracing with potential clustering tendency. (f) Scatter plots of six metabolites constructed the diagnostic panel among HDs, BRT, DRT, and ART. Orange lines referred to the average intensity of the metabolites in each group. (g) Dynamic alterations of lactic acid in low-risk and high-risk groups.

We have updated the related results (Fig. 4), experimental details, and discussion in the manuscript and Supplementary Information as follows.

Revision:

"To capture the dynamic metabolic snapshots at high resolution, we performed a design of high-density blood sampling on the longitudinal cohort constituting of 62 BSG patients." (Manuscript, Page 6)

"Importantly, we found lactic acid involved in pyruvate metabolism had different tendencies along with radiotherapy progression in low-risk and high-risk groups within the longitudinal cohorts of 62 BSG participants (Fig. 4g)." (Manuscript, Page 15)

"Finally, A total of 186 serum samples were collected longitudinally from 62 patients at three time points: before radiotherapy (BRT), during radiotherapy (DRT), and after radiotherapy (ART)[3]." (Supplementary Information, Page 2)

Minor comments:

Comment: *In the introduction the authors mention that small molecule metabolites can pass through the blood brain barrier; however, this is not true. Polar small molecules require transport though solute carriers for entry into the brain. In the context of blood brain barrier dysfunction there may be transport-independent mechanisms for metabolites to end up in the blood, but the authors should clarify this.*

Response: We thank the reviewer for the careful comment. In light of the reviewer's explanation, we have carefully reviewed and revised the statement in the Introduction concerning the passage of small molecule metabolites through the blood-brain barrier.

Revision:

"In the context of BBB dysfunction, there may be transport-independent mechanisms for metabolites (size < 1.8 nm) to cross the BBB. This is facilitated by the compatible pore size of brain microvessel endothelial cells, which typically range from about 1.4 to 1.8 nm, enabling metabolites enter the bloodstream[21-24]." (Manuscript, Page 4)

"Our previous study has validated the function of BBB in separating blood and

brain/cerebrospinal fluid (CSF) systems, as well as in regulating the permeability that allows for metabolite transport under disease status[25]." (Manuscript, Page 4)

REVIEWER COMMENTS

Reviewer #1 (Remarks to the Author):

Comment: *The authors have addressed most of my concerns. However, there is a critical concern about glioblastoma (GBM) cell lines used in the new experiments in response to the comment 1, 2, and 9. Author used human GBM cell lines, U251MG and U87MG, that are gold standard GBM cell lines for research and are genetically and biologically quite different from brainstem glioma (BSG). The results from using these GBM cell lines will not reflect BSG biology and incompatible with the clinical data from BSG patient. The readers in neuro-oncology field will not accept the results using the well-established GBM cells for the study of BSG. Because few BSG cell lines are commercially available, author should use those BSG cell lines in response to the comments 1, 2, and 9. In addition, author used subcutaneous model of U87MG that is also will not reflect BSG biology. Author should use orthotopic intracranial (i.e., brainstem) xenografts with patient-derived BSG cell lines.*

Response: We sincerely appreciate the reviewer's critical feedback regarding the validation experiments on glioblastoma (GBM) cell lines and subcutaneous models. We fully acknowledge the genetic and biological discrepancies between GBM and brainstem glioma (BSG) cell lines, which could potentially limit our study. To address this concern rigorously, we have implemented the following revisions and clarifications:

1. Prioritization of BSG-orthotopic models:

All key functional validations (e.g., diagnostic panel efficacy, prognostic panel efficacy, metabolic pathway modulation between cancer vs. normal) have now been performed using the patient-derived BSG (human diffuse intrinsic pontine glioma cell line (SHSMU-DIPG-01)) (Fig. R1-8) as well as SHSMU-DIPG-01-derived orthotopic brainstem xenografts (n $\geqslant$ 3/group, Fig. R1&3), ensuring anatomical and biological fidelity to human BSG.

2. Rationale for retaining BSG-subcutaneous models:

To evaluate the prognostic panel, we employed subcutaneous xenografts

exclusively in the context of radiotherapy (RT) response related studies. This approach was necessitated by the inherent limitations of the orthotopic BSG model, which exhibits a very narrow survival window of 35-42 days post-tumor cell implantation (Ref. 1: Katagi H, et al., Therapeutic targeting of transcriptional elongation in diffuse intrinsic pontine glioma. Neuro-oncology. 2021. 23. 1348). Our experimental observations corroborate this limited survival duration, which prevents the completion of fractionated RT regimens. In our experiments, a stable bioluminescence signal from intracranial orthotopic tumors was observed 38 days post-implantation (Fig. R1). At this point, the mice exhibited significant body weight loss (loss greater than 20% of initial weight or no weight gain for 7 consecutive days) along with severe neurobehavioral deficits, including unsteady gait, circular walking, and frequent falls. Consequently, these comorbidities necessitated premature euthanasia prior to completing the planned radiation regimen.

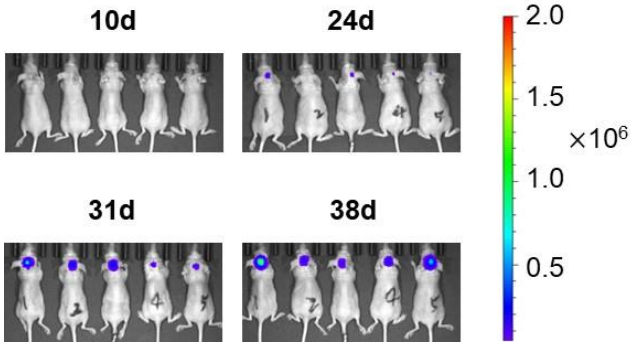

Fig. R1: Time-dependent bioluminescence detection of SHSMU-DIPG-01-derived orthotopic brainstem xenografts.

While subcutaneous tumors lack brainstem-specific microenvironmental interactions, they enable longitudinal monitoring (before and after RT therapy) of systemic metabolic perturbations that correlate with RT response in BSG, referring to similar practices in existing literature (Ref. 2: Liu T, et al., A positive feedback loop of lncRNA-RMRP/ZNRF3 axis and Wnt/β-catenin signaling regulates the progression and temozolomide resistance in glioma. Cell Death and Disease. 2021. 11. 12).

Importantly, our results revealed consistent trends (cosine similarity > 0.95)

between subcutaneous and orthotopic models in baseline biomarker expression via serum metabolic fingerprints (Fig. R2), supporting the utility of studying RT-induced metabolic adaptations. This is due to the serum metabolomic changes observed in subcutaneous models reflecting systemic tumor-induced metabolic perturbations (e.g., circulating lactic acid and polyamines) that are relevant to BSG biology (Ref. 3&4: Yasushi K, et al., Decreased liver B vitamin-related enzymes as a metabolic hallmark of cancer cachexia. Nature Communications. 2023, 14. 6246; Stribbling SM, et al., The cell-line-derived subcutaneous tumor model in preclinical cancer research. Nature Protocols. 2022. 17. 9). This approach aligns with prior studies evaluating therapy response kinetics in spatially accessible tumors (Ref. 5&6: Sun C, et al., Spatially resolved metabolomics to discover tumor-associated metabolic alterations. Proceedings of the National Academy of Sciences. 2019. 116. 1; Chen F, et al., Integrated analysis of the faecal metagenome and serum metabolome reveals the role of gut microbiome-associated metabolites in the detection of colorectal cancer and adenoma. Gut. 2022. 71. 7).

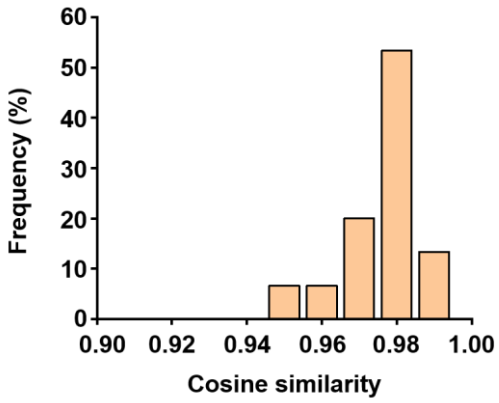

Fig. R2: Cosine similarities were analyzed between the reference serum metabolic fingerprint of orthotopic models and the fingerprints of subcutaneous models.

We agree with the reviewer's valuable concern that BSG-specific models are essential for translational relevance, and our revisions reflect this priority. By integrating orthotopic models for diagnostic validation and subcutaneous systems for RT studies, we aimed to balance biological fidelity with experimental feasibility. We believe these updates significantly strengthen the clinical applicability of our findings

to BSG.

The detailed responses and revisions to the previous comments 1, 2, and 9 can be found as follows.

Previous comment 1 regarding the respective roles of the metabolic markers in the diagnostic panel:

Response: To clarify the respective roles of the metabolic markers in distinguishing BSG from healthy donors (HDs), we integrated evidence from three key sources: (1) RNA-seq data from brainstem tissues in orthotopic murine models based on SHSMU-DIPG-01 cell lines, (2) in-vitro studies of metabolic markers in treated SHSMU-DIPG-01 cells, and (3) publicly available RNA-seq data from the GSE162976 database. BSG tumors exhibit metabolic reprogramming that involves the regulation of key genes such as Arg1, Arg2, Nos2, P4ha1, Hpgds, Nat8f6, Gldc, Pgam2, Enpp1, Enpp3, Aox4, and Hmgcs2, which are associated with the biosynthesis and metabolism of amino acids, glutathione, and pantothenate and coenzyme A (CoA). These regulatory changes enable the identified metabolites to serve as potential biomarkers for diagnostic purposes. These metabolites influence BSG cell proliferation in a concentration-dependent manner, suggesting their role in eliciting metabolic stress and modulating the metabolic reprogramming process in tumors.

1. RNA-seq results from orthotopic murine models

To mechanistically characterize the pathophysiological divergence between BSG and HDs, we conducted differential expression analysis on RNA-seq data from orthotopically xenografted BSG specimens (brainstem tissues, n = 4) and age-matched controls (normal brainstem tissues, n = 3). Specially, SPF-grade female BALB/c nude mice, aged 4-6 weeks and weighing 18-20 g, were used as experimental subjects in this study, following refinement of the experimental methods based on the previous study (Ref. 7 corresponding to Ref. 17 in Supplementary information: Grasso C S, et al., Functionally defined therapeutic targets in diffuse intrinsic pontine glioma. Nature Medicine. 2015. 21. 555). All animal care and experiments were approved (#XHEC-F-

2023-031) by the Animal Ethics Committee of Xinhua Hospital, School of Medicine, Shanghai Jiao Tong University. To establish the orthotopic intracranial xenograft model, SHSMU-DIPG-01 cells were transduced with lentiviral vectors encoding the enhanced green fluorescent protein (eGFP) and firefly luciferase (ffLuc). Positively transduced cells were subsequently sorted by fluorescence-activated cell sorting (FACS) to achieve a purity greater than 95% prior to implantation. Under deep anesthesia, mice were secured on a stereotactic frame, and a cranial burr hole was drilled at stereotactic coordinates relative to the lambda suture: 0.8 mm posterior, 1 mm lateral to the midline, and 4.5 mm depth. A total of 1×10^6 cells suspended in 3 μL phosphate-buffered saline (PBS) were infused via Hamilton syringe at a controlled rate of 0.3 μL/min. To minimize reflux, the injection needle was retained for 5 minutes post-infusion. Tumor engraftment was validated 72 hours post-surgery by intraperitoneal administration of D-luciferin potassium salt (75 mg/kg; Promega) followed by bioluminescent signal acquisition using the IVIS Spectrum In Vivo Imaging System (PerkinElmer). At the humane endpoint, mice were euthanized.

Our analysis revealed significant variances in gene expression within the perturbed metabolic pathways, consistently reflected in the RNA-seq expression data obtained in this study (Fig. R3, corresponding to Supplementary Fig. 9 in Supplementary Information). Notably, the genes Arg1, Arg2, Nos2, and P4ha1 were found to reprogram arginine and proline metabolism. Meanwhile, Arg1, Arg2, and Nos2 were shown to disturb arginine biosynthesis. Arginine was converted into ornithine through the action of arginase. Additionally, the genes Hpgds and Nat8f6 were identified as key regulators in glutathione metabolism. Gldc and Pgam2 were also found to influence the metabolism of glycine, serine, and threonine. Furthermore, Enpp1 and Enpp3, which encode two critical enzymatic components of the pantothenate and CoA biosynthesis pathway, were shown to be epigenetically regulated in brain tumors. These modulations closely related to the Warburg effect and the TCA cycle, and regulated the expression of lactate. Lastly, Aox4 was found to regulate tyrosine metabolism as well as the degradation of valine, leucine, and isoleucine, in conjunction with Hmgcs2.

These findings suggest that the unique metabolic signature of BSG arises from the

metabolic rewiring of the tumors.

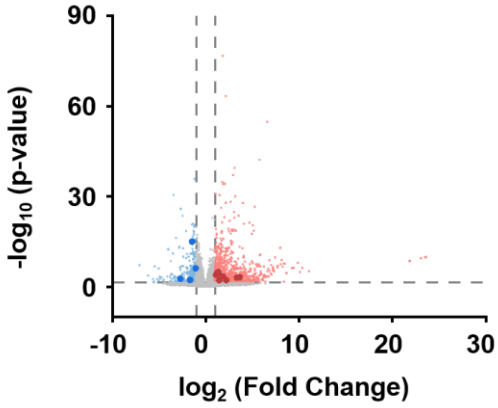

Metabolic pathway
Arginine and proline metabolism
Arginine biosynthesis
Glutathione metabolism
Glycine, serine and threonine metabolism
Pantothenate and CoA biosynthesis
Tryptophan metabolism
Valine, leucine and isoleucine degradation

Fig. R3: RNA-seq differential expression analysis from orthotopic murine models. RNAseq data were obtained from orthotopically xenografted BSG specimens (brainstem tissues, n = 4) and age-matched controls (normal brainstem tissues, n = 3). Significant variances in gene expression within the perturbed metabolic pathways were indicated by dark circles.

2. In-vitro study of metabolic markers in treated SHSMU-DIPG-01 cells

We further conducted in-vitro studies to investigate the biological effects of metabolite biomarkers on SHSMU-DIPG-01 cells. Our finding revealed concentration-dependent effects of these metabolites on DIPG cell proliferation, as validated by the cell counting kit-8 assay ($p < 0.05$; Fig. R4, corresponding to Supplementary Fig. 4 in Supplementary Information).

These results suggest that these metabolites play a regulatory role in DIPG cell behavior, potentially by modulating metabolic pathways or inducing metabolic stress. This aligns with the broader impact of metabolic reprogramming on tumor development and progression (Ref. 8 corresponding to Ref. 37 in manuscript: Faubert B, et al., Metabolic reprogramming and cancer progression. Science. 2020. 368. 152). The sensitive responses of DIPG cells to these metabolites further support their potential as biomarkers for distinguishing BSG from healthy individuals.

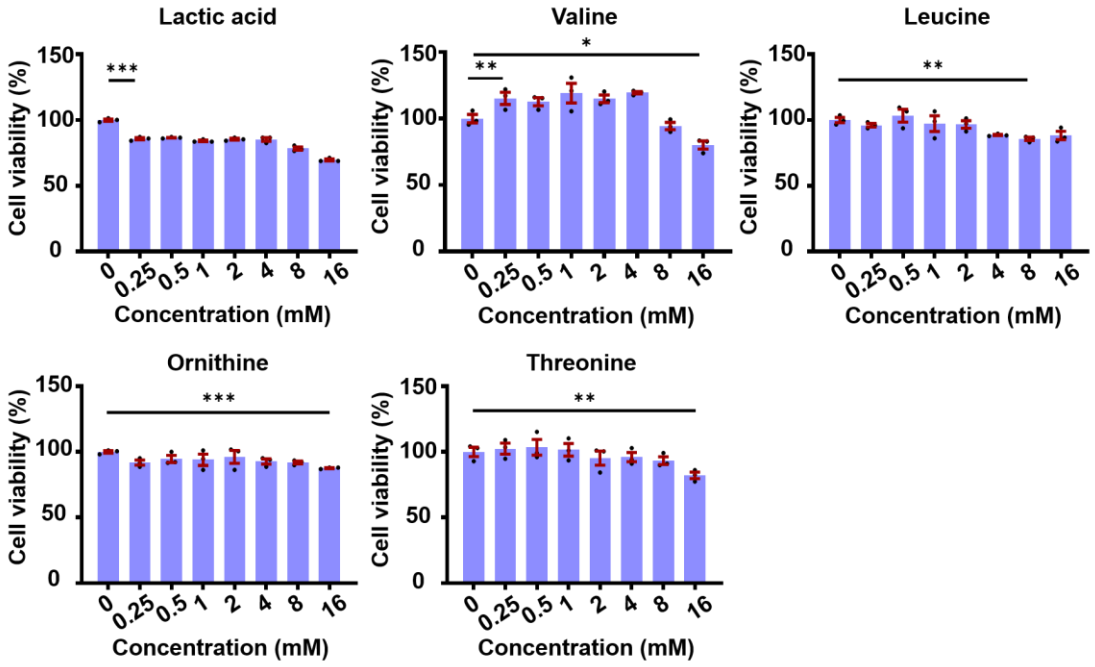

Fig. R4: The impact of diagnostic biomarkers on the proliferation of SHSMU-DIPG-01 cells after three days of treatment. Statistical analyses were conducted using one-way ANOVA, and only the first statistically significant differences were reported. Significance levels are indicated as follows: *p < 0.05, **p < 0.01, ***p < 0.001. All experiments were independently repeated three times.

3. RNA-seq results from publically available database

To validate our findings, we also performed differential expression analysis of publically available RNA-seq data from the GEO dataset GSE162976, comparing DIPG cells against two distinct neural progenitor controls: human neural stem cells (hNSC) and normal human astrocytes (NHA). Intersection analysis revealed a consistent overlap between differentially expressed genes ($|\log_2 FC| > 1$, $p < 0.05$) and the metabolic regulators associated with the adaptive metabolic reprogramming (e.g., arginine and proline metabolism, glycine, serine and threonine metabolism, pantothenate and CoA biosynthesis, and valine, leucine and isoleucine degradation) of tumor cells (Fig. R5, corresponding to Supplementary Fig. 10 in Supplementary Information).

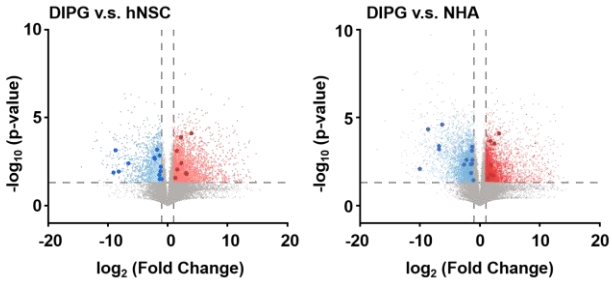

Metabolic pathway
Arginine and proline metabolism
Arginine biosynthesis
Glutathione metabolism
Glycine, serine and threonine metabolism
Pantothenate and CoA biosynthesis
Tryptophan metabolism
Valine, leucine and isoleucine degradation

Fig. R5: RNA-seq differential expression analysis from publically available database. RNAseq data were obtained from the public GEO dataset GSE162976 (DIPG/hNSC/NHA = 3/3/3). Significant variances in gene expression within the perturbed metabolic pathways were indicated by dark circles.

This consistency in both metabolic and transcriptomic results together validated the differentiation capability of the identified metabolic markers in the diagnostic panel for BSG.

We have included the related results (Supplementary Fig. 4, 9, 10), references (Ref. 37 in manuscript and Ref. 17 in Supplementary information), experimental details, and discussions in the manuscript and Supplementary Information as follows.

Revision:

"To further investigate the biological mechanisms underlying the differences between BSG and HDs, we performed differential expression analysis using RNAseq data obtained from orthotopically xenografted BSG specimens (brainstem tissues, n = 4) and age-matched controls (normal brainstem tissues, n = 3, Supplementary Fig. 9). We also validated the correlation based on the analysis of the GEO dataset GSE162976, comparing DIPG cells against two distinct neural progenitor controls: human neural stem cells (hNSC) and normal human astrocytes (NHA; Supplementary Fig. 10). As a result, we detected notable variances in gene expression within the perturbed metabolic pathways, which were reflected in the RNAseq expression data obtained in this study and further supported by the consistent results obtained from GEO database.

Moreover, our exploration revealed the regulation of specific genes associated with the adaptive reprogramming of tumor cells. Notably, the genes Arg1, Arg2, Nos2, and P4ha1 were found to reprogram arginine and proline metabolism. Meanwhile, Arg1,

Arg2, and Nos2 were shown to disturb arginine biosynthesis. Arginine was converted into ornithine through the action of arginase. Additionally, the genes Hpgds and Nat8f6 were identified as key regulators in glutathione metabolism. Gldc and Pgam2 were also found to influence the metabolism of glycine, serine, and threonine. Furthermore, Enpp1 and Enpp3, which encode two critical enzymatic components of the pantothenate and CoA biosynthesis pathway, were shown to be epigenetically regulated in brain tumors. These modulations closely related to the Warburg effect and the TCA cycle, and regulated the expression of lactate. Lastly, Aox4 was found to regulate tyrosine metabolism as well as the degradation of valine, leucine, and isoleucine, in conjunction with Hmgcs2. Therefore, we speculated that the unique metabolic signature arises from the metabolic rewiring of brain tumors, potentially offering valuable insights for BSG." (Manuscript, Page 9)

"SPF-grade female BALB/c nude mice, aged 4-6 weeks and weighing 18-20 g, were used as experimental subjects in this study, following refinement of the experimental methods based on previous study[17]. All animal care and experiments were approved (#XHEC-F-2023-031) by the Animal Ethics Committee of Xinhua Hospital, School of Medicine, Shanghai Jiao Tong University.

To establish the orthotopic intracranial xenograft model, SHSMU-DIPG-01 cells were transduced with lentiviral vectors encoding enhanced green fluorescent protein (eGFP) and firefly luciferase (ffLuc). Positively transduced cells were subsequently sorted by fluorescence-activated cell sorting (FACS) to achieve a purity greater than 95% prior to implantation. Under deep anesthesia, mice were secured on a stereotactic frame, and a cranial burr hole was drilled at stereotactic coordinates relative to the lambda suture: 0.8 mm posterior, 1 mm lateral to the midline, and 4.5 mm depth. A total of 1×10^6 cells suspended in 3 μL phosphate-buffered saline (PBS) were infused via Hamilton syringe at a controlled rate of 0.3 μL/min. To minimize reflux, the injection needle was retained for 5 minutes post-infusion. Tumor engraftment was validated 72 hours post-surgery by intraperitoneal administration of D-luciferin potassium salt (75 mg/kg; Promega) followed by bioluminescent signal acquisition using the IVIS Spectrum In Vivo Imaging System (PerkinElmer). At the humane endpoint, mice were

euthanized. Brain tumor tissue and normal mice brainstem tissues were collected and subjected to RNA sequencing.

To establish the subcutaneous tumor model, 3×10^6 SHSMU-DIPG-01 cells were resuspended in a 1:1 mixture with chilled Matrigel matrix (Corning), maintained on ice throughout preparation. A 100 μL aliquot of the cell-Matrigel suspension was injected subcutaneously into the left dorsal flank of mice using a sterile 25-gauge needle. Tumor volume was measured using a vernier caliper. Radiotherapy was initiated in subcutaneous tumor-bearing mice when the tumor size exceeded 100 mm^3. Mice in the radiotherapy group were administered a daily radiation dose of 2 Gy at the tumor site for five consecutive days."(Supplementary Information, Page 6)

Previous comment 2 regarding the respective roles of the metabolic markers in the prognostic panel:

Response: To delineate the respective roles of the metabolic markers within the prognostic panel, we employed the investigation through (1) in-vitro cell experiments and (2) RNA-seq analyses on tumor tissues in SHSMU-DIPG-01-derived murine models. The metabolic markers in the prognostic panel facilitate tumor progression and therapy resistance of BSG by collectively regulating the signaling pathways, including TNF signaling, NF-κB signaling, p53 signaling, HIF-1 signaling, hippo signaling, and MAPK signaling, which are closely associated with tumor cell proliferation and repair.

1. Cell viability results in in-vitro cell experiments

Our in-vitro experiments demonstrated the specific effects of metabolic markers on cell viability in SHSMU-DIPG-01 models (Fig. R6, corresponding to Supplementary Fig. 11 in Supplementary Information). In particular, we have already validated lactic acid in the diagnostic panel. Hence, its presence in the prognostic panel does not warrant further investigation. Besides, arginine, succinic acid, and lactic acid exhibited significant anti-proliferative effects on DIPG cells ($p < 0.05$). Glucose and niacinamide played a role in promoting cell growth ($p < 0.05$). These findings highlight the relevance of these metabolites in modulating tumor cell behavior.

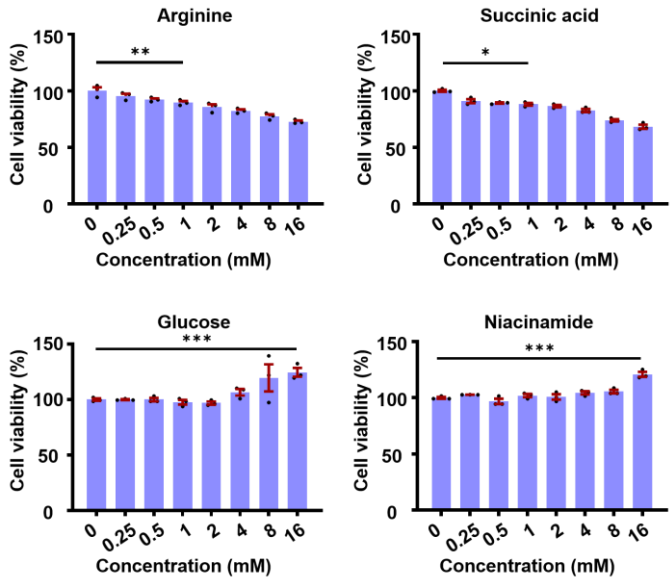

Fig. R6: The impact of prognostic biomarkers on the proliferation of SHSMU-DIPG-01 cells after three days of treatment. Statistical analyses were conducted using one-way ANOVA, and only the first statistically significant differences were reported. Significance levels are indicated as follows: *p < 0.05, **p < 0.01, ***p < 0.001. All experiments were independently repeated three times.

2. RNAseq results from in vivo mouse models

We conducted differential expression analysis on subcutaneous xenografted BSG specimens after radiotherapy (tumor tissues, n = 5) and age-matched BSG specimens before radiotherapy (tumor tissues, n = 6). In particular, 3×10^6 SHSMU-DIPG-01 cells were resuspended in a 1:1 mixture with chilled Matrigel matrix (Corning), maintained on ice throughout preparation. A 100 μL aliquot of the cell-Matrigel suspension was injected subcutaneously into the left dorsal flank of mice using a sterile 25-gauge needle. Tumor volume was measured using a vernier caliper. Radiotherapy was initiated in subcutaneous tumor-bearing mice when the tumor size exceeded 100 mm^3. Mice in the radiotherapy group were administered a daily radiation dose of 2 Gy at the tumor site for five consecutive days.

We identified 14 potentially altered metabolic pathways and highlighted 7 differentially expressed genes (ALDOC, CA9, FBP1, HKDC1, LOC102724560, NDUFA4L2, and P4HA2) linked to these pathways (Fig. R7a-b, corresponding to Supplementary Fig. 12a-b). In particular, glycolysis/gluconeogenesis appeared

enriched in tumor cells. Tumor growth is characterized by the upregulation of ALDOC, FBP1, and HKDC1 correlated with increased glucose and fructose consumption and lactate production (Ref. 9 corresponding to Ref. 42 in manuscript: De Vitis C, et al., ALDOC- and ENO2- driven glucose metabolism sustains 3D tumor spheroids growth regardless of nutrient environmental conditions: a multi-omics analysis. Journal of Experimental & Clinical Cancer Research. 2023. 42. 69). Similarly, amino acid metabolism, regulated by P4HA2 and LOC102724560, a significant hallmark of glioblastoma impacting patient prognosis, has been confirmed through our metabolic and sequencing results and supported by existing literature (Ref. 10&11 corresponding to Ref. 43&44 in manuscript: Chinnaiyan P, et al., The metabolomic signature of malignant glioma reflects accelerated anabolic metabolism. Cancer Research. 2012. 72. 5878; Ersuo J, et al., P4HA2 activates mTOR via hydroxylation and targeting P4HA2-mTOR inhibits lung adenocarcinoma cell growth. Oncogene. 2024. 43. 1813).

To mechanistically characterize the pathophysiological divergence between before RT (BRT) and after RT (ART) among BSG, we identified four significantly enriched pathways correlated with the prognostic metabolic signature in BSG through gene set enrichment analysis (Supplementary Fig. 12c). Enriched pathways involve TNF signaling, NF-κB signaling, p53 signaling, HIF-1 signaling, hippo signaling, and MAPK signaling, which have been demonstrated to impact on the sensitivity of tumors to RT (Ref. 12&13 corresponding to Ref. 45&46 in manuscript: Wang Y, et al., Mechanisms of radioresistance and radiosensitization strategies for triple negative breast cancer. Translational Oncology. 2025. 55. 102351; Ding M, et al., Newly developed strategies for improving sensitivity to radiation by targeting signal pathways in cancer therapy. Cancer Science. 2013. 104. 1401). Intensive studies indicate that the prognostic panel of metabolites could be involved in the regulation of these signaling pathways, which have the potential to influence radiation prognosis. Specifically, lactate enhances the stability of HIF-1α, which promotes its transcriptional activity and subsequently regulates tumor growth and sensitivity to RT (Ref. 15 corresponding to Ref. 47 in manuscript: Taneja N, et al., HIF-1 mediated metabolic reprogramming in cancer: Mechanisms and therapeutic implications. Life Sciences. 2024. 352. 122890).

Glucose stress induces O-GlcNAcylation and further activates hippo-YAP pathways to promote tumorigenesis (Ref. 16 corresponding to Ref. 48 in manuscript: Peng C, et al., Regulation of the hippo-YAP pathway by glucose sensor O-GlcNAcylation. Molecular Cell. 2017. 68. 591). Niacinamide activates p53 activation and suppresses PARP1 to mediate DNA repair and cell proliferation in tumors (Ref. 17 corresponding to Ref. 49 in manuscript: Nikas I, et al., The role of nicotinamide in cancer chemoprevention and therapy. Biomolecules. 2020. 10. 477). Succinic acid promotes not only cancer cell migration and invasion but also cancer metastasis, mediated by PI3K- HIF-1α axis (Ref. 18 corresponding to Ref. 50 in manuscript: Xu J, Richard S. Cellular pathways influenced by protein arginine methylation: Implications for cancer. Molecular cell. 2021. 81. 21). Arginine activates NF-κB signaling by regulating mTORC1-mediated lysosomal release of essential amino acids. It also induces the generation of intracellular nitric oxide, which stimulates HIF-1α signaling and further promotes tumor proliferation (Ref. 19 corresponding to Ref. 51 in manuscript: Yang J, et al., Arginine metabolism: a potential target in pancreatic cancer therapy. Chinese Medical Journal. 2020. 134. 28). Threonine metabolism influences tumor cell proliferation by driving abnormal tRNA modifications and protein translation within tumors (Ref. 20 corresponding to Ref. 52 in manuscript: Wu X, et al., Threonine fuels glioblastoma through YRDC-mediated codon-biased translational reprogramming. Nature Cancer. 2024. 5. 1024).

Taken together, these results indicate that the prognostic panel encapsulates BSG's metabolic reprogramming, linking cell proliferation and therapy resistance to patient prognosis.

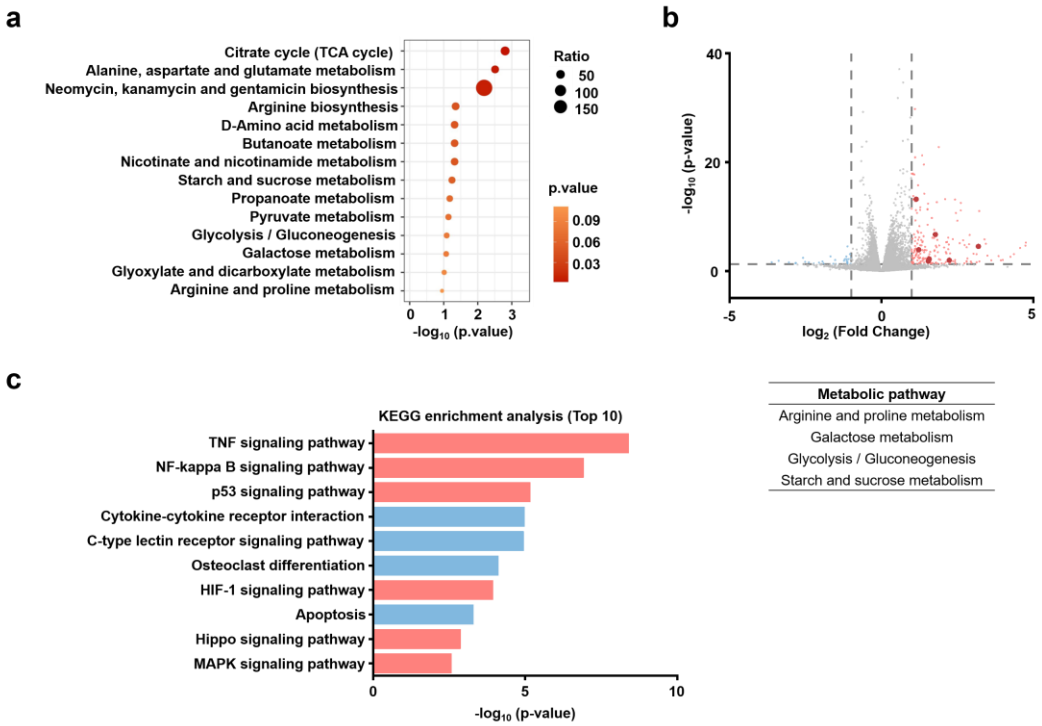

Fig. R7: Validation of prognostic panel. (a) Metabolite set enrichment analysis of metabolic biomarkers from the prognostic panel via the Kyoto Encyclopedia of Genes and Genomes (KEGG) database. (b) Differential expression analysis using RNA-seq data obtained from tumor tissues before (n = 6) and after (n = 5) radiotherapy in subcutaneous murine models. (c) The top 10 perturbed KEGG pathways ranked by p-value ($p < 0.001$).

We have included the related results (Fig. 11&12), references (Ref. 42-52), experimental details, and discussions in the manuscript and Supplementary Information as follows.

Revision:

"Our in-vitro experiments demonstrated the specific effects of metabolic markers on cell viability in SHSMU-DIPG-01 models (Supplementary Fig. 1). In particular, we have already validated lactic acid in the diagnostic panel. Hence, its presence in the prognostic panel does not warrant further investigation. Besides, arginine, succinic acid, and lactic acid exhibited significant anti-proliferative effects on DIPG cells ($p < 0.05$). Glucose and niacinamide played a role in promoting cell growth ($p < 0.05$). These findings highlight the relevance of these metabolites in modulating tumor cell behavior.

The prognostic panel consisted of differentially regulated metabolites together identified 14 potentially altered metabolic pathways (Supplementary Fig. 12a). We thus

conducted RNAseq experiments on subcutaneous xenografted BSG specimens after radiotherapy (tumor tissues, n = 5) and age-matched BSG specimens before radiotherapy (tumor tissues, n = 6). We highlighted seven differentially expressed genes (ALDOC, CA9, FBP1, HKDC1, LOC102724560, NDUFA4L2, and P4HA2), associated with the metabolic pathways identified in the prognostic panel and expression data (Supplementary Fig. 12b). In particular, glycolysis/gluconeogenesis appeared enriched in tumor cells. Tumor growth is characterized by the upregulation of ALDOC, FBP1, and HKDC1 correlated with increased glucose and fructose consumption and lactate production[42]. Similarly, amino acid metabolism, regulated by P4HA2 and LOC102724560, a significant hallmark of glioblastoma impacting patient prognosis, has been confirmed through our metabolic and sequencing results and supported by existing literature[43,44].

To mechanistically characterize the pathophysiological divergence between before RT (BRT) and after RT (ART) among BSG, we identified six significantly enriched pathways correlated with the prognostic metabolic signature in BSG through gene set enrichment analysis (Supplementary Fig. 12c). Enriched pathways involve TNF signaling, NF-κB signaling, p53 signaling, HIF-1 signaling, hippo signaling, and MAPK signaling, which have been demonstrated to impact on the sensitivity of tumors to radiotherapy[45,46]. Intensive studies indicate that the prognostic panel of metabolites could be involved in the regulation of these signaling pathways, which have the potential to influence radiation prognosis. Specifically, lactate enhances the stability of HIF-1 α , which promotes its transcriptional activity and subsequently regulates tumor growth and sensitivity to RT[47]. Glucose stress induces O-GlcNAcylation and further activates hippo-YAP pathways to promote tumorigenesis[48]. Niacinamide activates p53 activation and suppresses PARP1 to mediate DNA repair and cell proliferation in tumor[49]. Succinic acid promotes not only cancer cell migration and invasion but also cancer metastasis, mediated by PI3K- HIF-1α axis[50]. Arginine activates NF-κB signaling by regulating mTORC1-mediated lysosomal release of essential amino acids. It also induces the generation of intracellular nitric oxide, which stimulates HIF-1α signaling and further promotes tumor proliferation[51]. Threonine metabolism

influences tumor cell proliferation by driving abnormal tRNA modifications and protein translation within tumors[52]. Thus, we conclude that the prognostic panel reflects the rewired metabolism of tumors." (Manuscript, Page 11)

Previous comment 9 regarding the metabolite change in high-grade gliomas treatment course in brainstem tumor itself:

Response: We performed the preclinical animal study using mouse models to acquire paired samples (*i.e.*, mice brain tumor and mice serum with and without radiation) with the same analysis from discovery set. We demonstrated consistent metabolite changes, such as lactic acid, in the high-grade gliomas treatment course in brainstem tumor itself, as in the paired serum samples.

Paired serum and brain tumor samples from treated mice were collected five days after radiotherapy. Both the serum and tumor samples were subjected to metabolic analysis by NPELDI MS. The preclinical animal study indicated significant alterations in metabolite levels after radiotherapy treatment in tumors, aligning with observations in paired serum samples (Fig. R8, corresponding to Supplementary Fig. 15 in Supplementary Information).

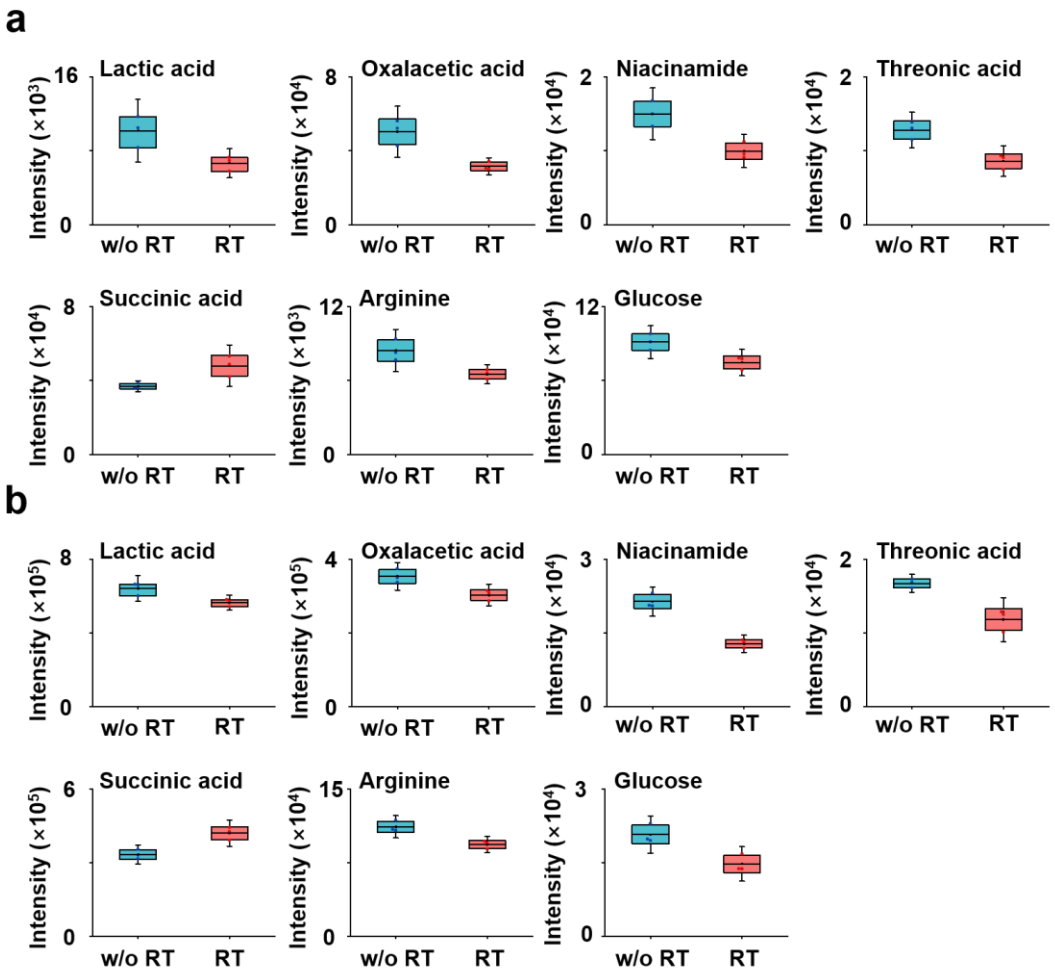

Fig. R8: Metabolic alterations throughout the treatment course of tumors. Metabolite levels before and after radiotherapy treatment in (a) paired serum samples (n = 3 vs. 3) and (b) BSG tumors themselves (n = 3 vs. 3) from subcutaneous tumor models. Data are presented as mean ± s.d.

We have added the related results (Supplementary Fig. 15), experimental details, and discussion in the manuscript and Supplementary Information as follows.

Revision:

"We further performed preclinical animal study using mouse tumor models to acquire paired samples (i.e., mice brain tumor and mice serum before and after radiation) with the same analysis from discovery set. The preclinical animal study also indicated significant alterations in metabolite levels before and after radiotherapy treatment in BSG, aligning with observations in paired serum samples (Supplementary Fig. 15)." (Manuscript, Page 14)

Reviewer #2 (Remarks to the Author):

Comment: *In the revised manuscript, Li and colleagues have extensively addressed all my concerns. The data presented in the current version supports the authors' conclusions. I recommend publication in Nature Communications.*

Response: We thank the reviewer for his/her time and careful consideration. The feedback provided by the reviewer has significantly enhanced the manuscript, and we appreciate your acknowledgment of our contributions. We are dedicated to upholding the manuscript's quality and precision to the utmost standard, and we value your input and guidance throughout this endeavor.

Reviewer #3 (Remarks to the Author):

Comment: *This revised manuscript has improved on the study and answered many of the questions posed in the original review, including a more in-depth description on how they identified the metabolite biomarkers and adding additional patients. However, I have two concerns remaining that should be addressed prior to publication.*

Response: We thank the reviewer for the feedback on the revised version of our manuscript. We have carefully addressed the concerns raised and made additional revisions to further strengthen the study. Detailed point-by-point responses and revisions can be found below.

Comment 1: *The authors have clarified that the 402 metabolic features are unidentified peaks detected in their NPELDI-MS platform and 287 features were different between healthy and glioma patients. It is fine to report these numbers; however, comparing groups by using unidentified features as is done in Figure 1 and Figure 2a is problematic. Mass spectrometers detect noise signals in the low mass range and without positive metabolite identifications it likely that many of the peaks don't actual represent biological metabolites but are artifacts of the detection method. I don't think the authors have to identify all 402 features, but they should either eliminate these comparisons or perform the same comparisons using only metabolites that have been identified.*

Response: We thank the reviewer for the very useful comment. We have eliminated these comparisons in Fig. R9 (corresponding to Fig. 1 in the manuscript) as well as in the main text. We also performed the same comparisons using only metabolites that have been identified as shown in Fig. R10c (corresponding to Fig. 2c in the manuscript).

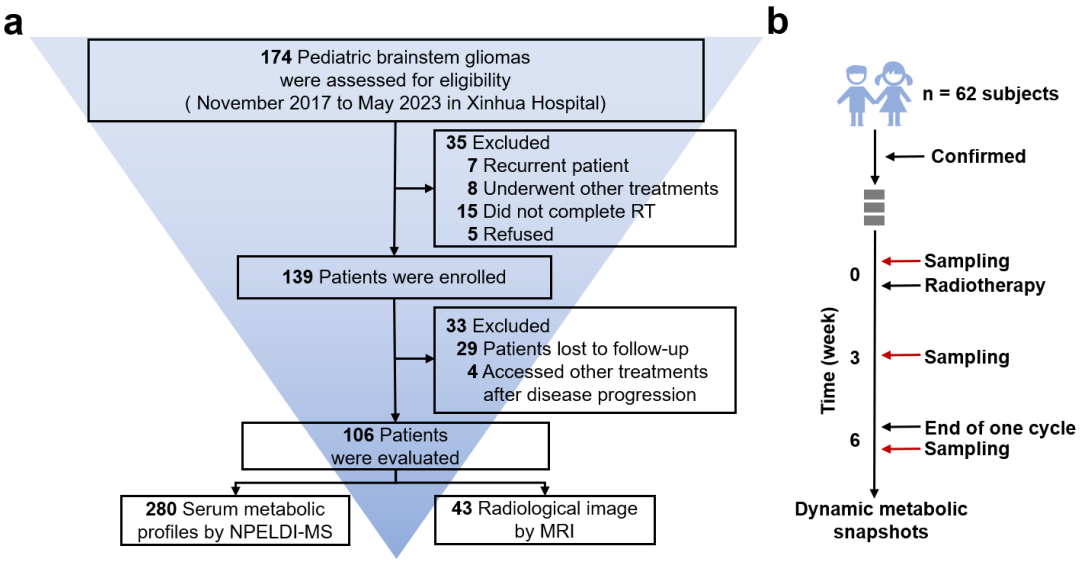

Fig. R9: Study design and patient cohort characteristics. (a) Study design of participant enrollment, including 125 HDs and 106 BSG patients. (b) Longitudinal sample collection of 62 BSG patients at three time points as the dynamic metabolic snapshots.

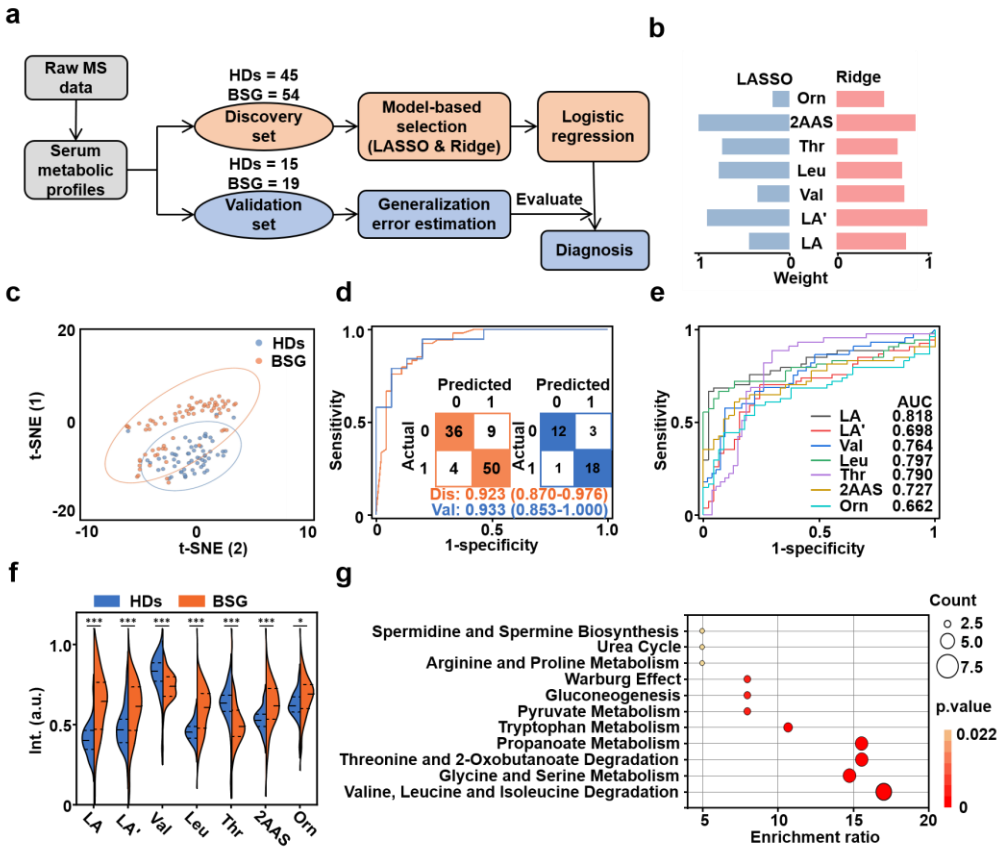

Fig. R10: Diagnostic value of circulating metabolites in BSG patients. (a) Study design for BSG diagnosis using machine learning. Static metabolic snapshots from 99 participants (45/54, HDs/BSG) in the discovery set for feature selection and model building. The optimized model was tested in an independent validation set (15/19, HDs/BSG). (b) Coefficients of the least absolute shrinkage and

selection operator (LASSO) and Ridge algorithms were shown as the evaluation index for seven metabolic features. (c) t-distributed stochastic neighbor embedding of serum metabolic profiles for 60 HDs and 73 BSG patients was plotted using the identified metabolites. (d) Receiver operating characteristic (ROC) curves of the discovery set and validation set to distinguish HDs and BSG patients within the metabolic panel. The corresponding confusion matrices were shown as the inset. (e) ROC curves analysis was shown with each single feature (AUC of 0.662-0.818). (f) Violin-plot illustrated the differential regulation of normalized intensities for metabolic features in HDs and BSG. (g) Potential pathways were differentially regulated in HDs and BSG patients. Color and size of each circle were correlated to the *p* value and enrichment ratio. *** represented $p < 0.005$, * represented $p < 0.05$. LA and LA': lactic acid; Val: valine; Leu: leucine; Thr: threonine; 2AAS: 2-Aminomuconic acid semialdehyde; Orn: ornithine.

We have revised the figures (Fig. 1 and 2) and related discussion in the manuscript as follows.

Revision:

"Among these, 287 features (71.4%) varied from HDs to BSG patients ($p < 0.05$, Student's t-test). Notably, the serum metabolic snapshot database, which contains a sufficient amount of signal intensity and feature number, serves as the foundation for the downstream analysis." (Manuscript, Page 6)

"We built diagnostic classification models based on machine learning algorithms on the discovery set (n = 45/54, HDs/BSG)." (Manuscript, Page 6)

"Unsupervised clustering analyses analysis partly intuitively distinguished BSG from HDs, including t-distributed stochastic neighbor embedding (Fig. 2c) and principal component analysis (Supplementary Fig. 2d)." (Manuscript, Page 7)

Comment 2: *It is appreciated that the authors tried to add biological context with cell culture experiments, but the rationale and approach for these studies is confusing. It is well-known that metabolites such as lactate can impact malignant cell phenotype, but presumably a better argument is that the serum biomarkers found in the study (and associated with BSG and response to therapy) would be secreted into circulation by the tumor. It is puzzling why the authors didn't just measure excretion of their metabolite biomarkers into media? In my opinion the RNA-seq data (matched tumor/serum from*

mice) support a biological role for the metabolite biomarkers better than the cell culture experiments. Perhaps the authors can modify the text to spend less time on the cell culture experiments and describe the RNA-seq experiments more fully.

Response: We appreciate the reviewer for the valuable feedback, particularly the suggestion to directly measure the excretion of our metabolite biomarkers into the media. However, conducting a comparison of excretion at the cell model level poses challenges due to the lack of suitable control cell models.

The inclusion of biological context through cell culture experiments offers insights into the association of the biomarkers with BSG occurrence and progression, a widely employed approach supported by previous metabolomics studies from existing literature (Ref: Daniel et al., Metabolomics in cancer research and emerging applications in clinical oncology. CA-A Cancer Journal for Clinicians. 2021. 71. 333; Wu et al., Cancer-derived succinate promotes macrophage polarization and cancer metastasis via succinate receptor. Molecular Cell. 2020. 77. 213).

To address the reviewer's concerns effectively, we have made the revisions to spend less time on the cell culture experiments and described the RNA-seq experiments more fully. The related revisions were listed as follows.

Revision:

"To further investigate the biological mechanisms underlying the differences between BSG and HDs, we performed differential expression analysis using RNAseq data obtained from orthotopically xenografted BSG specimens (brainstem tissues, n = 4) and age-matched controls (normal brainstem tissues, n = 3, Supplementary Fig. 9). We also validated the correlation based on the analysis of the GEO dataset GSE162976, comparing DIPG cells against two distinct neural progenitor controls: human neural stem cells (hNSC) and normal human astrocytes (NHA; Supplementary Fig. 10). As a result, we detected notable variances in gene expression within the perturbed metabolic pathways, which were reflected in the RNAseq expression data obtained in this study and further supported by the consistent results obtained from GEO database.

Moreover, our exploration revealed the regulation of specific genes associated with the adaptive reprogramming of tumor cells. Notably, the genes Arg1, Arg2, Nos2, and P4ha1 were found to reprogram arginine and proline metabolism. Meanwhile, Arg1, Arg2, and Nos2 were shown to disturb arginine biosynthesis. Arginine was converted into ornithine through the action of arginase. Additionally, the genes Hpgds and Nat8f6 were identified as key regulators in glutathione metabolism. Gldc and Pgam2 were also found to influence the metabolism of glycine, serine, and threonine. Furthermore, Enpp1 and Enpp3, which encode two critical enzymatic components of the pantothenate and CoA biosynthesis pathway, were shown to be epigenetically regulated in brain tumors. These modulations closely related to the Warburg effect and the TCA cycle, and regulated the expression of lactate. Lastly, Aox4 was found to regulate tyrosine metabolism as well as the degradation of valine, leucine, and isoleucine, in conjunction with Hmgcs2. Therefore, we speculated that the unique metabolic signature arises from the metabolic rewiring of brain tumors, potentially offering valuable insights for BSG." (Manuscript, Page 9)

"The prognostic panel consisted of differentially regulated metabolites together identified 14 potentially altered metabolic pathways (Supplementary Fig. 12a). We thus conducted RNAseq experiments on subcutaneous xenografted BSG specimens after radiotherapy (tumor tissues, n = 5) and age-matched BSG specimens before radiotherapy (tumor tissues, n = 6). We highlighted seven differentially expressed genes (ALDOC, CA9, FBP1, HKDC1, LOC102724560, NDUFA4L2, and P4HA2), associated with the metabolic pathways identified in the prognostic panel and expression data (Supplementary Fig. 12b). In particular, glycolysis/gluconeogenesis appeared enriched in tumor cells. Tumor growth is characterized by the upregulation of ALDOC, FBP1, and HKDC1 correlated with increased glucose and fructose consumption and lactate production[42]. Similarly, amino acid metabolism, regulated by P4HA2 and LOC102724560, a significant hallmark of glioblastoma impacting patient prognosis, has been confirmed through our metabolic and sequencing results and supported by existing literature[43,44].

To mechanistically characterize the pathophysiological divergence between before

RT (BRT) and after RT (ART) among BSG, we identified six significantly enriched pathways correlated with the prognostic metabolic signature in BSG through gene set enrichment analysis (Supplementary Fig. 12c). Enriched pathways involve TNF signaling, NF-κB signaling, p53 signaling, HIF-1 signaling, hippo signaling, and MAPK signaling, which have been demonstrated to impact on the sensitivity of tumors to radiotherapy[45,46]. Intensive studies indicate that the prognostic panel of metabolites could be involved in the regulation of these signaling pathways, which have the potential to influence radiation prognosis. Specifically, lactate enhances the stability of HIF-1 α , which promotes its transcriptional activity and subsequently regulates tumor growth and sensitivity to RT[47]. Glucose stress induces O-GlcNAcylation and further activates hippo-YAP pathways to promote tumorigenesis[48]. Niacinamide activates p53 activation and suppresses PARP1 to mediate DNA repair and cell proliferation in tumor[49]. Succinic acid promotes not only cancer cell migration and invasion but also cancer metastasis, mediated by PI3K- HIF-1α axis[50]. Arginine activates NF-κB signaling by regulating mTORC1-mediated lysosomal release of essential amino acids. It also induces the generation of intracellular nitric oxide, which stimulates HIF-1α signaling and further promotes tumor proliferation[51]. Threonine metabolism influences tumor cell proliferation by driving abnormal tRNA modifications and protein translation within tumors[52]. Thus, we conclude that the prognostic panel reflects the rewired metabolism of tumors." (Manuscript, Page 11)

Minor comments:

Comment 1: *Western blot in supplementary 10a doesn't look different between treatments in my opinion.*

Response: We thank the reviewer for the useful comment. To address the methodological concerns, we conducted additional qPCR analyses quantifying PD-L1 mRNA expression levels following treatment with glucose and the niacinamide analog (Fig. R11). While our original Western blot data from glioblastoma (GBM) cell lines remain valid, we recognize the critical need for disease-specific validation.

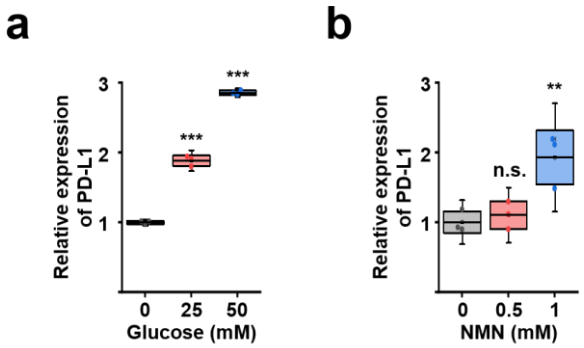

Fig. R11: Biological effects of prognostic biomarkers on human glioblastoma multiforme cells. Both (a) glucose and (b) nicotinamide mononucleotide (NMN) improved the mRNA expression of PD-L1 in U251MG cells, verified by quantitative polymerase chain reaction (qPCR) determination. One-way ANOVA was used to perform statistical analyses. * $p < 0.05$, ** $p < 0.01$, *** $p < 0.001$. Experiments were independently repeated 3 times with similar results in (a).

To tie our study mechanistically to brainstem glioma biology, we repeated all key vivo and vitro experiments using the human diffuse intrinsic pontine glioma (DIPG) cell line SHSMU-DIPG-01 – a brainstem glioma-specific model. In the current manuscript, Western blot data were intentionally omitted from the revised manuscript to prioritize mechanistically relevant findings from the DIPG system. Original GBM-derived Western blot results have been replaced with new in-vitro functional data in Fig. R6 (corresponding to Supplementary Fig. 11 in Supplementary Information).

We have replaced the original western blot data with new in-vitro cell experimental results in the figure (Supplementary Fig. 11) and the corresponding discussion in the manuscript as follows.

Revision:

"Our in-vitro experiments demonstrated the specific effects of metabolic markers on cell viability in SHSMU-DIPG-01 models (Supplementary Fig. 11). In particular, we have already validated lactic acid in the diagnostic panel. Hence, its presence in the prognostic panel does not warrant further investigation. Besides, arginine, succinic acid, and lactic acid exhibited significant anti-proliferative effects on DIPG cells ($p < 0.05$). Glucose and niacinamide played a role in promoting cell growth ($p < 0.05$). These findings highlight the relevance of these metabolites in modulating tumor cell behavior"

(Manuscript, Page 11)

Comment 2: *Language still needs to some editing. For example, Line 88 has resolution twice. Line 376-Our sampling focus on the HDs and BSG.*

Response: We thank the reviewer for the valuable feedback. We have carefully proofread the manuscript again for further validation. We have revised all grammatical errors present throughout the paper and ensured comprehensive corrections were made.

Typical revisions in the manuscript have been listed as follows.

Revision:

"This is facilitated by the compatible pore size of brain microvessel endothelial cells, which typically range from about 1.4 to 1.8 nm, enabling metabolites to enter the bloodstream[21-24]." (Manuscript, Page 3)

"Mass spectrometry (MS) is applied in the profiling and discovery of metabolic biomarkers by detecting the mass-to-charge ratio (m/z) of metabolites at a high resolution at ppm level." (Manuscript, Page 4)

"This technique features few pretreatment operations, fast detection speed, and trace sample consumption[28-30], making it ideal for scenarios where expeditious reporting is critical[31-33]." (Manuscript, Page 4)

"Based on the dichotomized label on the median risk score, the BSG patients were stratified into two groups: the high-risk group and the low-risk group." (Manuscript, Page 12)

"Our samples were mainly from the HDs and BSG (as cohort 3) in the different periods of radiotherapy, including 117 HDs, 101 BRT, 85 DRT, and 85 ART, revealed detailed temporal patterns of metabolic changes." (Manuscript, Page 13)

"Overall, regular monitoring of metabolic snapshots allows for prompt assessment of the patients' treatment effectiveness and provides valuable support in clinical decision-making processes." (Manuscript, Page 16)

REVIEWER COMMENTS

Reviewer #1 (Remarks to the Author):

Comment: *The revised manuscript has addressed my concerns about models system and metabolic makers between BSG and HDs. I recommended publication in Nature Communications.*

Response: We extend our sincere gratitude to the reviewer for his/her dedicated efforts and insightful critique throughout the peer review process. The expert suggestions have made invaluable contributions to refining the rigor and clarity of this work. We have meticulously implemented all recommended revisions as detailed in the point-by-point response document, ensuring full compliance with the journal's standards.

Reviewer #3 (Remarks to the Author):

Comment: *The authors have performed additional work that sufficiently addresses my previous concerns. I only have two minor comments to add.*

Response: We are grateful to the reviewers for his/her constructive comments on the revised manuscript. We have carefully considered all feedback, incorporated additional revisions to enhance the rigor and clarity of the study, and provided a point-by-point response to each suggestion as detailed below.

Comment 1: *The authors should indicate in the text and figure legend how many identified metabolites were used as input in their model and provide a list of metabolites in supplementary.*

Response: We thank the reviewer for the valuable comments. We have indicated the identified metabolites used in the diagnostic and prognostic models in Fig. 2e (seven features for six metabolites) and Fig. 3b (seven features for seven metabolites) of the main text, as well as in Supplementary Table 5 and Supplementary Table 7. We also added the number of identified metabolites in figure legends.

Revision:

"As a result, seven metabolic features corresponding to six metabolites were identified as highly ranked biomarkers (mean intensity > 200, p value < 0.05, and coefficient weight > 0.18), including 2-aminomuconic acid semialdehyde, lactic acid, valine, leucine, threonine, and ornithine (Supplementary Table 5)[38,39]." (Page 7, Manuscript)

"Importantly, we identified a seven-feature panel correlated with clinical outcomes, consisting of lactic acid, oxalacetic acid, niacinamide, threonic acid, succinic acid, arginine, and glucose (Supplementary Table 7)." (Page 11, Manuscript)

Comment 2: *I appreciate that the authors have now focused on the RNA-seq, I am still unsure how the in vitro viability assays validate the biological activity of metabolites in the paper. The magnitude in change in viability looks marginal at best and there is no confirmation of nutrient uptake in the cells or signaling through a receptor. One path perhaps to move forward would be to acknowledge the limitations of only looking at proliferation and emphasize that more biological validation studies need to be done.*

Response: We sincerely thank the reviewer for the insightful critique on the biological validation of metabolite activity. We fully agree that additional mechanistic studies will strengthen the biological relevance of our findings, and we acknowledge the limitations of the study and add them to the main text. The related revisions were listed as follows.

Revision:

"Although this work delineates the concentration-dependent effects of specific metabolites on tumor cell proliferation dynamics, additional biological validation is essential to confirm the metabolic regulatory networks involved in cellular nutrient uptake or receptor-mediated signaling pathways." (Page 19, Manuscript)